10-31-2023

# Examining the Role of Microglia in Diabetic Retinopathy: Phenotypes, Mechanisms, and Therapies

Charles W. Pfeifer
*Washington University in St. Louis*

WASHINGTON UNIVERSITY IN ST. LOUIS

Division of Biology and Biomedical Sciences
Neurosciences

Dissertation Examination Committee:
Aaron DiAntonio, Chair
Rajendra Apte
Vladimir Kefalov
Tristan Qingyun Li
Philip Ruzycki

# Examining the Role of Microglia in Diabetic Retinopathy: Phenotypes, Mechanisms, and Therapies

by
Charles W. Pfeifer

A dissertation presented to
Washington University in St. Louis
in partial fulfillment of the
requirements for the degree
of Doctor of Philosophy

December, 2023
St. Louis, Missouri

# Table of Contents

# List of Figures

# Acknowledgments

I would first like to thank my thesis advisor, Dr. Rajendra Apte, for guiding and supporting me through my doctoral work while shaping the way I approach science and life. I would also like to thank the other members of the Apte laboratory for creating and fueling an environment in which it was a joy to work each day.

To my family. Lisa, Rich, and Lily have always picked up the phone, celebrated me in times of joy, encouraged me in times of despair, and always believed in my pursuit of research despite the sacrifices it required. Special thank you to my parents for raising me to dream, move around the country, and seek out opportunities to challenge myself and grow – both inside and outside of science – for without them, I would not be where I am today.

Thank you to Sabrina, my companion in life, for sticking with me so we could train and grow alongside one another. You're the glue that steadies me, and the fire that motivates me.

Thanks to all my friends and supportive individuals in my life, particularly those that have stood by me in spirit from afar. I am forever grateful for your kind words, wisdom, laughter, and love.

Chas Pfeifer

*Washington University in St. Louis*

*December 2023*

Dedicated to my parents for their endless love and support.

ABSTRACT OF THE DISSERTATION

Examining the role of microglia in diabetic retinopathy: Phenotypes, mechanisms, and therapies

by

Charles W. Pfeifer

Doctor of Philosophy in Biology and Biomedical Sciences

Neurosciences

Washington University in St. Louis, 2023

Professor Aaron DiAntonio, Chair

Retinal microglia activation and function is a pivotal component of ocular disease pathology, but their involvement in diabetic retinopathy, a complex neurovascular complication of diabetes, remains unclear. The purpose of this thesis work is to thoroughly examine features of microglia activation in DR, identify mechanistic underpinnings of their contributions to neuroinflammatory features of disease pathogenesis, and assess immunotherapeutic targeting of microglia as a potential approach to treating early-stage DR. Here, we show that chronic hyperglycemia elicits morphological, ultrastructural, and transcriptional changes in retinal microglia during early-stage DR while other elements of the retinal neurovascular unit remain unperturbed. Through chronic ablation of retinal microglia in diabetic mice, we find that microglia are not only first responders to chronic hyperglycemia but also potent contributors to visual dysfunction and neurodegeneration. Furthermore, we find that microglia are particularly detrimental to amacrine cells, a critical interneuron subtype, through aberrant contact and phagocytosis. Through ligand-receptor analysis of DR-associated microglial transcriptomic changes, we discover that microglia upregulate CD200R while its immunomodulatory cognate protein CD200, is decreased in

amacrine cells of the diabetic retina, and correlates with retinal inflammation and pathological microglial contact. Lastly, we find that CD200-CD200R dysregulation is amenable to treatment via CD200 fusion protein (CD200Fc), which attenuates high glucose-induced inflammation, transcriptomic changes, and phagocytosis in microglia *in vitro.* Furthermore, we show that CD200Fc suppresses visual dysfunction, microglia activation, and retinal inflammation in the STZ mouse *in vivo,* demonstrating that CD200Fc treatment may be a promising therapeutic avenue for preventing microglia-mediated retinopathy in diabetic animals and patients. Together, these findings show that microglia are a significant contributor to features of early-stage DR and are amenable to treatment via correction of CD200-CD200R dysregulation *in vivo.* This work provides a valuable framework for future studies in microglia-mediated disease pathology as well as development of this novel therapy in the context of DR.

# Chapter 1: Introduction

## 1.1 Discovery, ontogeny, and longevity of microglia

In 1856, German pathologist Rudolf Virchow first identified a connective tissue in the brain, the 'nervenkitt' or nerve-cement, which he termed 'neuroglia'[1]. This initial discovery would be debated by scientists for several decades until 1913, when Spanish neuroscientist Santiago Ramón y Cajal described oligodendrocytes and microglia together as a new element of the central nervous system (CNS)[2]. This would gain further traction as Alois Alzheimer, Franz Nissl, and others began to recognize these apolar cells in various types of brain diseases, such as dementia and multiple sclerosis[3,4]. In 1919, another prominent Spanish neuroscientist Pio del Rio Hortega published a series of papers that distinguished microglia as a distinct population of immune cells in the brain parenchyma using a modified silver carbonate impregnation labeling method[5]. Using this technique, he differentiated microglia from oligodendrocytes based on their mesodermal origin, ramified morphology at rest, and phagocytic and migratory capacity[6].

For a time, there was much support for the notion that microglia shared a ectodermal origin with other glial cells[7]. In fact, a common progenitor for microglia, astrocytes, and oligodendrocytes was agreed upon up until the 1990s[8,9]. This view was later replaced by the concept that microglia were of blood monocytic origin, which has been upheld up until the last decade or so[10]. With the development of fate-mapping techniques, it has been shown that microglia arise from embryonic yolk sac (YS) precursors and migrate to the developing brain around embryonic day 9.5 in the mouse, and colonize the human cerebrum within the first 6 months of gestation[11,12,13,14]. As an independent lineage from hematopoietic stem cells, microglia maintain their population throughout the life span of the organism through slow self-replication

with little contribution from bone-derived myeloid precursors[15,16,17]. Using lineage tracing and conditional microglia ablation, this has also been upheld in the retina where nearly 90% of residing microglia are "long-lived" and repopulating microglia following ablation events are largely derived from a surviving minority of residual microglia and display transcriptional and functional properties similar to bona fide microglia[18,19,20]. These discoveries regarding microglial identity, ontogeny, and longevity set up the early frontier of microglial biology and built the foundation from which the field now flourishes. Furthermore, the distinction among microglia, tissue-resident macrophages, and blood-derived cells have ignited a rapidly growing discussion surrounding their discreet functional roles in development, adulthood, and disease.

## 1.2 Microglial precursor development and maintenance

The committed differentiation of myeloid precursors to microglia and their early maintenance is tightly controlled by various transcription factors, growth factors, chemokines, and microRNAs[21,22]. Runt-related transcription factor (RUNX1) is a transcription factor that binds directly to enhancer genes required for myeloid cell development. Its expression level is high during early embryonic development when amoeboid microglia are actively populating the CNS while progressive loss of expression correlates with conclusive transformation into resident, resting microglia around postnatal day 10[23]. Mutations of RUNX1 result in embryonic lethality as well as poor differentiation of myeloid progenitors in the developing embryo, however it remains unknown if RUNX1 is necessary to support function[24]. PU.1 is a member of the ETS (E-twenty six) family of transcription factors that are dynamically expressed in various cells, including macrophages, neutrophils, B cells, and microglia[25,26]. PU.1 is considered to be a master regulator of myelomonocytic differentiation during embryonic development as deficiency in

PU.1 is associated with immunocompromise and poor maturation of yolk-sac-derived myeloid progenitors[27]. Colony stimulating factor 1 receptor (CSF1R) is a receptor tyrosine kinase that regulates microglial survival, differentiation, and development. As such, CSF1R mutations or deficiency result in decreased numbers of microglia and other tissue macrophages[28,29]. CSF1R binds two ligands, CSF1 and interleukin-34 (IL-34), which are both secreted primarily by neurons in the CNS and when genetically modified, result in partial reduction in microglia numbers[30]. Interferon regulatory factor 8 (IRF-8) is an additional transcription factor that modulates the proliferative capacity and activation of microglia, as shown in studies demonstrating that IRF-8-deficiency results in increased abundance of morphologically activated microglia[31]. miR-124 is one of the most abundantly expressed microRNAs in the CNS and in addition to its role in neuronal differentiation it also maintains microglial quiescence by targeting the transcription factor C/EBP and its downstream target PU.1[32]. Through this developmental program, microglial genesis is guided towards appropriate colonization of CNS tissues and involvement in neurovascular development.

## 1.3 Organization of the retina and microglial colonization during development

The retina is part of the CNS due to its neuroectodermal origin and is structured in diverse layers of cell types that form morphologically and functionally distinct circuits to generate complex visual output. The outermost layer of the retina is the retinal pigment epithelium (RPE), a monolayer of pigmented cells that resembles the choroid-blood-retinal barrier with Bruch's membrane and choroid at the lateral retina and regulates metabolism and physiology in the retina[33,34]. Anterior to the RPE lies the outer nuclear layer (ONL), which

contains rod and cone photoreceptors that drive dim-light, low acuity, and bright-light, high acuity color vision, respectively. The inner nuclear layer (INL) contains cell bodies of bipolar cells, the second-order neurons that receive glutamatergic signals from photoreceptors within the outer plexiform layer (OPL) and depolarize (ON) or hyperpolarize (OFF) to increments in light intensity. Amacrine and horizontal cells are key interneuron subtypes that also exist within the INL and stratify laterally to modulate transmitted signals from bipolar and photoreceptor cells, respectively, and provide feedback in the inner plexiform layer (IPL) through GABAergic and glycinergic input. The ganglion cell layer (GCL) is primarily made up of retinal ganglion cells (RGC), which transmit these modified signals to the lateral geniculate nucleus (LGN) in the thalamus and superior colliculus in the midbrain using glutamate via long axons that make up the optic nerve[35,36].

Glia (Müller cells, astrocytes, and microglia) are also critical to maintaining homeostasis in the retina. Müller cells are the predominant subtype that span the entire thickness of the retina, regulating ion composition in the extracellular space, trophic and anti-oxidant support of neurons, and maintenance of the blood-retina-barrier[37,38]. Astrocytes are restricted to the superficial vessel and nerve fiber layer (NFL) where they radiate fibrous processes to drive important roles in vascular development, neurovascular coupling, and blood flow[39]. Lastly, the retina is supplied with an intricate vascular network that distributes within the RGC/NFL layers (superficial vascular plexus), IPL (intermediate vascular plexus), and OPL (deep capillary plexus). Supported structurally by endothelial cells and pericytes, and secondarily by glial cells, this vascular system supports the retinal parenchyma while providing a physical inner blood retina barrier (iBRB). The outer blood retina barrier (oBRB) is maintained by the RPE and choroidal vasculature that exists posterior to the RPE. While the concept of ocular immune

privilege, first introduced by Sir Peter Medawar over 70 years ago, remains controversial, these anatomical barriers do provide a degree of specialized protection against destructive inflammatory responses and tolerate foreign antigens[40,41]. The molecular basis of this tolerance has given rise to the development of therapeutic approaches to prevent destructive inflammation in the eye and other tissues and organs.

As part of the CNS, microglia migrate to, and aid the development of the retina. Microglia are first detected in the human retina by 10 weeks gestation and in the mouse retina by E11.5[42,43]. Based on the apparent localization of early-arriving microglia, there are two instances of microglia infiltration proposed for the developing retina. The first occurs prior to vascularization via the ciliary margin or non-neural ciliary regions in the periphery while the second occurs following vascularization via blood vessels or the optic disc[44,45,46]. At first, microglia cells with ameboid morphology are found at the primary vascular plexus in the GCL, where they radiate laterally. Until P10, microglia progressively colonize the IPL and OPL in parallel to development of the intermediate (IPL) and deep capillary (OPL) vascular plexuses[47,48]. In adulthood, microglia maintain primary networks within the IPL and OPL with consistent intercellular distances that are believed to be dictated by repulsive signaling mechanisms[49]. Occasional microglia are found in the GCL and INL but are not observed in the ONL in homeostatic conditions[50]. Through this process of retinal colonization and organization, microglia simultaneously witness and mediate various crucial facets of neurovascular development necessary for homeostatic retinal function in adulthood.

## 1.4 General microglial functions in development and adulthood

Following migration to, and differentiation within, developing CNS tissue, microglia participate in various ongoing facets of development that are consistent across tissue niches. As inferred by their paralleled temporal and spatial organization during development, microglia aid the growth of sprouting vessels during vasculogenesis via Mas1 and Notch1 receptors, secreted trophic factors, and direct contact with endothelial cells and pericytes[51,52,53]. Similarly, microglia selectively release trophic factors at proliferative zones during neurogenesis to regulate the rate of neuronal precursor production and axonal growth[54,55]. Given the amount of cell death that occurs during development, microglia provide an efficient cleanup force that phagocytoses cellular debris without initiating an inflammatory response. To speed up proper neuronal integration through elimination of these cells, microglia contribute to programmed cell death through production of superoxide ions and growth factors where necessary[56,57,58]. The shaping of nascent synapses during development is perhaps one of the main functions of postnatal microglia. This process is regulated by neuronal activity and expression of classical complement proteins (C1q, C3) by synapses which are then recognized and phagocytosed via microglia-specific expression of complement receptor CR3[59,60]. Additional mechanisms at play include the release of soluble fractalkine (CX3CL1) by damaged neurons which can promote phagocytosis via expression of milk fat globule-epidermal growth factor 8 (MFG-E8)[61]. At a broader scale, the synergistic involvement of microglia in vasculo- and neurogenesis, cell survival and proliferation, and synaptic refinement drive the establishment and active remodeling of whole neural circuits which directly impacts connectivity and function[62,63,64,65,66]. Following postnatal development, microglia form non-overlapping network mosaics within CNS tissue where they constantly survey and contact neural elements with their highly active processes[67,68,69]. Through

this active surveillance, microglia interact with virtually all neuronal cell types to establish and maintain CNS tissue homeostasis during development and adulthood[70].

## 1.5 Microglial heterogeneity and plasticity in disease

As resident immune cells, microglial activation is a pivotal feature of virtually all neurodegenerative diseases[71]. This response is generated by their recognition of pathogens, immunoglobulins, adhesion molecules and other subtle changes in the tissue micromilieu with chemokine receptors (CCR), Toll-like receptors (TLR), purinoreceptors, and scavenger/Fc receptors. These interactions result in morphological changes, release of cytokines and trophic factors, migration, and phagocytosis that influence surrounding tissue function and survival. Microglia activation was previously characterized similarly to classical macrophages, subdivided into either pro-inflammatory and neurotoxic (M1) or anti-inflammatory and neuroprotective (M2) based on the expression of a small set of markers[72]. However, with the emergence of single cell RNA sequencing (scRNA-Seq) and similar technologies there is now a greater appreciation for the complexity of microglia activation, which exists as a dynamic spectrum of ever-evolving 'states' unique to the tissue cues generated in a given pathological context[73]. This can be appreciated by the accumulating body of literature describing heterogenous microglial phenotypes that shape the landscape of disease pathogenesis, for better or for worse[74,75,76,77,78,79]. Activated microglia represent the first responders to tissue insults and thus a pivotal biomarker for pathology and therapeutic intervention. In disease, local chemokine signaling and antigen presentation, as well as compromise of the vascular network, results in the recruitment and infiltration of blood-derived monocytes and other immune cell types. Despite the similarity in markers for microglia and these infiltrating cell types, progress has been made in identifying the

differential contributions of infiltrating versus resident myeloid populations to disease pathogenesis[80,81,82]. Furthermore, microglia activation is susceptible to exogenous stimulation and reprogramming *in vitro* and *in vivo*, making this cell type a reputable target for early-disease therapeutic intervention[83,84,85]. Through these recent discoveries, careful study of microglia-specific contributions to early disease pathogenesis and identification of underlying biomarkers will generate unique therapeutic strategies to suppress detrimental activation features while augmenting beneficial features as an avenue of treatment options.

## 1.6 Retinal microglia activation and function in disease

Similar to the brain, retinal microglia subpopulations in the OPL and IPL form non-overlapping mosaic networks of cells that display ramified morphology and highly active processes[86]. Through this constant surveillance, retinal microglia contribute to synaptic maintenance and neurotransmission, elimination of cellular waste and debris, and immunological surveillance of the retinal parenchyma in homeostasis[46,87,88]. Importantly, while these subpopulations serve largely overlapping roles, more recent functional differences have been identified, mainly that microglial maintenance of synaptic health in the IPL is dependent upon Il-34 secretion by inner retinal neurons[20].

As sentinels of the retina, microglia are highly sensitive to an array of cytokines, chemokines, complement components, antibodies, and damage-associated molecular patterns meant to either elicit or inhibit activity[89]. This has led to a growing appreciation for the study of heterogenous microglial phenotypes in the context of retinal diseases, particularly those that directly impact neuronal function and survival[90,20,91]. While disease-associated molecules can impact microglial activation and function, various signaling mechanisms intrinsic to the retina

modulate microglial reactivity in homeostasis (Fig.1.1). Retinal pigment epithelial cells (RPE) release immunomodulatory factors into the outer retinal space such as transforming growth factor-beta (TGF-B), which downregulates expression of antigen presentation proteins and has the potential to reprogram microglia towards an anti-inflammatory phenotype[92,93]. Thrombospondin-1 (TSP-1) and somatostatin (SOM) are also released by RPE cells to inhibit migration of microglia to the subretinal space, a common feature of retinal disease[94]. Muller glia also limit microglial reactivity via release of diazepam binding inhibitor protein (DBI), which binds to microglial translocator protein (TSPO) to suppress activation[95,96]. Microglial activation is also controlled by direct physical interaction with other retinal cells. CD200 is a transmembrane glycoprotein expressed primarily by neurons in the retina which upon binding with its receptor (CD200R) specific to microglia, triggers inhibition of microglial activation, migration, and inflammation via Ras/MAPK pathways[97,98,99]. The importance of this pathway can be appreciated by studies that have observed CD200 deficiency resulting in microglial activation, enhanced pro-inflammatory markers, and more severe experimental autoimmune uveitis (EAU) development in mice[100,101]. Another key neuroimmune regulator is fractalkine (CX3CL1), a neuronal chemokine that is constitutively released from healthy retinal neurons and endothelial cells and binds to its cognate receptor CX3CR1 expressed by microglia[102]. This interaction regulates microglial process motility and migration, neurotoxicity, and overall surveillance[103,104]. Furthermore, disruption of CX3CL1-CX3CR1 signaling increases phagocytic activity of microglia, pro-inflammatory cytokine production, and acceleration of age-related macular degeneration and choroidal neovascularization[105,106]. Lastly, neuronal activity regulated primarily by glutamatergic and GABAergic signaling influences the release of adenosine

triphosphate (ATP), which binds to microglial ATP-gated purinergic P2 receptors (P2R) to influence process behavior and activation[107,108].

Despite only comprising a mere 0.2% of all cells in the retina, microglia are increasingly recognized as key mediators in ocular disease[109]. Laboratory and clinical research on leading blindness diseases such as glaucoma, retinitis pigmentosa (RP), age-related macular degeneration (AMD), and diabetic retinopathy (DR) have identified activated microglia as a prominent feature of disease pathogenesis[110,111,112,106,113]. However, the methods for targeting and suppressing detrimental features of activated microglia in disease are lacking. Depletion of microglia and broad anti-inflammatory treatments remain the most prominent strategies and while both have shown efficacy in preserving retinal neurons, cell ablation in human patients is impractical and current treatments yield highly variable outcomes across different disease models and stages of pathogenesis[114,115,116,20]. This suggests that there remain areas of microglial biology that require deeper investigation to substantially improve the precision and success of current therapies for treating blindness diseases. To this end, increasing efforts to identify dysregulated signaling mechanisms innate to the retinal microenvironment and interrogate microglial heterogeneity in disease will accelerate the development of microglia-based ocular therapeutics.

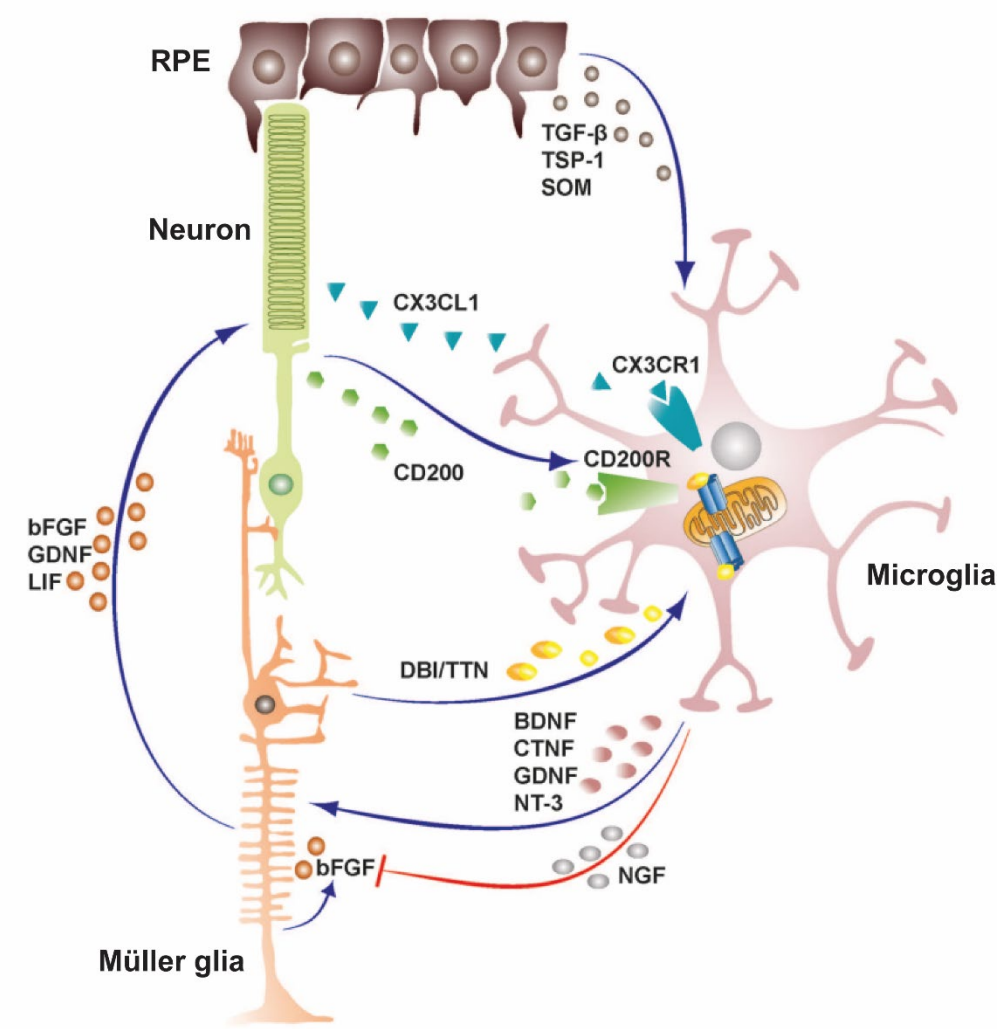


**Figure 1.1: Schematic of neuro-glial mechanisms underlying retinal microglial activation in homeostasis and disease. Figure adapted from**[117]

# 1.7 Diabetic retinopathy: Pathobiology and current outlook

Diabetes mellitus is a chronic disease in which the body's ability to produce or respond to insulin is impaired, resulting in poor conversion of food into energy and elevated levels of glucose in the blood and urine[118]. This dysfunction results from inadequate insulin secretion (type 1) or decreased tissue responses to insulin (type 2). The former category is characterized by autoimmune processes that damage the pancreatic islets or genetic predisposition while the latter,

more prevalent category, is characterized by a progressive resistance to insulin and an absent compensatory insulin secretory response. For both categories, excess glucose can accumulate in the blood, leading to hyperglycemia that varies in severity and duration depending on symptom onset and progression. Nearly half a billion people are living with diabetes worldwide and projections suggest that prevalence will increase by 25% in 2030 and 50% in 2045[119]. With increased numbers of individuals with diabetes comes higher incidence of diabetes-specific complications. Macrovascular complications of diabetes include coronary heart disease, peripheral vascular disease, and stroke while microvascular complications include end-stage renal disease (ESRD), neuropathy, and retinopathy[120].

Diabetic retinopathy (DR) is the primary cause of visual impairment in adults globally[121]. Affecting 1 in 3 individuals with diabetes, DR is a gradual neurovascular complication of prolonged hyperglycemic stress on the eye. This excess glucose leads to oxidative stress and increased levels of glycolytic metabolites in virtually all retinal cell types, which increases flux through the polyol and hexosamine biochemical pathways, advanced glycation end (AGE) product formation, and protein kinase-C (PKC) activation[122,123]. Over time, these harmful metabolic imbalances lead to neuronal dysfunction and apoptosis, gliosis and inflammation, and microvascular complications. Diagnosis and treatment of DR primarily focuses on microvascular changes as they can be identified through clinical examination and targeted with current therapeutics[122]. DR is subdivided into a non-proliferative (NPDR) stage characterized by vascular tortuosity, retinal hemorrhages, and lipid exudates, and a proliferative stage (PDR), characterized by the aberrant growth of new and fragile vessels[124]. Diabetic macular edema (DME), or the accumulation of fluid into the neural retinal, can also occur and lead to abnormal thickening of the retina. Despite the close attention paid to these stages of vascular abnormalities,

laboratory and clinical evidence demonstrate that retinal inflammation and neuronal alterations precede vasculopathy and contribute to neurodegeneration and vision loss during early stages of DR[125,126,127,128]. Unlike diabetic retinal vasculopathy, neuronal changes in early disease cannot be visualized through fundoscopic examination. Furthermore, currently approved therapeutic strategies for treating advanced DR only target vascular complications, require frequent pharmacologic and laser treatment, and do not reverse retinopathy in the long term[129,130,131,132]. Given the immense impact of DR on global health and inability of current treatment strategies to restore retinal structure and function, there remains a significant knowledge gap in our understanding of the cellular mechanisms underlying early DR pathogenesis and with that, appropriate treatment methods.

Microglia activation and neuroinflammation are prominent features of early-stage DR in patients and animal models, suggesting that microglia may play an early role in disease pathogenesis[113,133,134,135]. Given the simultaneous evidence of pro-inflammatory mediators in the ocular tissues and serum of DR patients, the current view is that microglia contribute to inflammation and neuroretinal decline in DR[136]. However, the bulk of laboratory and clinical research is conducted during established stages of DR when macroglial activation, blood-retina barrier (BRB) breakdown, and peripheral immune cell invasion have been observed[124,137,122]. This has led to the possibility that early-stage DR may provide an investigative window to properly interrogate the early response of microglia to hyperglycemic stress and acute retinal changes prior to compromise of the ocular immune environment[138]. Furthermore, discovery of novel mechanisms underlying microglial involvement in early-stage DR may generate immunotherapeutic treatment strategies to preserve retinal structure and function and prevent more robust features of retinopathy in later stages of disease. Within this conceptual framework,

we have conducted an extensive investigation of microglial phenotypes during early-stage DR, mechanisms underlying their contributions to disease, and preliminary demonstrations of a novel therapy for treating microglia-mediated retinopathy in a diabetes mouse model. We have presented and discussed these findings in the following chapters. Furthermore, we have added an additional chapter that discusses the implications and future directions of this work with regards to microglia-specific immunotherapy as a leading strategy for treating DR in patients.

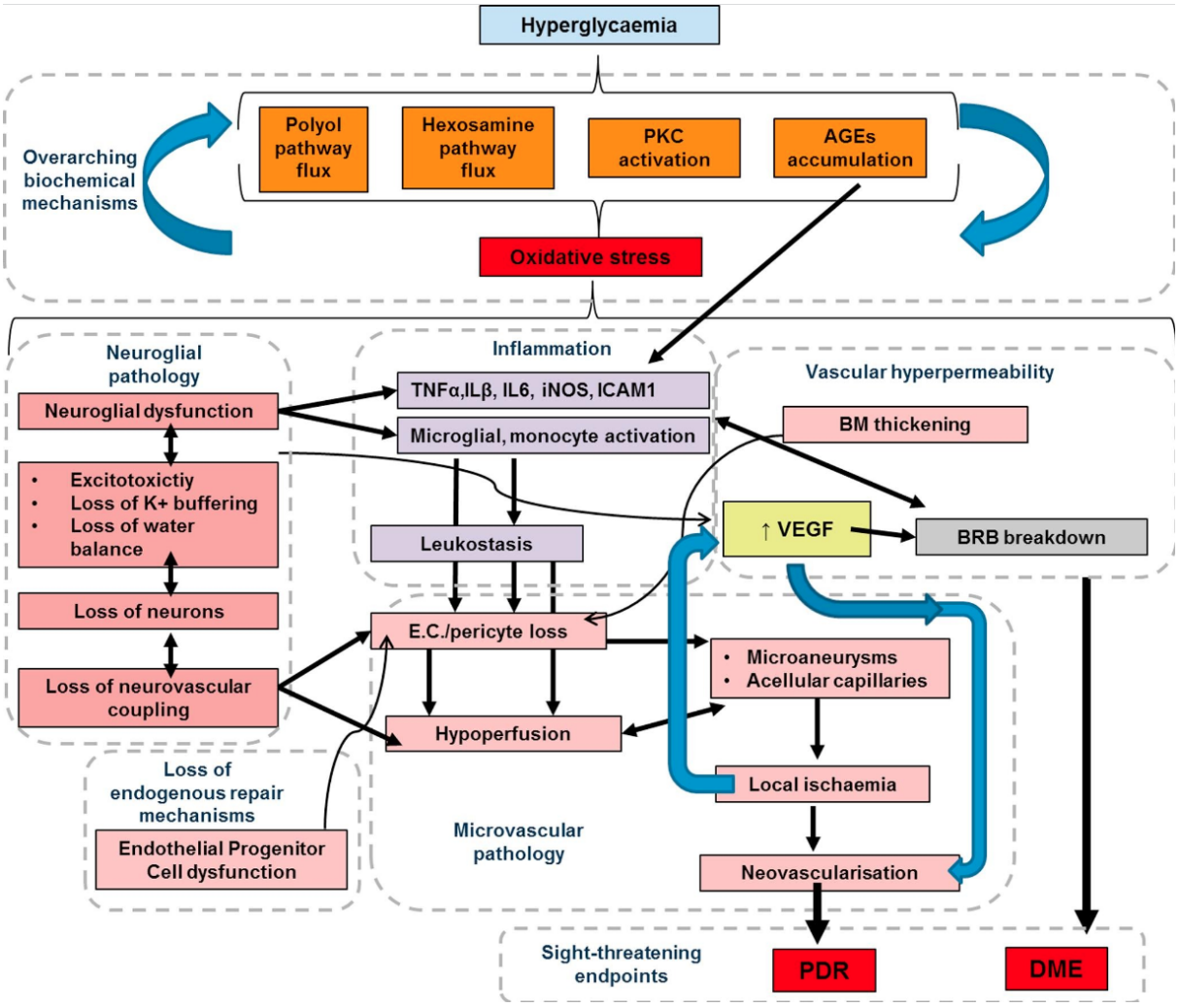


**Figure 1.2: Schematic overview of diabetic retinopathy pathobiology. Figure from**[139]

# Chapter 2: Features of the retinal neurovascular unit in homeostasis and early diabetes

*Adapted from unpublished data and manuscript in revision:*

Pfeifer, C.W., Walsh, J.T., Santeford, A., Lin, J.B., Beatty W.L., Terao, R., Liu, Y.A., Hase, K., Ruzycki, P.A., Apte, R.S. (2023). Dysregulated CD200-CD200R signaling in early diabetes modulates microglia-mediated retinopathy. Proc. Natl. Acad. Sci. U.S.A. (*revision submitted 8/10/23)*

# 2.1 Introduction

Clinical and laboratory research has traditionally focused on vascular dysfunction during DR but diabetic microvasculopathy does not explain associated peripheral nerve damage, cognitive impairment, or loss of vision. As a result, studies have shifted focus onto neurodegenerative and inflammatory features of DR, particularly due to their emergence prior to observable microvascular complications[125,140,141,142]. While genetic determinants of susceptibility and accelerating factors such as hypertension contribute to diabetes-associated tissue damage, hyperglycemia is believed to be the main determinant of comorbidities such as DR[143]. Exposure of diverse neuronal cell types in the retina to hyperglycemia, and their differential susceptibility to damage, has led to the discovery of dysfunctional intracellular glucose control mechanisms such as the polyol pathway, hexosamine pathway, and advanced glycation end product (AGE) formation as contributors to oxidative stress, dysfunction, and apoptosis[144,123]. However, simultaneous disturbance of neurovascular unit elements such as vascular endothelial cells and glial cells, and the invasion of peripheral immune cells, contribute to retinal inflammation that may modulate the progression of early DR[124,145]. The role of inflammation in DR has been extensively studied but the diverse landscape of contributing cell types and their involvement within the broad course of disease has made it difficult to characterize cell-specific contributions to DR pathogenesis and develop effective therapies[138]. This is reflected in the limited effectiveness of current immunosuppressive and anti-inflammatory treatments for DR.

Microglia are the resident immune cells of the retina. Morphological features of microglia activation have been reported during early stages of DR in patients and animal models[134,113,135]. Elevated levels of inflammatory cytokines and chemokines have been detected in ocular tissues from patients with non-proliferative DR, suggesting that activated microglia

may be directly contributing to local inflammation in the retina[146,147]. However, recruitment of peripheral immune cells to the retinal parenchyma has been reported during established stages of DR in rodent models, complicating efforts to distinguish contributions of resident vs. peripheral immune cells to DR-associated inflammation[148]. Vascular changes such as enhanced permeability permit the invasion of peripheral immune cells and have been observed during DR, but the precise emergence of blood-retina-barrier (BRB) compromise during early stages of disease remains unclear[149,150,151]. Lastly, activation of macroglia such as astrocytes and muller glia is reported during similar stages of disease but whether they precede and elicit microglia activation is unresolved[145]. Until the temporal progression of these contributing features is elucidated, treatments for early DR-associated neuroinflammation will continue to be imprecise and provide limited effectiveness.

Studying elements of the retinal neurovascular unit in the context of early-stage DR may provide the opportunity to interrogate the innate response of resident microglia prior to the emergence of later-stage disease elements. Furthermore, the plasticity of microglia makes this cell type a promising therapeutic target for early-DR intervention strategies that may preserve retinal neurons and vision as well as prevent later-stage pathology[83,84,85]. Here we show that microglia emerge as a solely activated component of the retina during early stages of streptozotocin-induced (STZ) DR in the absence of alterations to other features of the retinal neurovascular unit. This dynamic activation includes morphological, ultrastructural, and transcriptional features that not only identifies microglia as a uniquely affected cell type in the diabetic retina but also underscores their potential functional contributions to early disease phenotypes.

## 2.2 Materials and Methods

**Animals.** All animal use and experiments were approved by the Institutional Animal Care and Use Committee (IACUC) of Washington University in Saint Louis and performed according to the Washington University Animal Care and Use Guidelines. A Cx3cr1$^{GFP/GFP}$ mouse (stock no. 005582) was obtained from Jackson Laboratory (Bar Harbor, ME) and was backcrossed with C57BL/6J (stock no. 000664) mice for 10 generations prior to use (Cx3cr1$^{GFP/+}$) in experiments[152]. Genotyping of the resulting N10 generation was also performed to confirm the absence of the confounding rd8 mutation in the *Crumbs1* gene[153]. Hyperglycemia was induced in male mice via intraperitoneal delivery of a single streptozotocin injection (150mg/kg bodyweight) in sodium citrate buffer (pH 4.5; 15mg/mL buffer), while control animals received an equivalent volume of buffer. On post-injection day 7, fasting blood glucose levels of all mice were measured from the tail vein with a One Touch Basic blood glucose monitoring system. Mice that displayed hyperglycemic blood glucose levels (>250mg/dL) and exceeded this threshold for the duration of the study were considered diabetic and used for experiments. Mice were also weighed weekly to monitor weight loss. Due to the insensitivity of female mice to streptozotocin, only male mice were used for these studies[154].

**Flow cytometry.** Mice were anesthetized with a cocktail of ketamine (86.9mg/kg) and xylazine (10mg/kg), then cardiac-perfused with ice cold phosphate buffered saline (PBS) with heparin (3U/mL) prior to surgical dissection of eyes into ice-cold PBS with 10% fetal bovine serum (FBS) to isolate the retina from the retinal pigment epithelium-choroid complex. Retinas were then were digested for 25 minutes at 37ºC with constant agitation using 1 mL of pre-warmed digestion buffer (DMEM, 2% FBS, 1 mg/mL collagenase VIII (Sigma Aldrich), and 0.5 mg/mL

DNase I), and filtered through a 70µm cell strainer. Enzymes were then neutralized with 1 mL of FACS buffer (DMEM with 10% FBS). An additional 2 mL of FACS buffer was added, samples were centrifuged at 350 x g for five minutes, and samples were resuspended in FACS buffer with anti-CD16/32 (Biolegend, 101302) diluted 1:50 in FACS buffer and fluorescently conjugated antibodies added for 20 minutes at 4ºC. Samples were washed in FACS buffer and resuspended in FACS buffer with 133 ng/mL DAPI before running on a Cytek Aurora spectral flow cytometer (Cytek) and analyzed using FlowJo software (Tree Star). In addition to endogenous EGFP (*Cx3cr1*$^{GFP/+}$) the following antibodies were used: rat anti-mouse/human CD45R/B220-Alexa Fluor 700 (Biolegend, 103231), rat anti-mouse/human CD11b-APC/Cyanine7 (Biolegend, 101225), Armenian hamster anti-mouse CD11c-PE/Cyanine7 (Biolegend, 117317), Armenian hamster anti-mouse TCR(B)-APC (Biolegend, 109211), rat anti-mouse CD45-PE (Biolegend, 103105), rat anti-mouse Ly6G-Alexa Fluor 647 (Biolegend, 127609), mouse anti-mouse NK1.1-BUV 395 (BD Biosciences, 564144), rat anti-mouse MHCII-BV421 (BD Biosciences, 562564), and DAPI (Thermo, 62248).

**Retina dissociation.** Retinas were isolated as previously described. Retinas of both eyes were pooled for each animal before undergoing papain-based enzymatic digestion (Worthington Biochemical) with 0.5 mg/mL DNase I (Sigma Aldrich) for 40 minutes in a water bath at 28ºC. Samples were then moved to a separate water bath at 8ºC for 8 minutes. Digested material was then homogenized by gentle trituration with a pipette before being spun down by centrifugation at 300 x g for 5 minutes at 4ºC. Supernatant was then discarded and the sample resuspended with FACS buffer (PBS, 1% FBS, 1mM EDTA) containing ovomucoid inhibitor.

**Fluorescence-activated cell sorting (FACS).** FACS was carried out with a Beckman Coulter MoFlo cytometer at the Siteman Cancer Center Flow Cytometry core (Washington University St. Louis) equipped with a 120μm nozzle and 350nm (UV)/530nm (green) excitation lasers to isolate GFP-positive, DAPI-negative (viable) microglia. Fluorescence-minus-one controls were used for gating analyses to distinguish positively and negatively stained cell populations. Cells were sorted directly into RLT lysis buffer (Qiagen) and snap-frozen for storage (-80ºC) and future use.

**Immunohistochemistry.** Mice were euthanized and eyeballs were enucleated and fixed in 10% formalin overnight at 4ºC. For retinal flat mounts, retinas were dissected gently from fixed eyecups and remaining choroid and vitreous were removed. Retinas were submerged in blocking solution (PBS, 5% BSA, 0.3% Triton X-100) overnight at 4ºC. Primary antibody incubation was carried out overnight at 4ºC followed by washing and secondary incubation at 4ºC. Four radial incisions were made to flatten the retinas on glass slides before mounting (VECTASHIELD, Vector Laboratories). For frozen sections, the cornea and lens were removed from fixed eyeballs and remaining eyecups were submerged in successive rehydration solutions of 15% and 30% sucrose (PBS). Eyecups were then submerged in OCT solution, snap-frozen, and sectioned at 20μm. Sections were then rinsed with PBS and submerged in blocking solution (3% BSA, 0.1% Triton X-100) at room temperature for 1 hour in a humidified chamber. Primary antibody incubation was carried out overnight at 4ºC followed by washing and secondary antibody incubation at room temperature for 1 hour with inclusion of nuclear staining with DAPI. Sections were then washed and mounted. The following antibodies were used: Dylight-594 labeled tomato lectin (Vector Laboratories, DL-1177-1), anti-GFAP (Invitrogen, 13-0300), anti-GS (Sigma-Aldrich, G2781).

**Morphological analysis.** For microglia morphology analysis, CX3CR1-positive microglia in the OPL and IPL layers of the retina were visualized using confocal laser scanning microscopy (Zeiss LSM 800, 20x) and 20µm Z-stacks (0.5µm slices). Images were taken at 50% eccentricity in relation to the optic nerve and in proximity to vascular elements of similar order. Microglia completely captured within images were reconstructed using the semi-automated, interactive FilamentTracer tool in Imaris 9.9 software (Oxford Instruments). Following the automatic tracing of microglial cells, manual editing was performed to delete erroneous process segments. Quantification of cell area, volume, process length, and branching points were then automatically generated for all reconstructed microglia captured entirely within Z-stack images.

**Transmission electron microscopy.** Whole mouse eyes were fixed in 2% paraformaldehyde/2.5% glutaraldehyde (Ted Pella Inc., Redding, CA) in 100 mM sodium cacodylate buffer for 1 hour at room temperature and then overnight at 4°C. Samples were then washed in sodium cacodylate buffer and postfixed in 2% osmium tetroxide (Ted Pella Inc.) for 1 hour at room temperature. After three washes in $dH_2O$, samples were en bloc stained in 1% aqueous uranyl acetate (Electron Microscopy Sciences, Hatfield, PA) for 1 hour. Samples were then rinsed in $dH_2O$, dehydrated in a graded series of ethanol, and embedded in Eponate 12 resin (Ted Pella Inc). Vertical and lateral sections of 95 nm were cut with a Leica Ultracut UCT ultramicrotome (Leica Microsystems Inc., Bannockburn, IL), and stained with uranyl acetate and lead citrate. Sections were viewed on a JEOL 1200 EX transmission electron microscope (JEOL USA Inc., Peabody, MA) equipped with an AMT 8 megapixel digital camera and AMT Image Capture Engine V602 software (Advanced Microscopy Techniques, Woburn, MA).

**Fundus imaging and fluorescein angiography.** Digital color fundus and angiography photography was performed using the Micron IV retinal imaging system (Phoenix Research Laboratories). Prior to fundus imaging, mice were anesthetized with ketamine/xylazine and administered 1.0% atropine sulfate to dilate pupils. For angiography, fluorescein (AK-Fluor, 10mg/mL) was injected intraperitoneally and images were taken once peak vessel fluorescence was reached.

**Quantitative RT-PCR.** For mRNA expression analysis, samples were isolated from flow-sorted microglia using the RNeasy Plus Micro Kit (Qiagen) as per manufacturer's instructions. We prepared cDNA with 1-2ng total RNA per sample using the High Capacity Reverse Transcription kit (Thermo Fisher Scientific). We then amplified cDNA using the TaqMan PreAmp Master Mix (Thermo Fisher Scientific) with pooled gene expression probes. We then performed qPCR using TaqMan Fast Advanced Master Mix (Thermo Fisher Scientific) with n=2 technical replicates per sample. We used the ΔΔCt methods and normalized to the geometric mean of *Actb, Gapdh,* and *Hprt* housekeeping genes. The following TaqMan Gene Expression probes were utilized: *Actb* (Mm00607939_s1), *Gapdh* (Mm99999915_g1), *Hprt* (Mm00446968_m1), *Ccl3* (Mm00441259_g1), *Tnf* (Mm00443258_m1), *Lpl* (Mm00434764_m1), *Cyp4f18* (Mm07298284_m1), *Il1b* (Mm00434228_m1), *Apoc1* (Mm00431816_m1), *Alox5* (Mm01182747_m1), *Fxyd5* (Mm00435435_m1), *Ctse* (Mm00456010_m1), *Gale* (Mm00617772_g1), *Tlr2* (Mm00442346_m1).

**Bulk RNA-Sequencing.** Total RNA was isolated from flow-sorted microglia using the RNeasy Plus Micro Kit (Qiagen). RNA quantity and integrity was determined using a 2100 Bioanalyzer and RNA Pico kit (Agilent Technologies). All samples (n = 10) contained 2.0 – 4.0ng RNA and

had RIN > 8.0. Library preparation was performed by the Genome Technology Access Center (GTAC) through the McDonnell Genome Institute (MGI) with 1-2ng of total RNA per sample. Ds-cDNA was prepared using the SMARTer Ultra Low RNA kit for Illumina Sequencing (Takara-Clontech). Fragments were sequenced on an Illumina NovaSeq-6000 using paired end reads extending 150 bases. Basecalls and demultiplexing were performed with Illumina's bcl2fastq software with a maximum of one mismatch in the indexing read. RNA-Seq reads were then aligned to the Ensembl release 101 primary assembly with STAR version 2.7.9a1. Gene counts were derived from the number of uniquely aligned unambiguous reads by Subread:featureCount version 2.0.32. Raw gene counts were then filtered based on a ≥1 CPM threshold for (n-1) samples in a given condition. Next, a standard EdgeR-limma analysis of gene-level features was performed, defining significant up- or downregulated genes as a |fold-change| > 1.50 with a FDR < 0.05. All further analysis and figures were generated in R (R Core Team).

# 2.3 Results

## 2.3.1 Microglia dominate retinal immune cell composition during homeostasis and early-stage DR

Altered morphologies and laminar organization of microglia have been previously observed during early stages of DR in the retinas of diabetic patients and animals models but the features of DR that trigger this phenotype are unclear. STZ-induced early-stage DR has been shown to promote retinal transcriptome changes reflective of neurovascular degeneration and inflammation[155]. Thus, we first assessed whether or not perturbed elements of the retinal neurovascular unit and infiltrating immune cells may indirectly promote morphological activation of resident microglia. To test this, we first longitudinally evaluated retinal immune cell

composition in STZ-treated *Cx3cr1*$^{GFP/+}$ mice during the canonical early-stage of DR in the STZ model (onset – 8 weeks) (Fig.2.1; Fig.2.2A). In line with previous studies using this model, STZ-injected animals displayed hyperglycemic blood glucose levels within one week of treatment and static weight trends compared to normoglycemic vehicle-injected animals that persisted for the duration of the study (Fig.2.2B)[156].

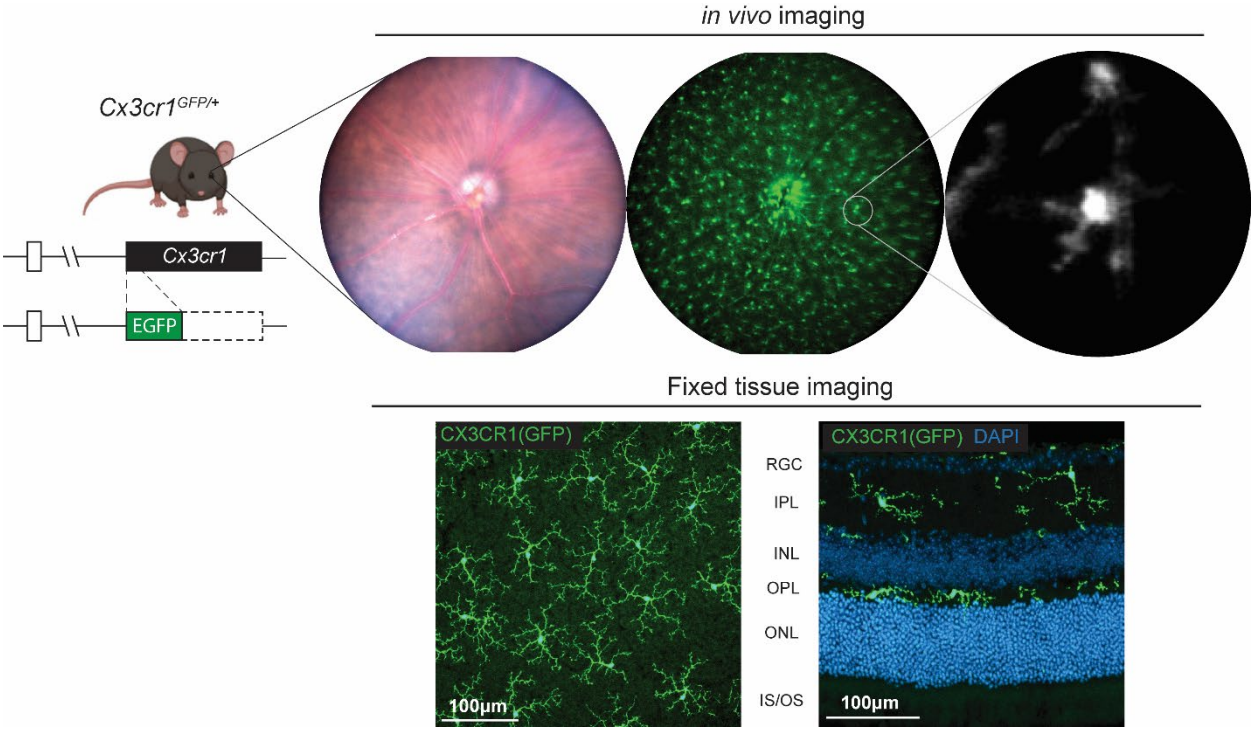


**Figure 2.1. Endogenous labeling and visualization of retinal microglia with fluorescent reporter mouse.** Genetic construct of *Cx3cr1*$^{GFP/+}$ mouse (left) used to visualize microglia *in vivo* using fundus and two-photon imaging (right, top) and in fixed retinal tissue using confocal microscopy (right, bottom).

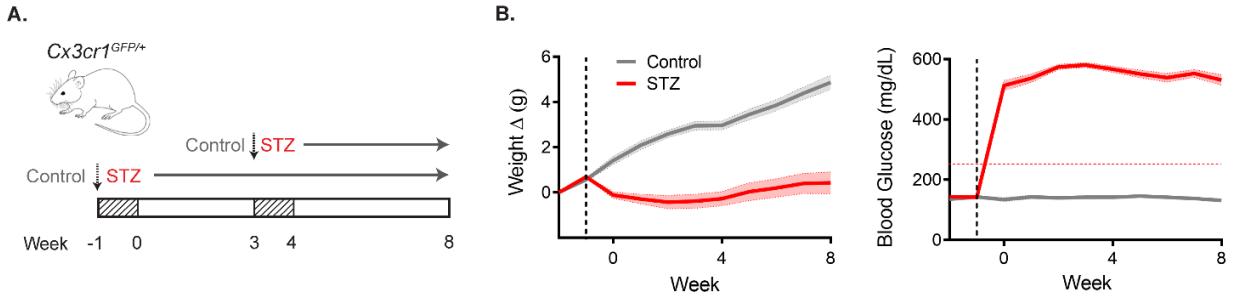

**Figure 2.2. Single-dose streptozotocin induces chronic hyperglycemia in mice.** (A) Schematic depicting injection schedule for 4 week- and 8 week-STZ and control *Cx3cr1*$^{GFP/+}$ mouse groups. (B) Line graphs showing weight change (left) and blood glucose measurements (right) in STZ- and vehicle-injected mice. Each line (Control, n=21; STZ, n=47) indicates the mean ± SEM calculated for animals used in the study. Black vertical dashed line indicates time of injection and red horizontal dashed line indicates hyperglycemic threshold (250mg/dL).

To characterize the immune cell profile of the retina we applied a comprehensive antibody panel to retinal single cell suspensions generated from diabetic (4wk STZ, 8wk STZ) and control animals for flow cytometry (Fig.2.3A). Overall immune cell counts (CD45$^{+}$) were not altered during the course of hyperglycemia (Fig.2.3B). Control retina suspensions revealed that microglia (CD45$^{lo}$, CD11b$^{+}$, CX3CR1$^{+}$) made up the vast majority (>90%) of the immune cell fraction, with minor fractions of dendritic cells (DC; CD45$^{hi}$, CD11c$^{+}$, CD11b$^{-}$) natural killer cells (NK; CD45$^{hi}$, NK1.1$^{+}$), neutrophils (NΦ; CD45$^{hi}$, Ly6G$^{+}$), T cells (CD45$^{hi}$, TCRβ$^{+}$), B cells (CD45$^{hi}$, B220$^{+}$), monocyte-derived macrophages (Mo-Mφ; CD45$^{lo}$, CD11b$^{+}$, CD11c$^{+}$, CX3CR1$^{+}$), and border-associated macrophages (BAM; CD45$^{lo}$, CD11b$^{+}$, CX3CR1$^{+}$, MHCII$^{+}$) (Fig.2.3C). Analysis of these immune cell fractions showed no significant changes in immune cell-specific proportions during early DR. These data indicate that microglia dominate retinal immune cell composition during homeostasis and early-stage DR without significant infiltration by peripheral immune cells.

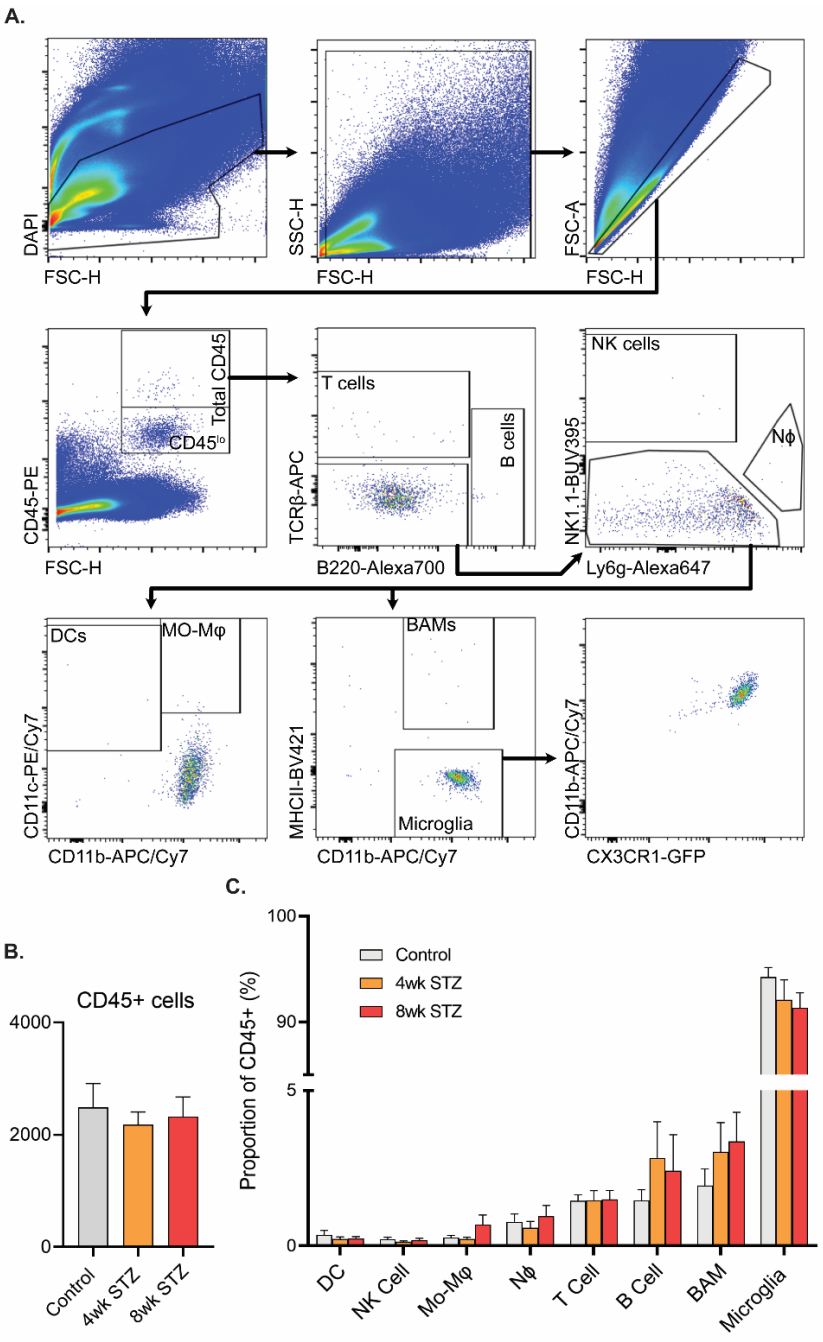


**Figure 2.3. Local immune composition of the retina is dominated by microglia in homeostasis and early diabetes.** (A) Flow cytometry gating strategy for exclusion of dead cells, non-cellular events, and doublets (top panel), and capture of CD45+ immune cell fractions (middle, bottom panels) within mouse retina cell suspensions. (B) Bar graphs showing raw CD45+ cell counts (left) and CD45+ immune cell fractions (right) for STZ and control mouse retinal single cell suspensions. Each bar (n=7 mice per group) indicates the mean ± SEM cell count or proportion of CD45+ cells. Statistical significance among groups for each cell type was determined using the Kruskal-Wallis test.

### 2.3.2 Blood-retina-barrier and macroglia are unperturbed during early DR

Blood-retina-barrier (BRB) changes such as enhanced vascular permeability, endothelial cell and pericyte dropout, and macroglial reactivity have been observed during established stages of DR in rodent models and may contribute to inflammation, microglia activation, and disease progression. However, the precise emergence of these features within the time course of DR progression and whether they impact microglia reactivity remains unclear. To evaluate potential changes to the vascular network in the retina, we first performed *in vivo* fundus imaging and fluorescein angiography but did not find evidence of primary vessel attenuation or vascular leakage among control or diabetic mouse groups (Fig.2.4A). We next examined the structure of lower-order vessels contained within the intermediate and deep capillary plexus of the retina using lectin immunostaining but did not find any changes in broad vascular structure or acellular capillaries (Fig.2.4B). Next, we used immunostaining to survey macroglial reactivity or loss. Astrocyte density and coverage of primary arteriole vessels, as well as Müller glia density and reactivity as measured by glial fibrillary acid protein (GFAP), were unchanged across all tested mouse groups (Fig.2.5A). These data suggest that, similar to immune composition, vascular and macroglial alterations do not emerge during early-stage DR in the STZ mouse.

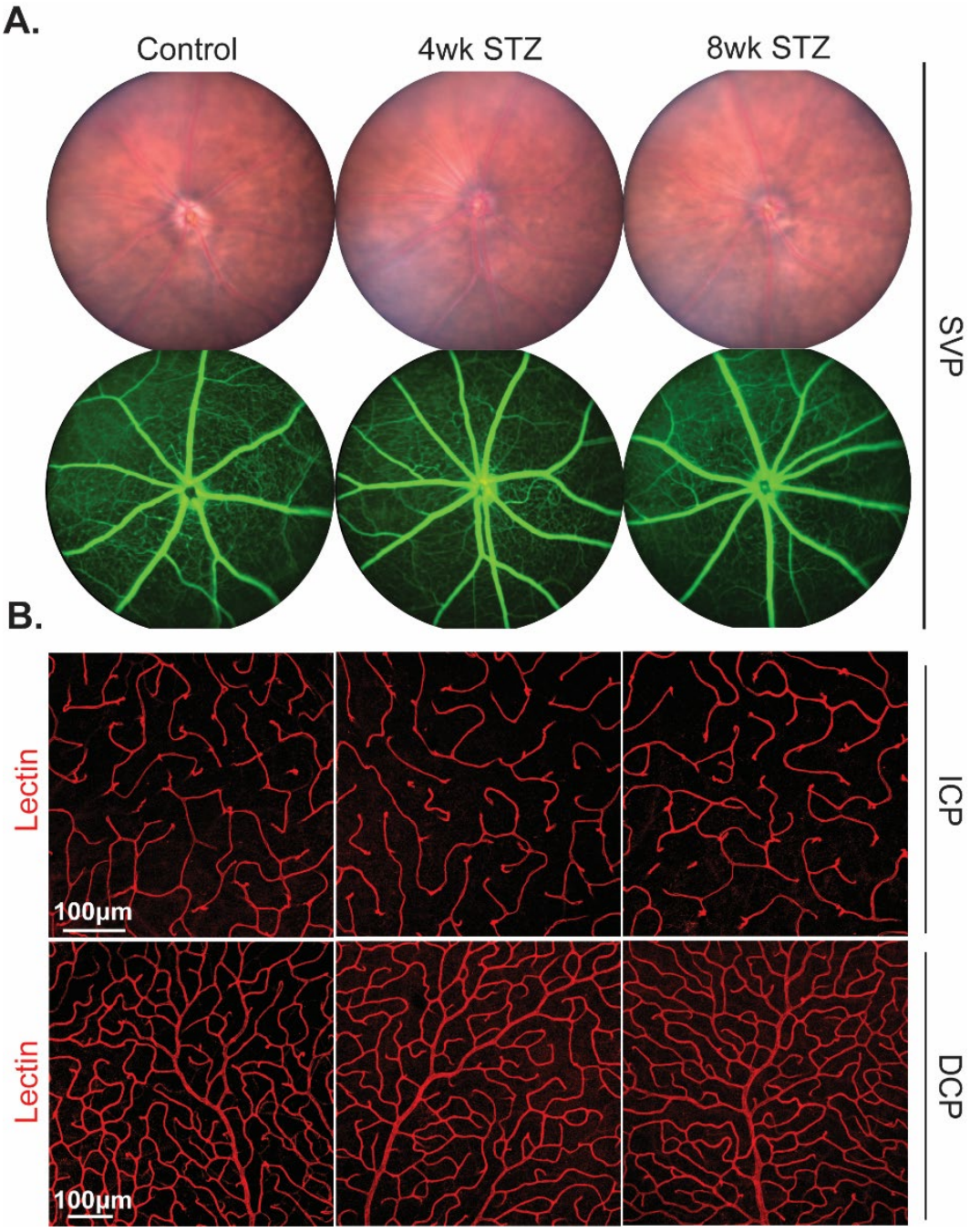


**Figure 2.4. Blood-retina-barrier permeability, structure, and organization is unchanged in early diabetes.** (A) Representative images of STZ and control mouse eyes and superficial vascular plexus (SVP) using the Phoenix Micron IV retinal imaging microscope equipped with bright field (top panel) and angiography (bottom panel) modalities. Images were acquired in anesthetized mice before (top panel) and after (bottom panel) sodium fluorescein injection. (D) Representative confocal images of intermediate (ICP, top panel) and deep capillary plexus (DCP, bottom panel) layers. These images are of immunostained flat-mounted retinas and are maximum projections of the lamina shown.

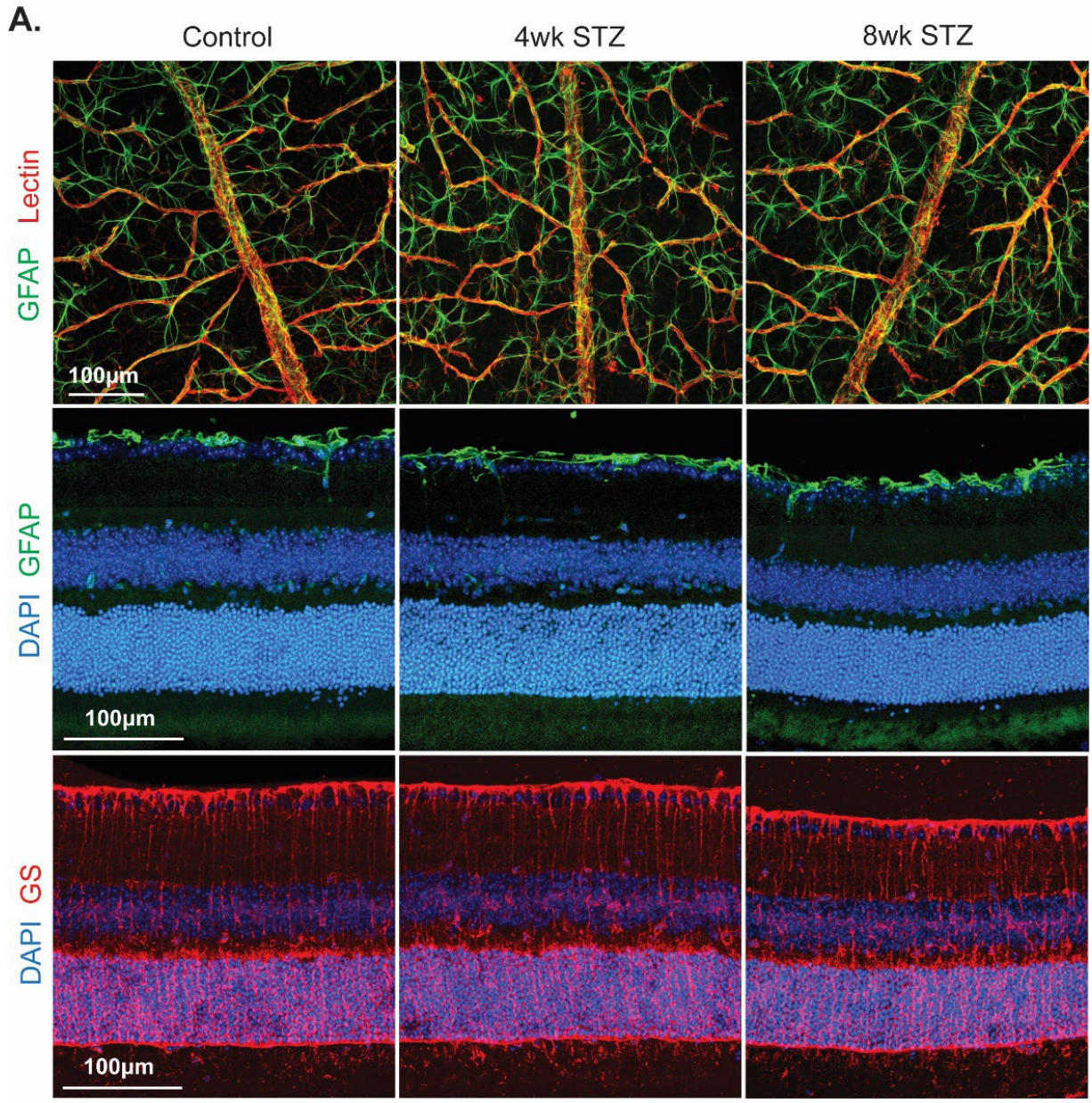


**Figure 2.5. Astrocyte and Muller glia density and reactivity is unchanged in early diabetes.** (E) Representative confocal images of astrocyte density and end-feet coverage of SVP vessels (top panel), GFAP reactivity (middle panel), and Müller glia density (bottom panel). These images are of immunostained flat-mounted (top panel) and cryo-sectioned (middle, bottom panels) retinas and are maximum projections of the vascular lamina and retina section shown, respectively.

### 2.3.3 DR-associated microglia exhibit changes in morphology and temporo-spatial distribution

We next wanted to assess potential temporal changes in microglia morphology and localization in our STZ model to investigate if morphological features of microglia activation occur without alterations to other neurovascular unit elements. Given the differential functions attributed to anatomically distinct pools of outer plexiform (OPL) and inner plexiform (IPL) microglia, we also wanted to evaluate potentially divergent properties of these niches in DR[20]. We found that microglia in both plexiform niches displayed significantly reduced cell area and volume, combined process length, and branching as early as 4 weeks after onset of STZ-induced hyperglycemia compared to controls (Fig.2.6A-D). Since flow cytometry analysis revealed no change in retinal microglia counts during early-stage DR, we hypothesized that the apparent loss in microglia density in the plexiform layers could be explained by changes in temporo-spatial distribution within the retinal laminae. Indeed, retinal cross sections revealed that microglia soma density was significantly reduced in the OPL and increased in the inner nuclear (INL) and ganglion cell layers (GCL) of the inner retina during early stages of DR compared to controls (Fig.2.6E-F). Microglia somas contained within inner retina neuronal layers also exhibited a cross-laminar orientation compared to the typical uniplanar morphology, suggesting migratory behavior. These data suggest that microglia are highly responsive to hyperglycemia within 4 weeks of exposure, and redistribute within retinal laminae with an affinity for neuronal layers of the retina. Given that the inner retina is susceptible to dysfunction and neurodegeneration during early phases of DR, this may also highlight a microglial response to neuro-synaptic dysfunction.

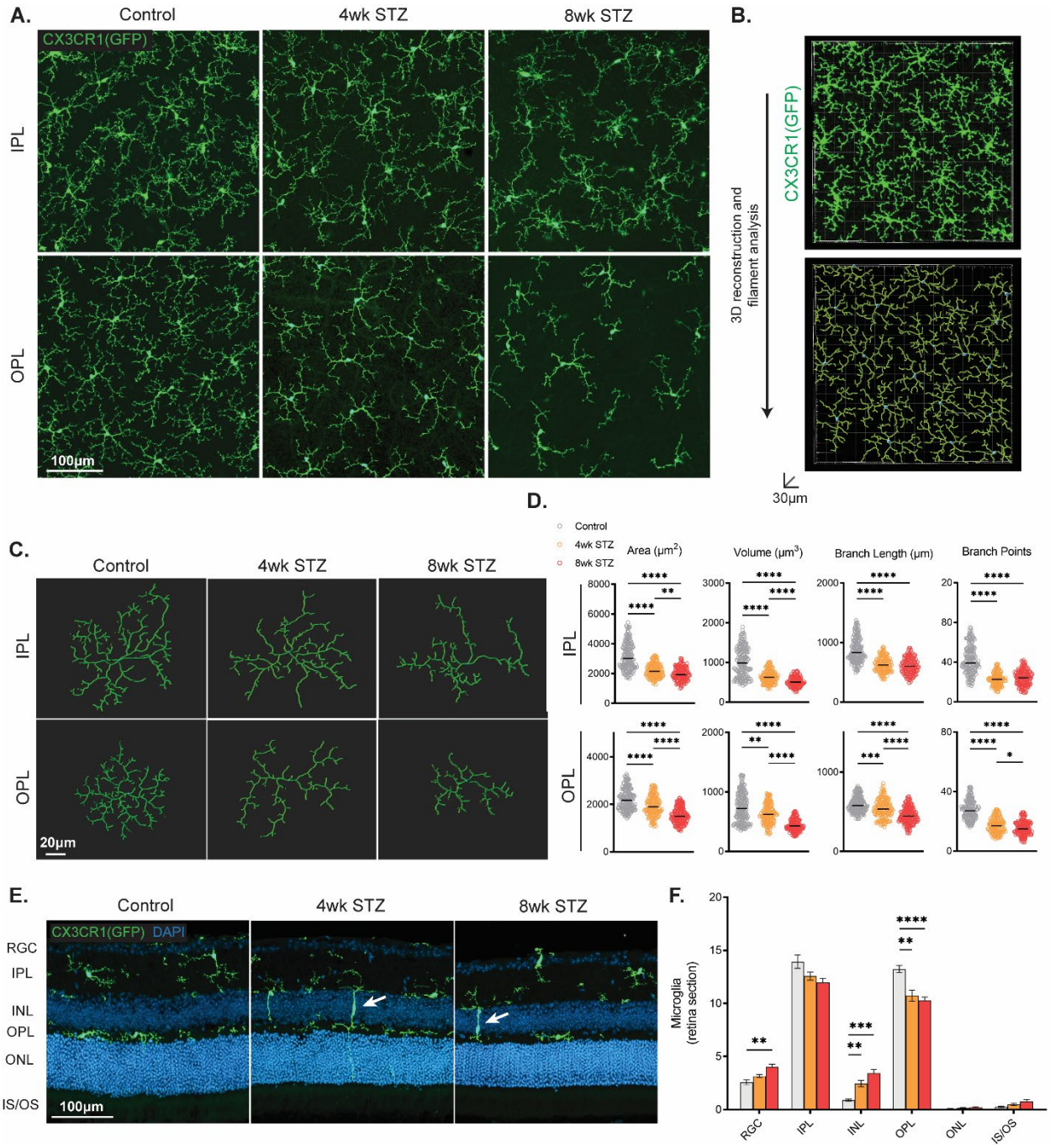


**Figure 2.6. DR-associated microglia exhibit changes in morphology and temporo-spatial distribution.** (A) Representative confocal images showing microglia morphology and organization in the IPL and OPL of control and STZ mouse retinas. These images are of flat-mounted retinas and are maximum projections of the retinal layers shown. (B) Representative 3D reconstruction of confocal Z-stack image taken of retinal OPL microglia (top) and filament traces of individual microglia (bottom) generated using Imaris software. (C) Representative filament traces of individual OPL and IPL microglia in retinas of control and STZ mice. (D) Dot plots showing filament area, volume, cumulative branch length, and branch points of

reconstructed microglia in control and STZ retinas. Each plot (OPL, n=146-201 cells per group; IPL, n=141-181 cells per group) indicates the median with each dot representing one microglia cell. Cell reconstructions and quantification are derived from four retinal Z-stack images per layer (n=5 mice per group). Statistical significance among groups for the IPL and OPL was determined using the Kruskal-Wallis test followed by Dunn's post hoc test for multiple comparisons. (E) Representative confocal images and bar graph (F) showing microglia soma counts in individual layers of control and STZ retinas. These images are of cryo-sectioned retinas and are maximum projections of the retina section shown. White arrows point to microglia in trans-laminal orientation. Each bar (n=8-10 mice per group) indicates the mean ± SEM of microglia soma counts per retina section. Each mouse count is an average of counts from three to four retina sections. Statistical significance among groups for each retina layer was determined using Brown-Forsythe and Welch's ANOVA tests followed by Dunnett's T3 post hoc test for multiple comparisons (*P<.05; **P<.01; ***P<.001; ****P<.0001).

### 2.3.4 DR-associated microglia undergo ultrastructural remodeling

During CNS disease, chronic stress, and aging, microglia adopt unique ultrastructural features that correlate with their activation and function[157]. We hypothesized that the morphological characteristics of activation we uncovered may indicate other changes at the ultrastructural level. To explore this, we prepared horizontal and vertical sections of control and 8 week-STZ retinas for transmission electron microscopy (TEM). Interestingly, we found a subtype of microglia that exhibited darkened cytoplasm, chromatin remodeling, and irregular shape in the inner retina (IPL/INL) of STZ retinas that was not observed in control retinas (Fig.2.7A). We also frequently observed these DR-associated microglia (*dmg)* at the junction of the INL and IPL with electron-dense processes leading into the inner retina neuropil (Fig.2.7B). In horizontal retina sections, we found that these electron-dense cells and processes were observed at a significantly higher frequency in STZ retinas compared to control retinas (Fig.2.7C). Furthermore, the neuropil of the IPL in the STZ retinas appeared more disorganized than that of control retinas, potentially indicating neuro-synaptic degeneration. Upon further examination of DR-associated microglial ultrastructure, we also observed irregularities in mitochondria shape and cristae number compared to those of control microglia, indicating

potential oxidative stress (Fig.2.7D). These findings provide evidence of a previously reported microglial ultrastructural phenotype in the diabetic mouse retina. Additionally, the ultrastructural evidence of irregular mitochondria and chromatin remodeling suggests that microglia undergo oxidative stress and transcriptional changes that may impact broader features of DR progression.

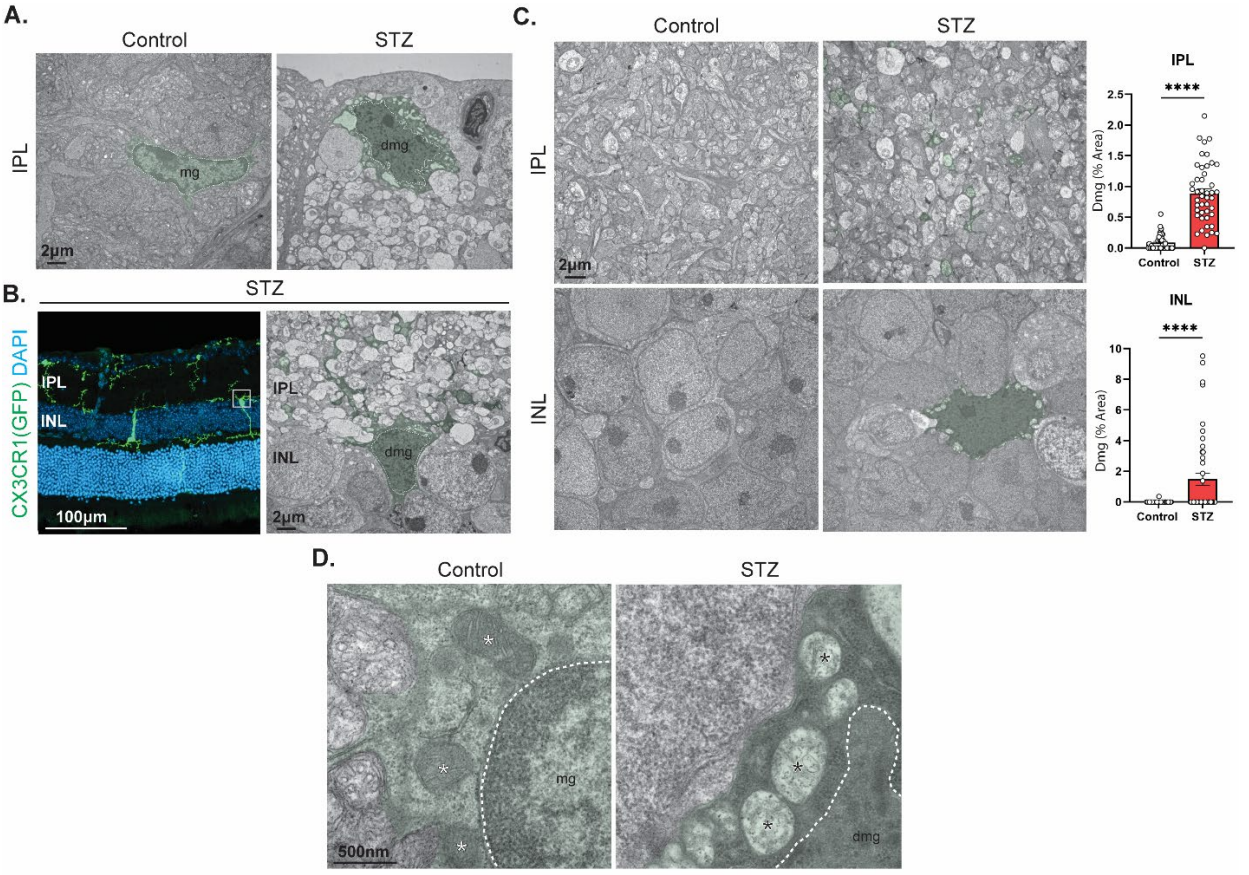


**Figure 2.7. DR-associated microglia exhibit ultrastructural remodeling.** (A) Representative transmission electron microscopy (TEM) images showing IPL microglia in control and STZ retinas. These images are of vertically-sectioned retinas. Control microglia (*mg)* and DR-associated microglia (*dmg)* are shaded in green with dotted white lines outlining nuclear compartments. (B) Representative confocal (left) and TEM (right) images of microglia in trans-laminal orientation positioned between the inner plexiform (IPL) and nuclear (INL) layers in STZ retinas. (C) Representative TEM images (left) and bar graphs (right) showing *dmg* frequency in the IPL (left, top panels) and INL (left, bottom panels) of control and STZ retinas. These images are of horizontally-sectioned retinas with *dmg* somas and processes shaded in green. Each bar (IPL, n=45 images per group; INL, n=45 images per group; n=3 mice per group) indicates the mean ± SEM of *dmg* frequency displayed as a percentage of standardized retinal

area. Statistical significance between groups was determined using Mann-Whitney U test. (D) Representative TEM images showing microglial mitochondria in control and STZ retinas. These images are of vertically-sectioned retinas with mitochondria in control and STZ retinas labeled with white and black asterisks, respectively (****P<.0001).

### 2.3.5 DR-associated microglia transcriptome supports inflammation, phagocytosis, and metabolic reprogramming

Microglia adopt transcriptional signatures that reflect their dynamic functional roles during inflammation and disease[158,159,160]. While microglia transcriptome changes have been described in a rat model of DR, we wanted to examine the microglia transcriptome longitudinally during early DR progression in the STZ mouse to assess the emerging response of microglia to hyperglycemia that may also explain their affinity for the inner neuroretina[161]. To do this, we first generated purified mRNA samples from pooled microglia using fluorescence-activated cell sorting (FACS) of viable, $GFP^+$ microglia (Fig.2.8A). Following assessment of FACS event counts, RNA quantity, and purity, we performed RNA sequencing (RNA-Seq) using samples ($n \geq 3$) from each diabetic (4wk STZ, 8wk STZ) and control condition. To validate the specificity of our FACS protocol, we first analyzed normalized gene counts and found that microglia-specific genes (*P2ry12, Tmem119, Hexb)* were among the highest expressed genes across all samples (Fig.2.8B). We then performed a standard EdgeR-limma pipeline analysis on all samples (n = 10) and compiled differentially expressed genes (DEG; >|1.5|FC; FDR< .05) for each diabetic condition compared to control. The resulting 825 DEGs compiled from both conditions were then used to analyze variance across samples using multidimensional scaling, which revealed consistent clustering within conditions and separation of condition clusters (Fig.2.9A-B). Interestingly, of the 825 DEGs identified we found that 767 resulted from analysis of 8wk STZ vs. control conditions while only 108 resulted from analysis of 4wk STZ vs. control conditions, with 50 shared in both STZ conditions. We also performed hierarchal clustering

based on DEGs, which further revealed a stark contrast between 8wk STZ microglia transcriptome compared to that of control microglia while 4wk STZ microglia occupied a largely intermediate state (Fig.2.9C). These data indicated that microglia undergo temporal changes to their transcriptome during early-stage DR that are substantially altered after 8 weeks of hyperglycemia.

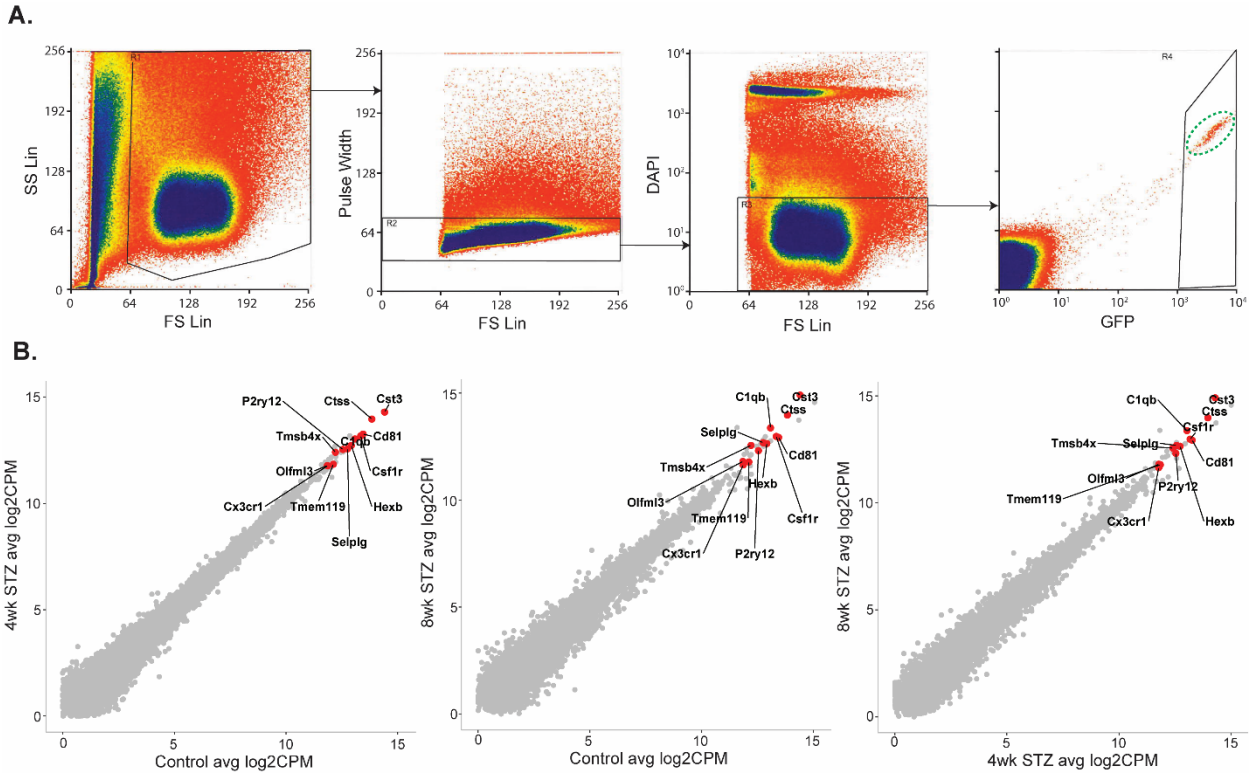


**Figure 2.8. FACS-driven isolation of retinal microglia results in mRNA samples enriched in microglia-specific genes.** (A) Fluorescence-activated cell sorting (FACS) gating strategy showing exclusion of non-cellular debris, doublets, and dead cells. Green dashed-line circle indicates the resulting population of *Cx3cr1*$^{GFP}$-positive microglia cells. (B) Dot plots showing normalized gene counts (counts per million, CPM) from RNA-Seq data for each sample condition. All genes are represented by grey dots while red dots with labels correspond to genes that are microglia-specific.

Next, we analyzed gene sets and biological pathway enrichment to relate transcriptional changes of microglia to potential functions in response to chronic hyperglycemia. Among the

DEGs unique to the 4wk STZ group, we identified several upregulated genes related to disease-associated microglial activation (*Cd44, Clec7a),* antigen presentation and nuclear factor kappa B signaling pathways (*Ctse, Tnfrsf8),* and *Klf10*, an inhibitor of gluconeogenesis that increases in response to high glucose levels[162]. In fact, several downregulated 4wk STZ DEGs genes were those related to glucose metabolism (*Slc2a8, Idua)*. In examining the DEGs unique to the 8wk STZ group, we found that upregulated genes were primarily related to pro-inflammatory signaling and chemotaxis *(Ccl2, Ccl3, Nfkbid, Tnf, Il1b, Map3k8, Cxcl14)*, as well as proliferation (*Mki67*), and lipid metabolism (*Apoc1, Ch25h).* Conversely, downregulated genes were primarily related to glycolysis *(Pkm, Pgam1, Eno1, Eno2)*. Lastly, we analyzed genes that were differentially expressed at both time points to examine the temporal relationship between duration of hyperglycemia and changes to microglia transcriptome. While several homeostatic microglia genes were expectedly downregulated *(Fcrls, Serpine2)* we also identified commonly upregulated genes related to inflammation (*Adora1, Serping1, Cd200r4*), lipid metabolism *(Cyp4f18, B3galt1)*, and insulin secretion disruption (*Igf2bp2)*.

To examine the larger 8wk STZ gene set further, we ran gene ontology (GO) pathway enrichment analysis and found that biologic pathways enriched in 8wk STZ microglia included those related to lysosome assembly, phagocytosis, and tumor necrosis factor (TNF) signaling (Fig.2.10A-B). Conversely, pathways enriched in microglia derived from control samples were related to glycolysis and negative regulation of fatty acid oxidation. Lastly, we isolated a separate batch of mRNA samples to validate expression levels of genes of interest through qPCR and found that there was a disease chronicity-dependent upregulation of these genes across STZ time points (Fig.2.9D). Taken together, we show that chronic hyperglycemia induces longitudinal alterations to retinal microglia transcriptome that reflect an acute activation after 4

weeks of hyperglycemia followed by a robust phenotypic shift after 8 weeks. Furthermore, the phenotype described by these experiments after 8 weeks seems to largely favor pro-inflammatory signaling and phagocytosis, which may underlie critical functional properties of DR-associated microglia.

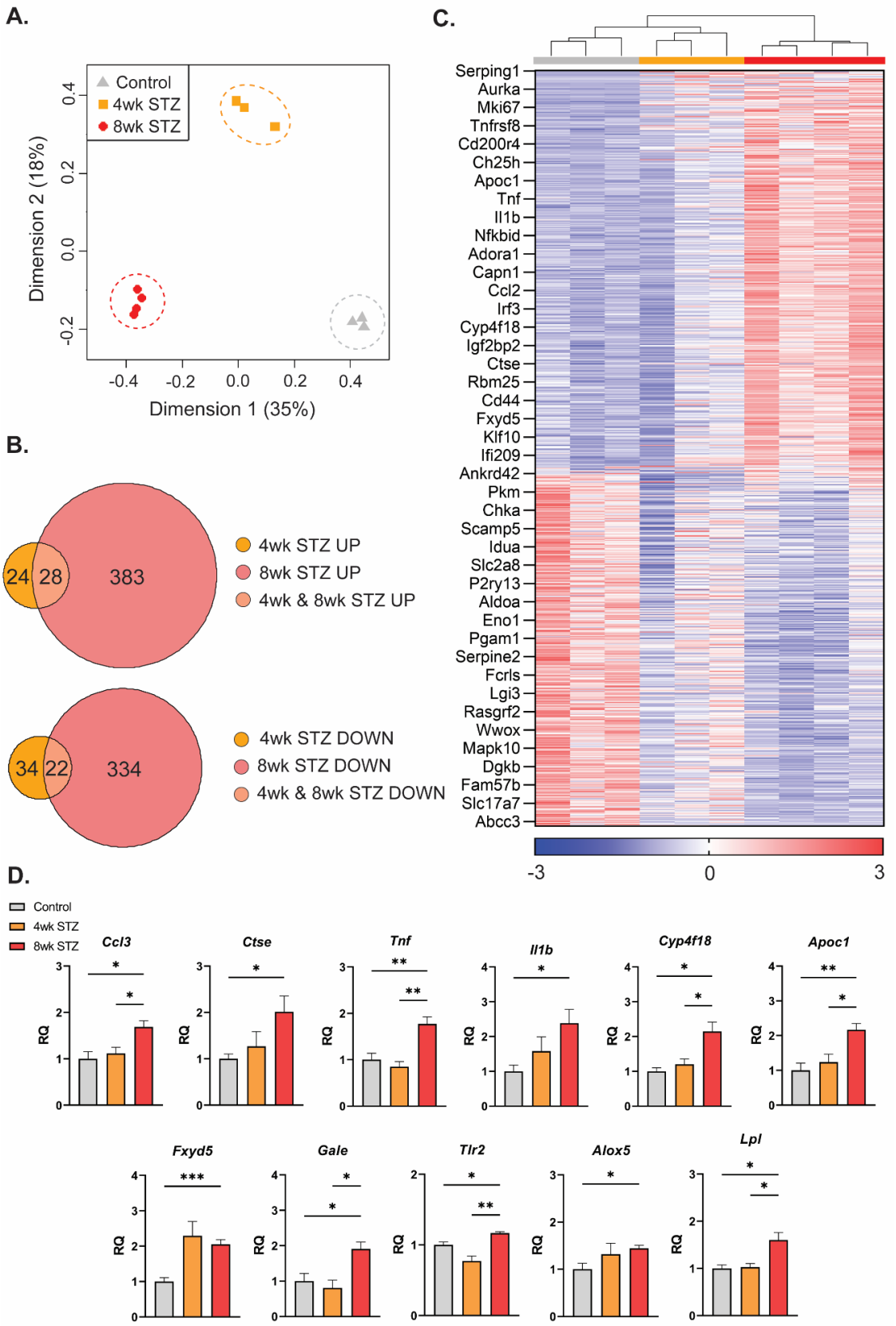
A.
Control
4wk STZ
8wk STZ
Dimension 2 (18%)
Dimension 1 (35%)
B.
24
28
383
4wk STZ UP
8wk STZ UP
4wk & 8wk STZ UP
34
22
334
4wk STZ DOWN
8wk STZ DOWN
4wk & 8wk STZ DOWN
C.
Serping1
Aurka
Mki67
Tnfrsf8
Cd200r4
Ch25h
Apoc1
Tnf
Il1b
Nfkbid
Adora1
Capn1
Ccl2
Irf3
Cyp4f18
Igf2bp2
Ctse
Rbm25
Cd44
Fxyd5
Klf10
Ifi209
Ankrd42
Pkm
Chka
Scamp5
Idua
Slc2a8
P2ry13
Aldoa
Eno1
Pgam1
Serpine2
Fcrls
Lgi3
Rasgrf2
Wwox
Mapk10
Dgkb
Fam57b
Slc17a7
Abcc3
-3
0
3
D.
Control
4wk STZ
8wk STZ
Ccl3
Ctse
Tnf
Il1b
Cyp4f18
Apoc1
Fxyd5
Gale
Tlr2
Alox5
Lpl
RQ

**Figure 2.9. Microglia transcriptome is altered in early-stage DR.** (A) Multidimensional scaling plot (MDS) showing clustering of, and separation of, RNA-Seq samples (n=3-4 mice per group) for control, 4wk STZ, and 8wk STZ conditions. (B) Euler diagrams showing the number of differentially expressed genes (DEGs) for 4wk- and 8wk-STZ conditions that are either increased (top) or decreased (bottom) in expression compared to control. Intersection regions of diagrams indicate DEGs identified in both conditions. (C) Heatmap showing hierarchical clustering of DEGs for all samples. Data (825 DEGs) are shown as Z-scores for each sample on a color gradient scale derived from normalized gene counts. Example DEG rows are labeled on the left. (D) Bar graphs showing expression levels of genes validated by quantitative polymerase chain reaction (qPCR). Each bar (n=6-7 mice per group) indicates the mean ± SEM of gene expression standardized to control values. Statistical significance among groups for each gene was determined using the Kruskal-Wallis test followed by Dunn's post hoc test for multiple comparisons (*P<.05; **P<.01).

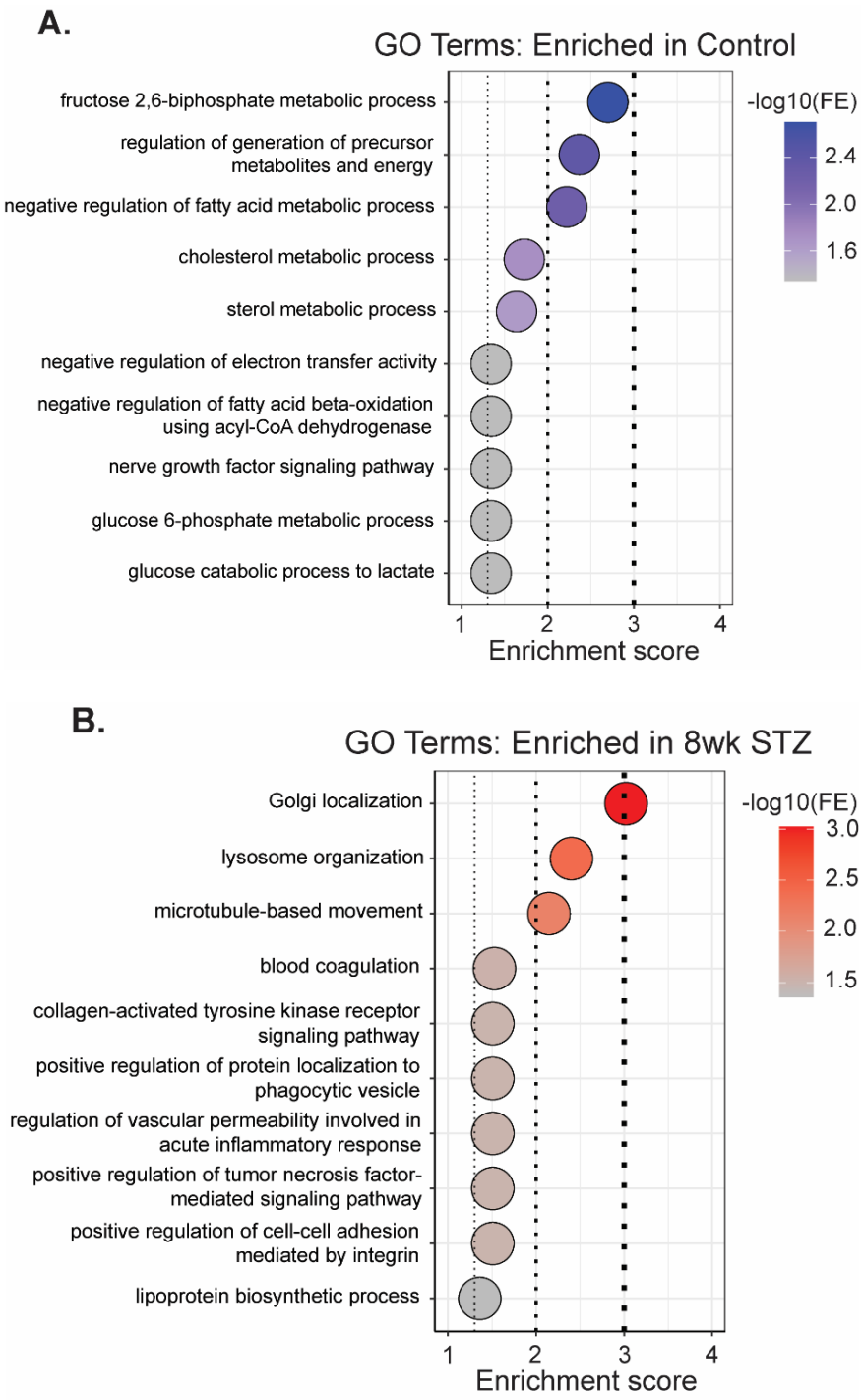


**Figure 2.10. DR-associated microglia upregulate gene programs related to inflammation, phagocytosis, and lipid metabolism.** (A-B) Top GO biological process pathways enriched in control (A) and 8wk STZ (B) microglia. Enrichment scores were calculated using Fisher's exact (FE) test.

## 2.4 Discussion

We show that microglia remain the predominant immune cell type (>92%) in the retina and uniquely respond to hyperglycemia during early stages of DR in the STZ mouse. Our analysis of retinal immune fractions also supports the use of *Cx3cr1*-based strategies to further evaluate these cells. BRB compromise, peripheral immune cell infiltration, and macroglial activation and death are reported features of DR but we show that these facets of disease are not significantly altered within 8 weeks of chronic hyperglycemia[125,137,148]. However, the limited approach we use to study these features does not rule of more acute vascular changes or macroglial phenotypes during early-stage DR that others have observed[149,150,151,163,145]. Furthermore, while local immune composition does not change significantly, we appreciate that cell types such as monocyte-derived macrophages do increase longitudinally in proportion and indicate a potential trend in infiltration that may become significant during later stages of disease. Importantly, we present this data in the same context as the majority of previous DR rodent studies in implementing STZ to model DR[164]. Multiple low-dose administration of STZ has been shown to only partially damage pancreatic islets, triggering a primarily systemic inflammatory response followed by delayed hyperglycemia. Conversely, the single high-dose STZ model used in the present study sufficiently ablates pancreatic beta cells and provides a more powerful system for examining neuroinflammation in early DR elicited by chronic hyperglycemia[165]. Future work is required to examine how retinal neurovascular unit elements are impacted by early-stage DR across various models and species.

We report on robust alterations to microglia size, ramification, and spatio-temporal distribution that occur as early as 4 weeks after the onset of hyperglycemia. Additionally, we identify regional changes in recruitment of microglia to inner retinal neuronal layers. Since the

inner retina is susceptible to dysfunction and neurodegeneration during early stages of DR in patients and animal models, these morphological observations suggest that microglia may be involved in these facets of DR pathogenesis[166]. While ultrastructural phenotypes of microglia can be heterogeneous, the subtype we aligns with previous reports of aberrant synapse remodeling by microglia in the context of chronic stress and disease[157,167]. Our findings also align with one study that reported on a similar phenotype in the brain of diabetic mice, suggesting that diabetes may elicit similar microglia phenotypes across CNS tissues[168]. Microglia undergo oxidative stress and inflammatory activation in response to acute glucose fluctuations *in vitro.* As such, our findings suggest that chronic hyperglycemia may induce a similarly pathologic state *in vivo*[169]. Future work will be focused on examining longitudinal alterations to, and potential heterogeneity among, retinal microglia ultrastructure during DR and its impact on surrounding neuroretina.

Our RNA-Seq dataset provides further resolution of microglia activation in identifying gene expression patterns that support pro-inflammatory signaling, phagocytosis, and metabolic reprogramming. While this is the first depiction of microglia transcriptome alterations in response to chronic hyperglycemia in the STZ mouse, we can identify shared patterns with similar studies. High glucose stimulation of microglia *in vitro* results in upregulation of *Tnf* and *Ccl2* through reactive oxygen species and nuclear factor kappa B pathways[170]. Additionally, whole-retina single cell RNA-Sequencing studies have reported on microglia-derived production of *Il1b* and metabolic reprogramming that may support inflammation in DR[171]. Energetic needs of phagocytic macrophages favor a reduction in glucose uptake and glycolysis while increasing fatty acid oxidation and lipid metabolism, which are consistent with what we report in the present study[73,172]. While these features have been described as a feature of less inflammatory microglia, the combination of metabolic reprogramming and pro-inflammatory priming we

observe may underscore a more complex and dynamic role that microglia play in early DR[173]. Furthermore, without implementation of single cell RNA sequencing we cannot rule out the possibility of heterogenous microglial subpopulations that may serve divergent roles in pathogenesis.

Taken together, we provide a thorough report on the immune, vascular, and glial features of the diabetic mouse retina during early stages of STZ-induced DR that clarifies their emergence following the onset of hyperglycemia. More importantly, in identifying microglia as a prominent responder to hyperglycemia in the STZ model, we describe novel morphological, ultrastructural, and transcriptional features of microglia activation in DR that may further inform their functional contributions to retinopathy.

# Chapter 3: Microglia-mediated features of early-stage diabetic retinopathy

*Adapted from unpublished data and manuscript in revision:*

Pfeifer, C.W., Walsh, J.T., Santeford, A., Lin, J.B., Beatty W.L., Terao, R., Liu, Y.A., Hase, K., Ruzycki, P.A., Apte, R.S. (2023). Dysregulated CD200-CD200R signaling in early diabetes modulates microglia-mediated retinopathy. Proc. Natl. Acad. Sci. U.S.A. (*revision submitted 8/10/23)*

# 3.1 Introduction

Morphological features of microglia activation been observed during early DR pathogenesis in patients and animal models but the functional contribution underlying activation remains unclear[134,113,135,133,174,175,176]. A recent study has reported on inflammatory markers associated with microglia activation during early and established stages of DR in the mouse but whether these phenotypic changes contribute to retinal dysfunction and neurodegeneration is still unresolved[177]. This can be appreciated by the complex metabolic, inflammatory, and functional changes that occur in the retinal environment during DR progression[130]. We have previously clarified the temporal progression of these changes in the STZ mouse by showing that the immune landscape of the diabetic retina is predominantly presided over by resident microglia. Microglia also robustly alter morphology, ultrastructure, and transcriptome in response to early-stage DR hyperglycemia while other components of the retinal environment remain unchanged. This suggests that microglia are potentially the first responders to hyperglycemic stress in the retina and may play a pivotal role in the emergence of visual dysfunction, neurodegeneration, and inflammation.

Previous studies have used microglia ablation strategies to uncover detrimental and beneficial contributions of microglia to pathogenesis[178,179,114,90,20]. Thus, we hypothesized that chronic ablation of retinal microglia during early-stage DR may impact these features of disease and in doing so, reveal which components of disease if any, are uniquely impacted by the input of activated retinal microglia. We show that chronic microglia ablation in the retina prevents visual dysfunction and neurodegeneration of the inner retina. Through immunostaining of different retinal cell and synapse types, we find that amacrine cell dysfunction and loss – an early feature of DR in patients and animal models – is particularly impacted by the contributions of

microglia. Using 3D image reconstruction techniques and transmission electron microscopy (TEM), we find that activated microglia increase contact and engulfment of amacrine cells and synapses in the diabetic retina, suggesting that aberrant phagocytosis is a feature of DR-associated microglia that contributes to neurodegeneration. Lastly, we find that chronic microglia ablation suppresses DR-associated changes to the retinal transcriptome such as leukocyte migration and cytokine production, synapse remodeling, and antigen presentation. These studies provide novel insight into specific features of early-stage DR that are impacted by the contributions of activated microglia. Furthermore, we provide evidence of enhanced phagocytosis by microglia as an explanation for their detrimental contribution to the dysfunction and loss of amacrine cells, a key interneuron cell type implicated in DR pathology. Lastly, this work provides a framework for future studies of molecular substrates underlying aberrant activation and function of microglia that may be targeted with immunotherapeutics to prevent these features of early DR in animal models and perhaps patients.

# 3.2 Materials and Methods

**Animals.** All animal use and experiments were approved by the Institutional Animal Care and Use Committee (IACUC) of Washington University in Saint Louis and performed according to the Washington University Animal Care and Use Guidelines. For experiments implementing microglia ablation in the retina, two separate mice ($Cx3cr1^{CreER/CreER}$, stock no. 0221160 and $Rosa26^{DTA/DTA}$, stock no. 009669) were obtained from Jackson Laboratory and crossed in our animal facility[180,181]. To induce *Cre*-driven ablation of microglia, tamoxifen-infused chow (500mg/kg chow) was provided in cages ad libitum for 8 weeks on a 6 days-on/1 day-off weekly

schedule to manage potential weight loss or toxicity. STZ-induced diabetic mice were prepared and monitored as previously described (Chapter 2.2*).*

**Electroretinography.** Mice were dark adapted overnight. Under red light illumination, animals were anesthetized with ketamine/xylazine. Pupils were dilated with 1% atropine sulfate and a small amount of hypromellose was applied to the surface of the corneas before placement of corneal lens electrodes and reference/ground electrodes. Body temperature was maintained at 37ºC with a heating pad. Stimuli were brief white flashes delivered via a Ganzfeld integrating sphere, and signals were recorded with bandpass settings of 0.3 Hz to 500 Hz. After a 10-minute adaptation period, a 9-step scotopic intensity series was recorded that included rod-specific/scotopic bright flash responses. After a 10-minute light adaptation period on a steady white background, a 7-step cone-specific/photopic intensity series was recorded. Quantitative measurements were extracted from ERG waveforms using an existing Microsoft Excel macro that defines the a-wave amplitude as the difference between the average pre-trial baseline and the most negative point of the average trace and defines the b-wave amplitude as the difference between this most negative point to the highest positive point, after subtracting oscillatory potentials. The eye with the larger recorded b-wave amplitude was used for each mouse. Oscillatory potentials were isolated using a digital Butterworth 45 Hz high-pass filter.

**Immunohistochemistry.** Retina flat mounts and frozen sections were prepared as previously describe (Chapter 2.2). Mice were euthanized and eyeballs were enucleated and fixed in 10% formalin overnight at 4ºC. The following antibodies were used: anti-Iba1 (FUJIFILM Wako, 019-19741), anti-PKCα (Sigma-Aldrich, P4334), anti-RBPMS (Raygene, A008712), anti-ChAT

(Sigma-Aldrich, AB144P), anti-vGlut3 (Synaptic Systems, 135204), anti-VGAT (Sigma-Aldrich, AB5062P), anti-GFP (Abcam, ab13970).

**Histology.** Mice were euthanized and eyeballs were enucleated and fixed in 4% glutaraldehyde for 1 hour followed by 10% formalin at 4ºC overnight. Eyeballs were then washed with PBS and embedded in paraffin for sectioning and staining with hematoxylin and eosin (H&E).

**Contact analysis.** For microglia-amacrine contact analysis, CX3CR1-positive microglia and amacrine cell subtypes ($CHAT^+$, $VGLUT3^+$) were visualized and imaged as previously described (Chapter 2.2). Z-stack images were then processed in Imaris to first identify voxels within reconstructed Z-stacks that were colocalized to fluorescence channels corresponding to microglia and amacrine cell subtypes using the ImarisColoc tool. Surface renderings were then created for fluorescence channels corresponding to microglia and amacrine cell subtypes, as well as colocalized voxels ("contacts"). Before quantification of contact number and volume, all contact segments were screened to remove erroneous segments produced from non-specific fluorescence.

**Quantitative RT-PCR.** For mRNA expression analysis, samples were isolated from mouse retinas using the RNeasy Plus Mini Kit (Qiagen) as per manufacturer's instructions. cDNA was prepared using the High Capacity Reverse Transcription kit (Thermo Fisher Scientific). We then performed qPCR using TaqMan Fast Advanced Master Mix (Thermo Fisher Scientific) with n=2 technical replicates per sample. We used the ΔΔCt methods and normalized to the geometric mean of *Actb* and *Gapdh* housekeeping genes. The following TaqMan Gene Expression probes were utilized: *Actb* (Mm00607939_s1), *Gapdh* (Mm99999915_g1), *Cx3cr1* (Mm02620111_s1).

**Bulk RNA-Sequencing.** Total RNA was isolated from mouse using the RNeasy Plus Mini Kit (Qiagen). Total RNA quantity and integrity was determined using 4200 Tapestation. All samples (n = 10) contained 0.5-4.0ug RNA and had RIN > 8.0. Library preparation was performed by the Genome Technology Access Center (GTAC) through the McDonnell Genome Institute (MGI) with 0.5-1.0ug of total RNA per sample. Ribosomal RNA was removed by an RNase-H method using RiboErase kits (Kapa Biosystems). mRNA was reverse transcribed to yield cDNA using Super Script III RT enzyme (Life Technologies, per manufacturer's instructions) and random hexamers. Fragments were then amplified and sequenced on an Illumina NovaSeq-6000 using paired end reads extending 150 bases. Basecalls and demultiplexing were performed with Illumina's bcl2fastq software with a maximum of one mismatch in the indexing read. RNA-Seq reads were then aligned to the Ensembl release 101 primary assembly with STAR version 2.7.9a1. Gene counts were derived from the number of uniquely aligned unambiguous reads by Subread:featureCount version 2.0.32. Raw gene counts were then filtered based on a ≥1 CPM threshold for (n-1) samples in a given condition. Next, a standard EdgeR-limma analysis of gene-level features was performed, defining significant up- or downregulated genes as a |fold-change| > 2.0 with a P value < 0.05. All further analysis and figures were generated in R (R Core Team).

# 3.3 Results

## 3.3.1 Continuous tamoxifen administration in Cx3cr1$^{CreER\text{-}YFP/+}$;*Rosa26*$^{DTA/+}$ mice results in retinal microglia ablation

One of the earliest features of DR in patients and animal models is progressive degeneration of inner retinal neurons and visual function deficits as measured by retinal electrophysiological output[125,182,183]. In observing enhanced migration of microglia into the inner retina (Figure 2.6E-

F) we proposed that microglia might play a role in early loss of inner retinal structure and function. To test this, we developed an approach to ablating microglia in the retinas of diabetic mice to examine whether these features of DR were dependent on their involvement. Using the Cx3cr1$^{\text{CreER-}YFP/+}$;*Rosa26*$^{DTA/+}$ mouse, continuous administration of tamoxifen-infused chow was used to express diphtheria toxin fragment A (DTA) in *Cx3cr1*-expressing microglia followed by immediate translocation and apoptosis (Fig.3.1A). Given that this technique has not been implemented beyond 4 weeks of treatment, we assessed microglia ablation efficacy by immunostaining retinas for microglia in the retinas of treated mice along 8 weeks of continuous tamoxifen chow administration[87]. We found that tamoxifen-treated mice exhibited >93% reduction in retinal microglia density through 8 weeks of treatment compared to untreated control mice (Fig.3.1B-C). We next combined STZ and vehicle injections with regular or tamoxifen-infused chow to compare diabetic animals that were retinal microglia-depleted (STZ DTA) or retinal microglia-privileged (STZ), while controlling for potential phenotypes related to *Cre* activity and microglia ablation (DTA) in healthy retinas (Fig.3.1D). In diabetic and non-diabetic animals (CTRL), tamoxifen-induced ablation of microglia did not induce changes to weight or blood glucose that differed from regular chow-fed mice through 8 weeks (Fig.3.1E). These findings demonstrated that this method of ablation maintains a sufficiently microglia-ablated retina without the confounding effects of residual microglia repopulation or neuroinflammatory phenotypes associated with other models of microglia ablation[184,185,186].

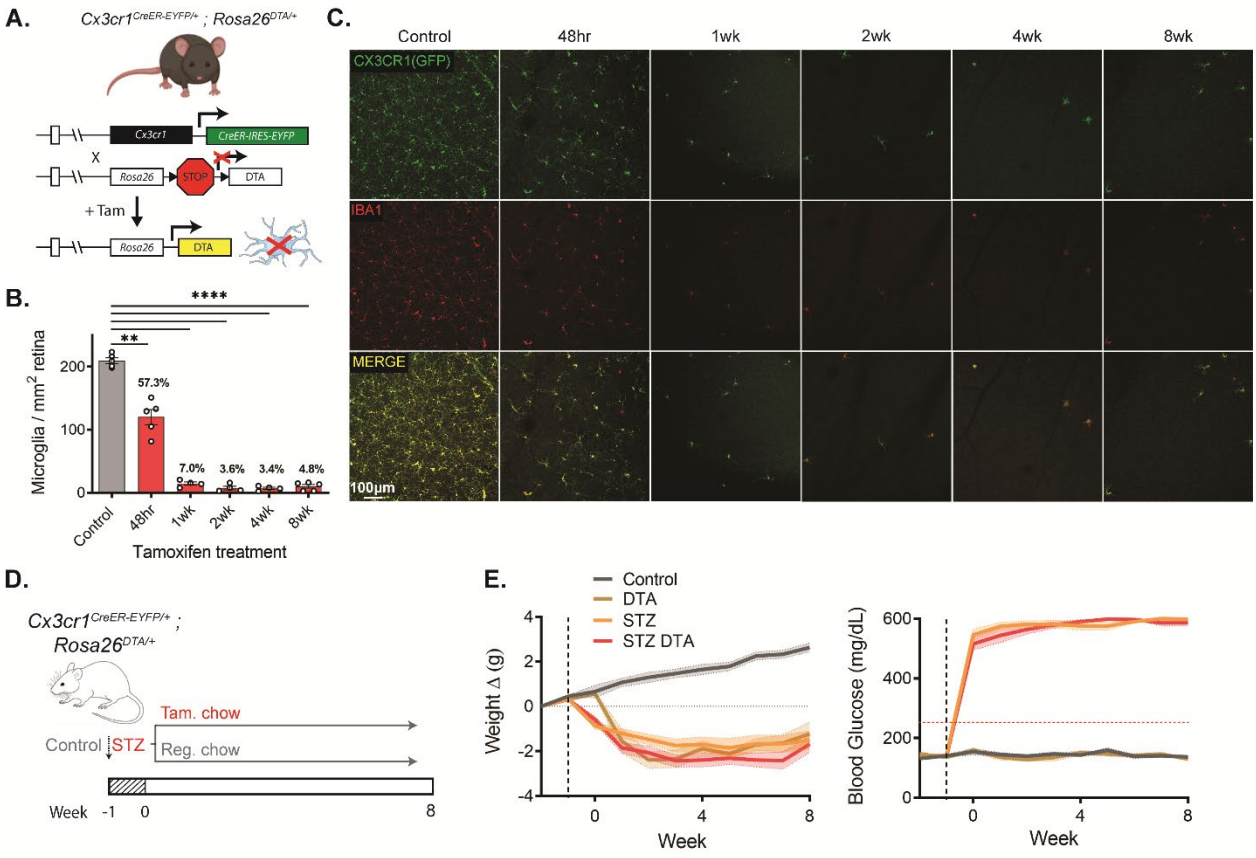


**Figure 3.1: Continuous tamoxifen administration in Cx3cr1$^{\text{CreER-}YFP/+}$;*Rosa26*$^{DTA/+}$ mice results in a microglia-ablated retina through 8 weeks of treatment.** (A) Schematic showing the mechanism by which microglia are genetically ablated by *Cre*-mediated expression of diphtheria toxin fragment A (DTA*)* following tamoxifen (TAM) administration in *Cx3cr1*$^{\text{CreER-YFP/+}}$;*Rosa26*$^{\text{DTA/+}}$ mice. (B) Bar graph and (C) representative confocal images showing retinal microglia (Cx3cr1+, Iba1+) density in the retinas of control and tamoxifen-treated *Cx3cr1*$^{\text{CreER-YFP/+}}$;*Rosa26*$^{\text{DTA/+}}$ mice. These images are of immunostained flat-mounted retinas and are maximum projections of the retina. Each bar (n=4-5 mice per group) indicates the mean ± SEM of microglia counts per standardized area of the retina. Statistical significance among groups was determined using Brown-Forsythe and Welch's ANOVA tests followed by Dunnett's T3 post hoc test for multiple comparisons. (D) Schematic of injection (STZ | vehicle) and feeding (Tamoxifen-infused chow | regular chow) schedule for *Cx3cr1*$^{\text{CreER-YFP/+}}$;*Rosa26*$^{\text{DTA/+}}$ mice. (E) Line graphs showing weight change (left) and blood glucose measurements (right) in control (CTRL), microglia-ablated (DTA), diabetic (STZ), and diabetic microglia-ablated (STZ DTA) mice. Each line (CTRL, n=10; DTA, n=10; STZ, n=20; STZ DTA, n=20) indicates the mean ± SEM weight or blood glucose calculated for animals used in the study. Black vertical dashed line indicates time of injection and red horizontal dashed line indicates hyperglycemic threshold (250mg/dL) (**P<.01; ****P<.0001).

### 3.3.2 Microglia ablation prevents visual dysfunction and neurodegeneration during early-stage DR

We next wanted to examine the impact of chronic microglia ablation on visual function and neurodegeneration during early-stage DR. To accomplish this, animals from four cohorts (CTRL, DTA, STZ, STZ DTA) were administered a scotopic (dark-adapted) and photopic (light-adapted) electroretinogram (ERG) to assess various components of rod- and cone- photoreceptor driven visual responses (Fig.3.2A). As expected from previous reports, photopic b-wave amplitudes were not significantly different among all groups, but scotopic a- and b-wave amplitudes were significantly reduced in STZ mice compared to each of the two normoglycemic groups (control and DTA) (Fig.3.2B). In normoglycemic mice, tamoxifen treatment had no effect on measured ERG parameters; however scotopic a- and b-wave amplitudes surprisingly showed a partial rescue in STZ DTA mice compared to STZ mice. Similarly, the response latency of individual oscillatory wave potentials (OP) filtered from ERG waveforms (OP1-4) were increased in STZ mice compared to control mice as reported previously, but were completely rescued in STZ DTA mice (Fig.3.2C)[166].

We next examined histology sections of retinas from tested mouse groups to appreciate potential differences in retinal neurodegeneration. In agreement with other studies, we found that the retinas of STZ mice were significantly thinner compared to those of controls, particularly the inner retina (Fig.3.3A-B)[140,134,187,188]. However, STZ DTA mouse retina thickness was significantly increased compared to STZ mice, indicating microglia ablation rescues early DR-associated neurodegeneration of the inner retina. Previous reports have suggested microglia contribute to maintenance of the blood-retina-barrier (BRB) in homeostasis and DR[189]. To investigate if microglia ablation may impact vascular permeability and structure, we performed

standard fundus imaging and fluorescein angiography of mouse groups but did not find any evidence of retinal lesions or vascular leakage (Fig.3.4). Taken together, these data demonstrate that chronic microglia ablation preserves components of rod-driven visual responses and retinal thinning in diabetic mice. This suggests that DR-associated microglia are significant contributors to the emergence of these functional and structural deficits associated with early-stage DR in the STZ mouse model. Furthermore, the strongly-preserved oscillatory potential response timing in STZ DTA mice suggests that microglia may differentially impact certain retinal cell types that drive unique components of vision.

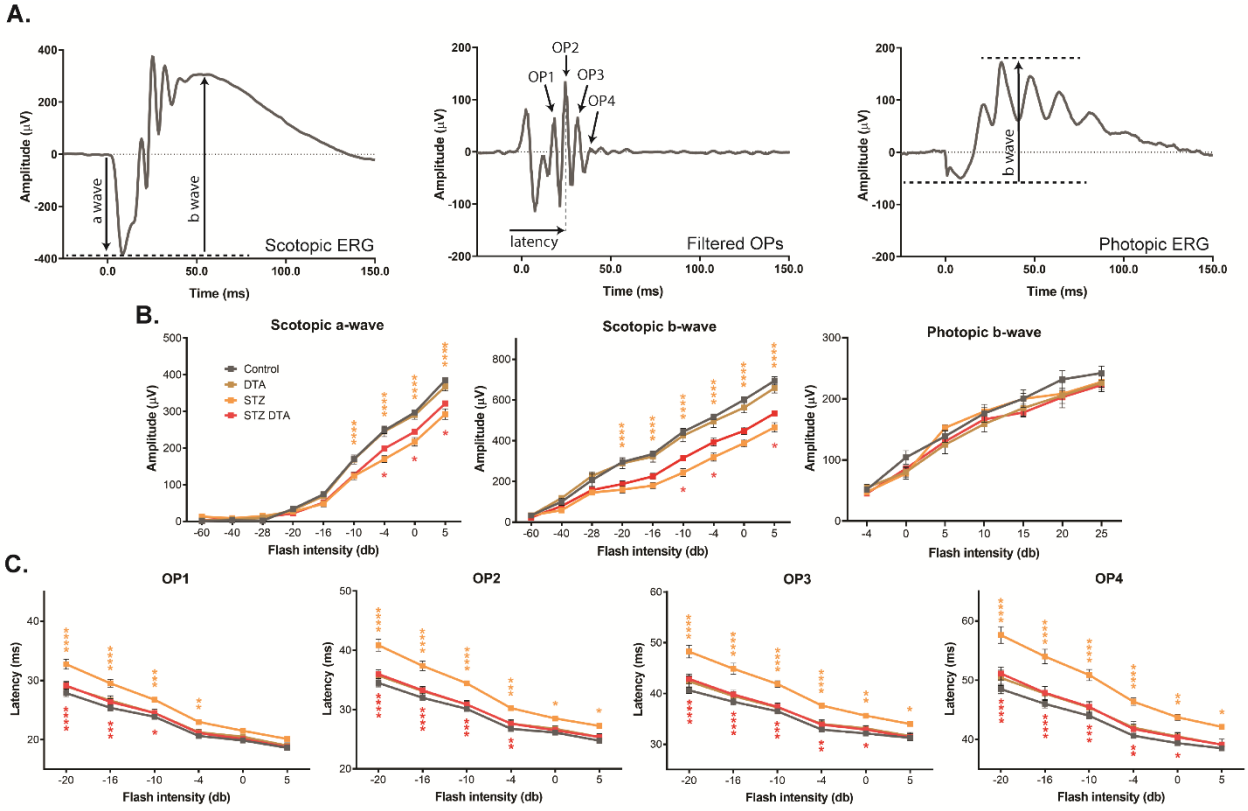


**Figure 3.2: Chronic retinal microglia ablation prevents features of scotopic visual dysfunction during early-stage DR.** (A) Waveforms showing scotopic (left), filtered oscillatory potential (OP, middle), and photopic (right) electroretinogram (ERG) responses. Each waveform (n=8 mice) indicates the control group mean annotated with individual wave components measured in (B-C). (B) Line graphs showing scotopic a- and b-wave, and photopic b-wave amplitudes for tested light intensities. (C) Line graphs showing scotopic OP latencies for tested light intensities that elicit Ops (-20-5db). Each line (n=8 mice per group) indicates the mean ±

SEM amplitude (D) or latency (E). Statistical significance among groups was determined using two-way ANOVA tests followed by Bonferonni's post hoc test for multiple comparisons. Orange asterisks in (B-C) indicate multiple comparisons test results between STZ and CTRL groups while red asterisks indicate results between STZ DTA and STZ groups (*P<.05; **P<.01; ***P<.001; ****P<.0001).

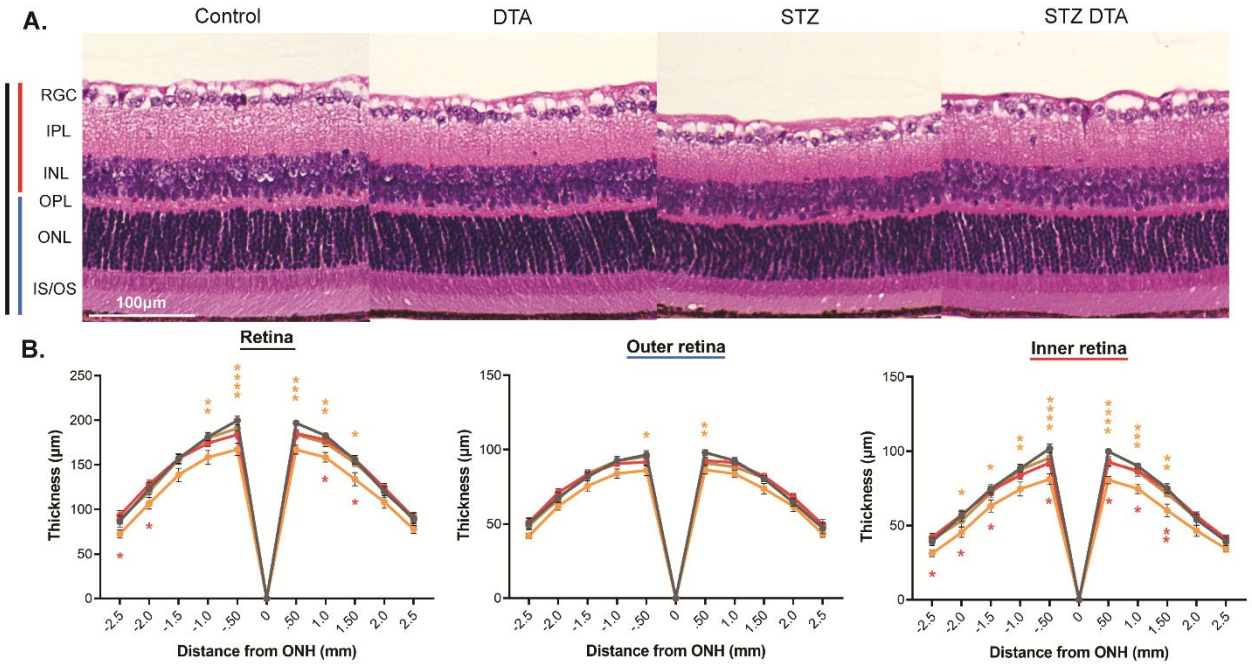


**Figure 3.3: Microglia ablation prevents inner retinal neurodegeneration during early-stage DR.** (A) Representative confocal images and (B) spider plots showing retinal layer histology and thickness for tested mouse groups. Images are maximum projections of paraffin-embedded hematoxylin and eosin-stained (H&E) retina sections taken at 0.50mm from the optic nerve head (ONH). Black, blue, and red vertical lines indicate entire, outer (OPL/ONL/IS/OS) and inner (RGC/IPL/INL) retina, respectively. Each line (n=7-8 mice per group) indicates the mean ± SEM retina thickness at incremental distances from the ONH. Statistical significance among groups was determined using two-way ANOVA tests followed by Bonferonni's post hoc test for multiple comparisons. Orange asterisks in (B) indicate multiple comparisons test results between STZ and CTRL groups while red asterisks indicate results between STZ DTA and STZ groups (*P<.05; **P<.01; ***P<.001; ****P<.0001).

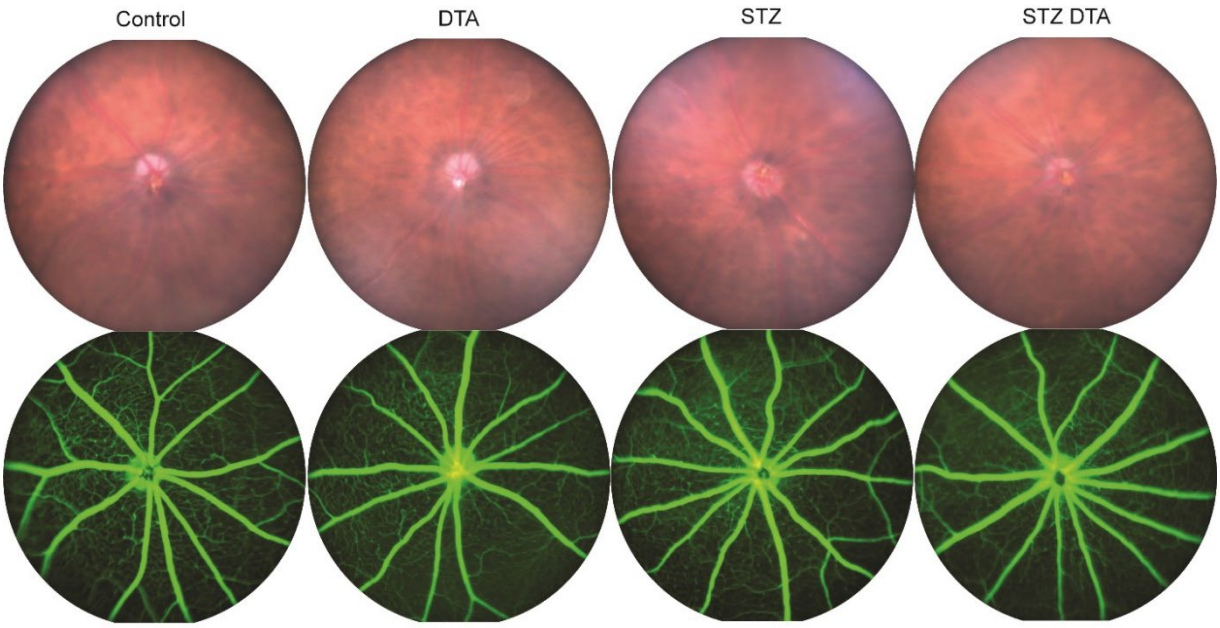


**Figure 3.4: Chronic microglia ablation does not impact BRB integrity in homeostasis or early-stage DR.** Representative fundus images of mouse eyes using bright field (top panel) and fluorescence (bottom panel) imaging modalities. Images were acquired in anesthetized mice before (top panel) and after (bottom panel) sodium fluorescein injection.

### 3.3.3 Microglia ablation preserves amacrine cells and synapses during early-stage DR

OP responses are broadly generated from modulatory feedback pathways between bipolar cells (BPC), amacrine cells (AC), and ganglion cells (RGC)[190]. Pharmacological studies have found that GABAergic and glycinergic transmission between ACs and BPCs, in addition to AC and RGC-generated action potentials, are necessary for maintaining normal OP latency responses[191]. Since neurodegeneration of these inner retinal subtypes has been reported during early stages of disease in animal models of DR, we hypothesized that rescued OP response latencies in diabetic microglia-depleted mice may indicate a causative link between microglia and selective neurodegeneration of these cell types[188,192,193]. To test this, we performed immunostaining of these cell and synapse types in retina sections taken from mouse cohorts. We first found that BPC axon terminal density was significantly reduced in STZ and STZ DTA retinas compared to

controls (Fig.3.5A-B). Similarly, RGC soma density was reduced in STZ retinas, but not in STZ DTA retinas, as compared to control and DTA retinas (Fig.3.5C). Previous studies have shown that ACs are among the first neurons to be affected by hyperglycemia[192,194]. In line with this, we found that the densities of two subtypes of ACs ($CHAT^+$, $VGLUT3^+$) that provide GABAergic, cholinergic, and glycinergic synaptic input were significantly reduced in STZ retinas compared to those of control and DTA groups (Fig.3.5D-E). Interestingly, cell densities for these AC subtypes were significantly increased in STZ DTA retinas compared to STZ, suggesting that microglia are a necessary contributor to loss of these AC cell subtypes during DR. Further, we also observed a significant reduction in GABAergic inhibitory synaptic ribbon (VGAT) density in the IPL of STZ retinas compared to controls while STZ DTA retina density was significantly increased compared to that of STZ retinas, suggesting greater preservation of this synaptic layer (Fig.3.5.F). Importantly, we did not observe any significant differences in cell or synapse density staining between control and DTA groups, ruling out tamoxifen toxicity or effects related to microglia ablation in healthy retinas. These data supported our hypothesis that microglia could be contributing to the reduction of AC-driven oscillatory potential responses by mediating the loss of at least two AC subtypes and their inhibitory synapses that are necessary for normal OP responses.

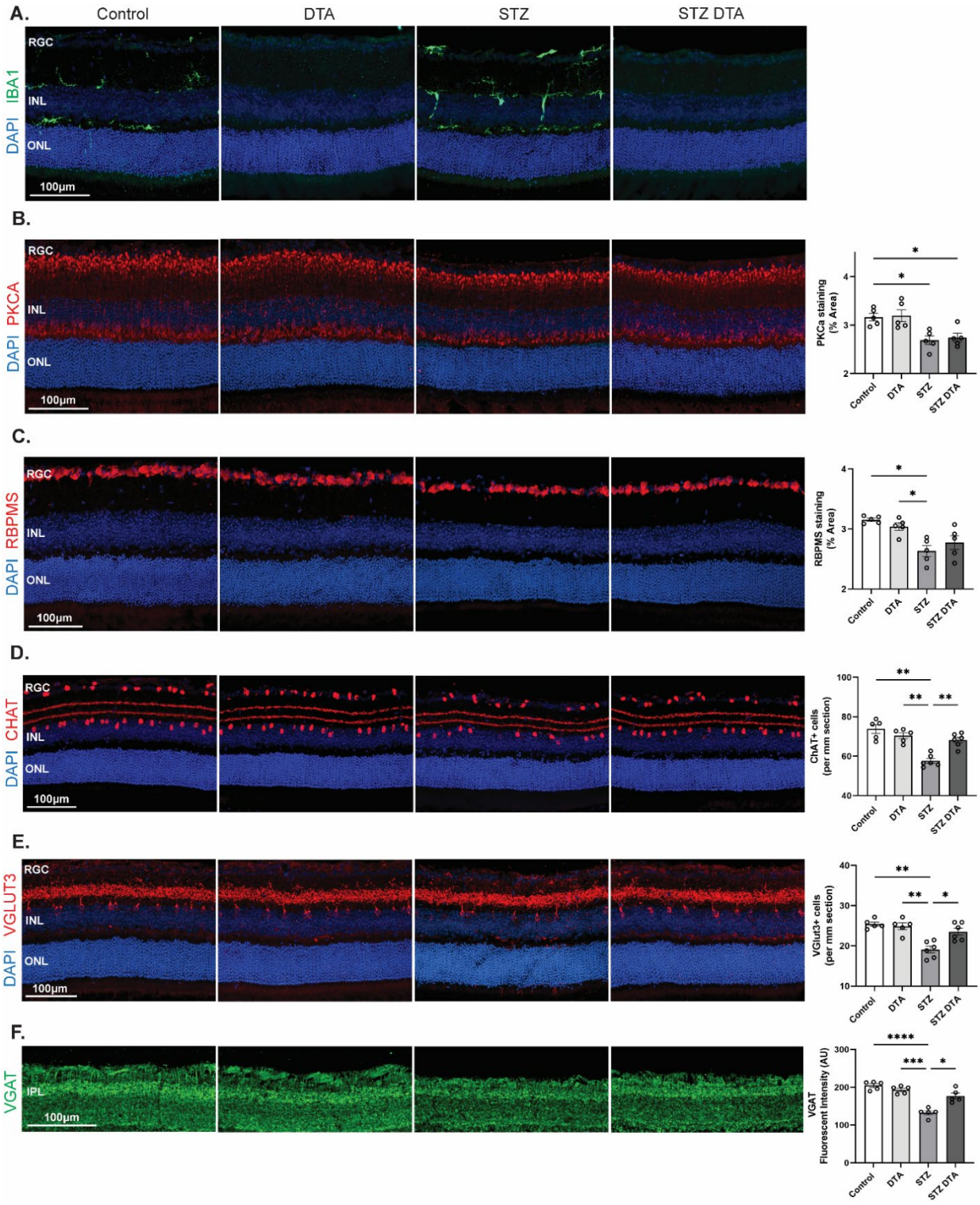


**Figure 3.5: Chronic microglia ablation prevents amacrine cell subtype and synapse loss during early-stage DR.** (A) Representative confocal images showing (IBA1+) microglia in the retinas of CTRL, DTA, STZ, and STZ DTA mouse groups. (B-F) Representative confocal images (left) and bar graphs (right) showing bipolar cells (BPC, PKCA+), ganglion cells (RGC,

RBPMS+), amacrine cells (AC, ChAT+, VGLUT3+), and inhibitory synapse ribbon (VGAT+) density in the retinas of each mouse group. Each bar (n=5-6 mice per group) indicates the mean ± SEM of fluorescence area (B-C), cell counts (D-E), and fluorescence intensity (F) for standardized area of retina section. Each mouse count is an average from four to five retina sections. Statistical significance among groups was determined using Brown-Forsythe and Welch's ANOVA tests followed by Dunnett's T3 post hoc test for multiple comparisons. (A-F) These images are of immunostained cryo-sectioned retinas and are maximum projections of the section shown (*P<.05; **P<.01; ***P<.001; ****P<.0001).

### 3.3.4 Microglia increase contact and engulfment of amacrine cells and synapses during early-stage DR

During retinal degeneration, microglia migrate to sites of neurodegeneration to engulf and degrade cell debris but if pathologically activated, can exacerbate degeneration of the neuroretina through aberrant phagocytosis and synapse remodeling[90,114,]. We have determined that DR-associated microglia are drawn to neuronal layers of the inner retina, increase transcriptional programs related to phagocytosis, and are a necessary contributor to amacrine cell dysfunction and loss (Figures 2.5; 2.8; 3.3). Thus, we hypothesized that aberrant engulfment of AC subtypes and synapses by DR-associated microglia may mediate microglia-dependent AC dysfunction and loss. To test this, we performed confocal Z-stack imaging of flat-mounted retinas immunostained for AC subtypes ($CHAT^+$, $VGLUT3^+$) in 8-week STZ and control mice, generated 3D reconstructions of image stacks, and quantified microglia-AC contact in the inner retina (Fig.3.6A). Early DR led to a significant increase in the percentage of $CHAT^+$ ACs in contact with microglia (Fig.3.6B). Consistent with data from retina cross sections, whole-mount quantification recapitulated significant reductions in $CHAT^+$ ACs in STZ retinas compared to control retinas. Interestingly, we also observed that morphologically activated microglia in STZ retinas displayed increased average size of contacts with $CHAT^+$ ACs. Upon further investigation, we observed instances of $CHAT^+$ AC encircling and engulfment by microglia, perhaps explaining the increased average volume of contact between these cell types (Fig.3.6C).

We also found similar results for VGLUT3$^{+}$ ACs (Fig.3.6D-F). To examine microglia-synapse interactions we revisited TEM imaging of the inner retina in STZ and control mice and once again identified DR-associated microglia and processes leading into the IPL neuropil. Interestingly, DR-associated microglia within the IPL exhibited close apposition and encircling of synaptic dyads with compromised clefts that was not observed in control retinas (Fig.3.6G). Furthermore, we observed occasions of encircled synapses of ACs, as indicated by their vesicular density and cytoplasmic detail[195]. These data indicate that DR-associated microglia increase contact with and engulfment of AC subtypes and synapses, which may explain preservation of ACs and the OP response in STZ DTA mice.

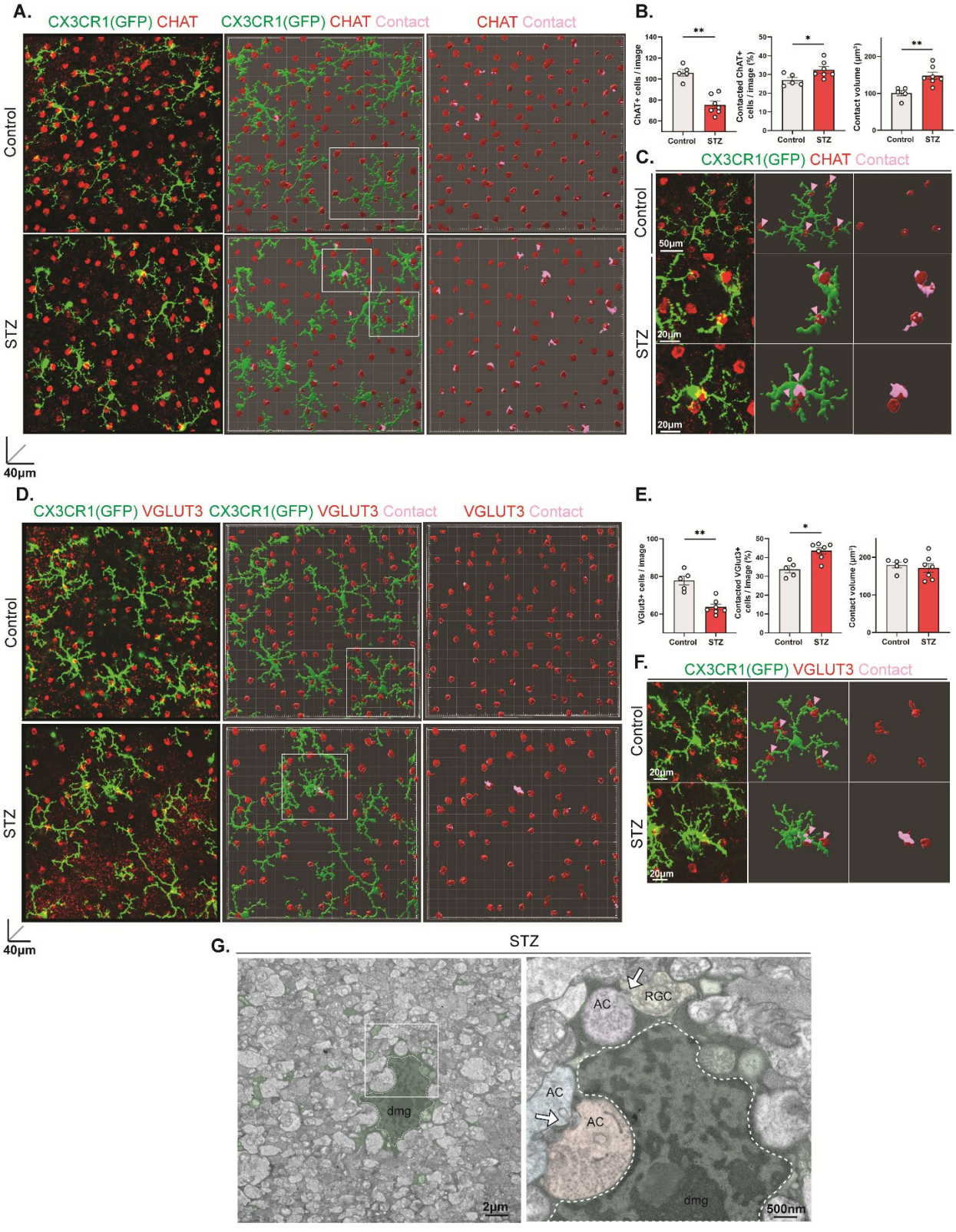
A.
CX3CR1(GFP) CHAT
CX3CR1(GFP) CHAT Contact
CHAT Contact
Control
STZ
40μm
B.
ChAT+ cells / image
Contacted ChAT+ cells / image (%)
Contact volume (μm³)
Control
STZ
C.
CX3CR1(GFP) CHAT Contact
50μm
20μm
D.
CX3CR1(GFP) VGLUT3
CX3CR1(GFP) VGLUT3 Contact
VGLUT3 Contact
E.
VGlut3+ cells / image
Contacted VGlut3+ cells / image (%)
F.
CX3CR1(GFP) VGLUT3 Contact
G.
STZ
AC
RGC
dmg
2μm
500nm

**Figure 3.6: DR-associated microglia increase contact and engulfment of amacrine cell subtypes and synapses.** (A,D) Representative 3D reconstructions of confocal Z-stack images showing contacts between microglia (CX3CR1+) and amacrine cells (CHAT+, VGLUT3+) in control and 8wk STZ mouse retinas. These images are of immunostained flat-mounted retinas and surface reconstructions (middle, right) of microglia, amacrine cells, and colocalized contacts were produced using Imaris imaging analysis software. (B,E) Bar graphs showing cell density (left), contacted cells (middle), and contact volume (right) for amacrine cells (CHAT+, VGLUT3+) in control and STZ retinas. Each bar (n=5-7 mice per group) indicates the mean ± SEM. Cell density and percentage of contacted cells for each mouse is an average from four to five confocal images of the retina. Contact volume for each mouse is an average from (n=78-161) individual contacts identified in four to five confocal images of the retina. Statistical significance among groups was determined using the Mann-Whitney U test. (C,F) Representative images of microglia as outlined in (A,D) showing contact and engulfment profiles between microglia and amacrine cells in control and STZ retinas (*P<.05; **P<.01). (G) Representative low-magnification (left) and high-magnification TEM image (right) showing synaptic remodeling by *dmg* in STZ retina. These images are of vertically-sectioned retina. White arrows are directed at compromised synaptic clefts shared between amacrine cells (AC; orange, blue, purple) and ganglion cells (RGC; yellow) that are encircled by *dmg* shaded in green (*P<.05; **P<.01).

### 3.3.5 Chronic microglia ablation suppresses diabetic retinal gene expression programs related to inflammation and synapse remodeling

During early-stage DR in the mouse, the retinal transcriptome changes to reflect an affinity for gene programs related to inflammation[155]. Thus, we wanted to investigate potential transcriptomic changes in the diabetic microglia-ablated mouse retina to identify broader biological implications of microglia ablation in the diabetic retina. To do this, we isolated purified mRNA samples from STZ and STZ DTA mouse retinas. Following assessment of RNA quantity and purity, we performed RNA-Sequencing using samples (n=5) from each condition. We then performed a standard EdgeR-limma pipeline analysis on all samples (n = 10) and compiled differentially expressed genes (DEG; >|2.0|FC; PValue< .05) when comparing STZ DTA against STZ. We first identified that samples appeared to cluster and separate from one another based on condition, as shown through multi-dimensional scaling (Fig.3.7A). To validate our microglia ablation approach in these samples, we first looked at the most downregulated

genes in STZ DTA samples compared to STZ and confirmed that most were microglia-specific (*Siglech, Tmem119, Selplg, Sall1, Cx3cr1)* (Fig.3.7C). We also performed confirmatory qPCR and found that while whole-retina transcript levels of *Cx3cr1* in STZ samples were similar to control littermates, transcripts in STZ DTA samples were 84% lower than STZ samples (Fig.3.7B). These initial assessments indicated that STZ DTA samples were indeed derived from diabetic microglia-ablated retinas.

Following comparison of STZ DTA against STZ samples we identified 110 DEGs. Through hierarchical heatmap analysis, we found that there was consistency in normalized gene counts across samples and stark contrasts in expression levels between conditions (Fig.3.7E). Among the 110 DEGs not directly related to ablation of microglia, we found genes related to photoreceptor-RPE function (*Oxtr, Rgsl1, Stra6l)*, connective tissue and cell-cell adhesion (*Col5a2, Cdh3),* and inflammation (*Cd40)* upregulated in STZ DTA samples compared to STZ (Fig.3.7D). We also identified genes related to lysosome function (*Laptm5)*, vesicle trafficking in antigen-presenting cells (*Fgd2, Myo1h),* and leukocyte activation and migration (*Vsir, Il6ra, Inpp5d, Pld4)* that were downregulated in STZ DTA samples compared to STZ. Lastly, to enhance our understanding of broader biological functions impacted by microglia ablation in DR, we performed biological pathway enrichment analysis on our entire dataset to identify the most suppressed gene sets. Through this analysis we found that pathways related to innate immune response and cytokine production, leukocyte motility and cytotoxicity, and synapse pruning and cell junction disassembly were among the top gene sets downregulated in STZ DTA retinas (Fig.3.7F). These data indicate that at a transcriptional level, microglia ablation suppresses gene expression patterns related to detrimental biologic functions such as inflammation and synapse pruning, which further supports our findings that microglia provide

detrimental contributions to DR progression. Furthermore, we provide demonstrations of microglia ablation as a preliminary method for ameliorating microglia-mediated features of DR.

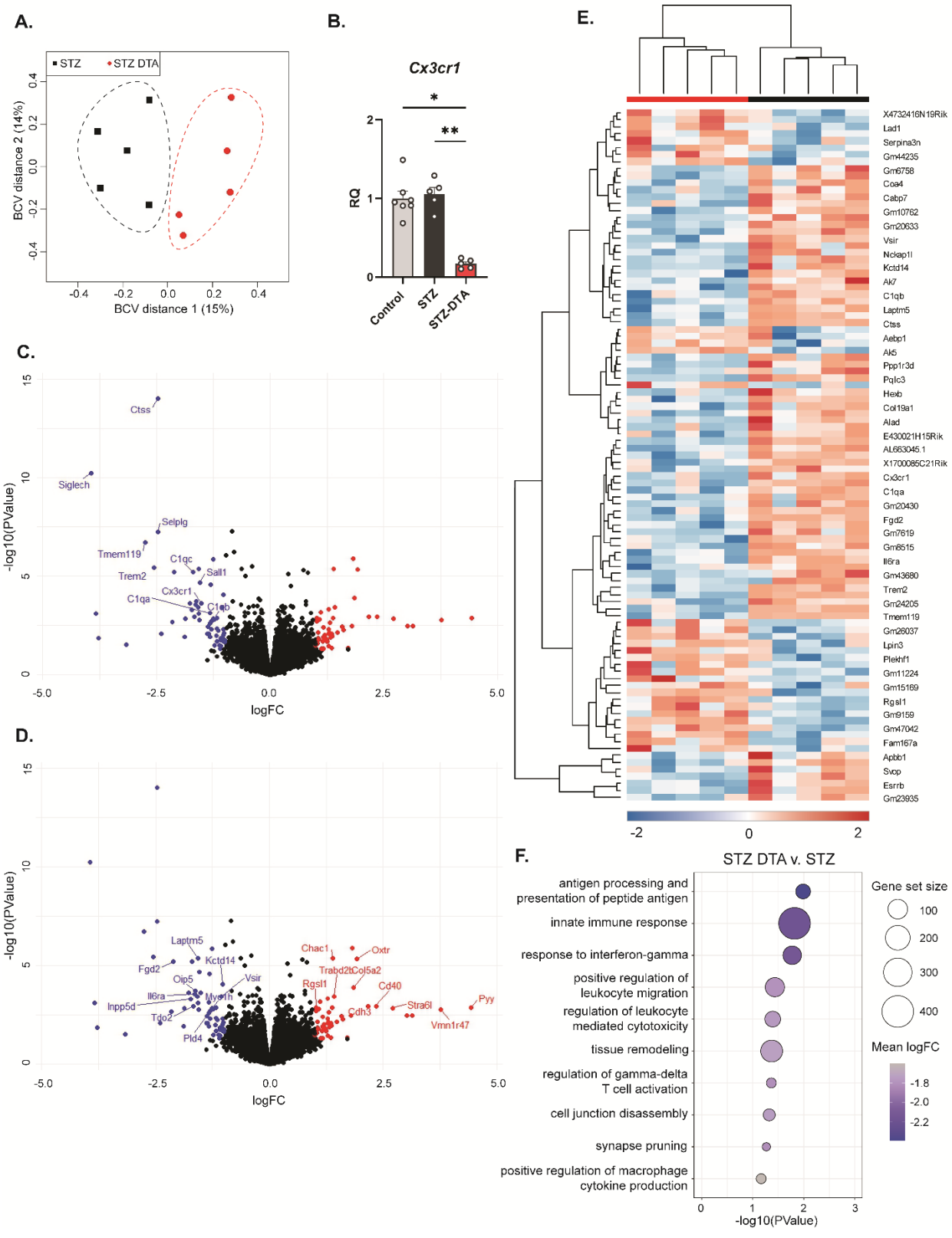
A.
STZ
STZ DTA
BCV distance 2 (14%)
BCV distance 1 (15%)
B.
Cx3cr1
RQ
Control
STZ
STZ-DTA
C.
-log10(PValue)
logFC
Ctss
Siglech
Selplg
Tmem119
C1qc
Trem2
Sall1
Cx3cr1
C1qa
C1qb
D.
Laptm5
Kctd14
Fgd2
Oip5
Vsir
Il6ra
Myo1f
Inpp5d
Tdo2
Pld4
Chac1
Oxtr
Trabd2b
Col5a2
Rgsl1
Cd40
Cdh3
Stra6l
Pyy
Vmn1r47
E.
X4732416N19Rik
Lad1
Serpina3n
Gm44235
Gm6758
Coa4
Cabp7
Gm10762
Gm20633
Vsir
Nckap1l
Kctd14
Ak7
C1qb
Laptm5
Ctss
Aebp1
Ak5
Ppp1r3d
Pqlc3
Hexb
Col19a1
Alad
E430021H15Rik
AL663045.1
X1700085C21Rik
Cx3cr1
C1qa
Gm20430
Fgd2
Gm7619
Gm6515
Il6ra
Gm43680
Trem2
Gm24205
Tmem119
Gm26037
Lpin3
Plekhf1
Gm11224
Gm15169
Rgsl1
Gm9159
Gm47042
Fam167a
Apbb1
Svop
Esrrb
Gm23935
F.
STZ DTA v. STZ
antigen processing and presentation of peptide antigen
innate immune response
response to interferon-gamma
positive regulation of leukocyte migration
regulation of leukocyte mediated cytotoxicity
tissue remodeling
regulation of gamma-delta T cell activation
cell junction disassembly
synapse pruning
positive regulation of macrophage cytokine production
-log10(PValue)
Gene set size
Mean logFC

**Figure 3.7: Chronic microglia ablation suppresses DR-associated whole-retina transcriptome changes related to inflammation and synapse remodeling.** (A) Multidimensional scaling plot (MDS) showing clustering of, and separation of, RNA-Seq samples (n=5 mice per group) for STZ and STZ DTA conditions. (B) Bar graph showing expression levels of *Cx3cr1* by quantitative polymerase chain reaction (qPCR). Each bar (n=5-7 mice per group) indicates the mean ± SEM of gene expression standardized to control values. Statistical significance among groups for each gene was determined using the Kruskal-Wallis test followed by Dunn's post hoc test for multiple comparisons. (C) Volcano plot showing DEGs either upregulated (red) or downregulated (blue) in STZ DTA samples compared to STZ samples with microglia-specific genes annotated. (D) Volcano plot showing DEGs either upregulated (red) or downregulated (blue) in STZ DTA samples compared to STZ samples with genes that are not microglia-specific annotated. (E) Heatmap showing hierarchical clustering of DEGs for all samples. Data (110 DEGs) are shown as Z-scores for each sample on a color gradient scale derived from normalized gene counts. Example DEG rows are labeled on the right. (F) Gene set enrichment analysis for downregulated genes in STZ DTA compared to STZ. Top 10 gene sets are shown and organized by mean logFC, PValue, and gene set size (*P<.05; **P<.01).

# 3.4 Discussion

Morphological features of microglia activation and inner retinal neurodegeneration have been previously characterized in DR, but we present evidence of these phenomena emerging in parallel and being uniquely interconnected[134,192,193,196]. We show that ablating microglia from the diabetic retina preserves inner retinal visual function and structure but reveals a specific susceptibility of amacrine cells. While it remains likely that microglia are mediating the phenotypes we observe, we cannot exclude that depletion of resident non-microglial macrophages (<1%), intravascular adherent leukocytes, and a portion of circulating monocytes via tamoxifen treatment in *Cx3cr1*$^{CreER\text{-}YFP/+}$*;Rosa26*$^{DTA/+}$ mice may also contribute to visual dysfunction and neurodegeneration[197]. We also show that microglia ablation in healthy adult mice for 8 weeks does not significantly impact visual function or neurodegeneration, which conflicts with previous reports[87]. However, the study in question implemented tamoxifen administration via injection and used exclusively young, female mice. We suspect that the differences in outcomes can be explained by these differences in approaches. Future work is

required to examine how ablation or inhibition of microglia and other myeloid cell species impacts features of DR across various models and stages of disease.

In showing that microglia increase contact and engulfment of ACs within this area of the retina, and are necessary for the lengthening of OP response latency, we postulate that these findings point to an underlying mechanism specific to ACs. Reduced GABA activity in the brain has been shown to result in enhanced microglial activity and contact with neuronal synapses, often resulting in aberrant remodeling[198]. More so, inflammatory cytokines disrupt synaptic homeostasis and trigger apoptotic cell death. To this end, we propose that dysfunctional inhibitory AC synapses during early-stage DR may in part elicit initial activation of retinal microglia. However, as we have demonstrated in other parts of this work, elicitation of a response from microglia and their subsequent contact and disposal of ACs may be dictated by different signaling mechanisms. Future work will be devoted to untangling the importance, and temporal emergence of, these potential explanations of microglia-driven loss of ACs and synapses.

We show that chronic ablation of microglia suppresses DR-associated retinal transcriptome changes associated with immune responses, tissue remodeling, and leukocyte migration and cytotoxicity. We attribute many of these suppressed biological pathways to the absence of microglia, which we describe previously as an activated and migratory cell type upregulating pro-inflammatory signaling molecules and phagocytosis (Fig.2.5-2.10). However, some of the changes we discovered may reveal indirect consequences of microglia ablation. Increased co-expression of *Cd40* and ATP in muller glia has been identified as a trigger of microglia activation and inflammatory cytokine production in a mouse model of DR[199]. To this end, we suspect that the increase in *Cd40* we see in STZ DTA retinas may reveal an inhibitory

role of microglia in muller glia function during DR that is yet to be elucidated. We also describe several gene changes related to photoreceptor-RPE communication and function. While alterations to the inner retina are observed earlier than those to the outer retina in DR literature, dysfunctional visual cycle metabolism and photoreceptor-RPE junctions lead to outer segment thinning and detachment[200]. We observe outer segment shortening in STZ histology retina sections, suggesting that microglia may contribute to early stages of outer retinal dysfunction in DR through mechanisms we have yet to elucidate. Future work will be devoted to enhancing our understanding of microglia-mediated outer retinal dysfunction and features of DR during more established stages.

Overall, this work provides a significant advancement in our understanding of microglia function during early stages of DR in the STZ mouse. Through chronic microglia ablation, we have uncovered unique structural, functional, and transcriptional features of the diabetic mouse retina uniquely dependent upon microglial involvement. These findings provide a framework for future studies devoted to uncovering the molecular substrates of microglia-mediated retinopathy necessary for developing microglia-specific immunotherapeutic strategies for treating DR.

# Chapter 4: Dysregulated CD200-CD200R signaling during early diabetes modulates microglia-mediated neuroretinopathy

*Adapted from unpublished data and manuscript in revision:*

Pfeifer, C.W., Walsh, J.T., Santeford, A., Lin, J.B., Beatty W.L., Terao, R., Liu, Y.A., Hase, K., Ruzycki, P.A., Apte, R.S. (2023). Dysregulated CD200-CD200R signaling in early diabetes modulates microglia-mediated retinopathy. Proc. Natl. Acad. Sci. U.S.A. (*revision submitted 8/10/23)*

# 4.1 Introduction

We and others have shown that microglia contribute to features of diabetic retinopathy such as neurodegeneration, vascular breakdown, and inflammation[201,202,203]. However, ablation of microglia is not a sustainable strategy for treating DR given that some of their functions or indirect effects on other retinal cell types may be beneficial. For this reason, reprogramming microglia or mitigating the detrimental features of their response to hyperglycemia is a more precise and desirable therapeutic approach. However, the molecular mechanisms underlying harmful microglia phenotypes during DR remain unknown thus inhibiting progress with regards to immunotherapeutic research. Systemic administration of minocycline, a tetracycline antibiotic, has been shown to reduce microglia activation, retinal inflammation, and neuronal apoptosis in diabetic rats but its benefit in treating diabetic macular edema in clinical trials was minimal[204,205]. Inhibition of fractalkine-receptor signaling (CX3CL1-CX3CR1) between retinal neurons and microglia has been shown to exacerbate vascular permeability and other features of DR in the diabetic mouse, but it remains unclear whether this signaling axis is perturbed in DR to begin with[148]. Lastly, neutralization of potent pro-inflammatory cytokines such as *Il1b* and *Tnf* with monoclonal antibodies has shown some effectiveness in preserving retinal neurons and visual function in animal models and small clinical trials but fail to target and reprogram microglia directly[206,207,208,209]. Seeing as current therapeutic strategies are lacking in effectiveness and specificity, we sought out to identify microglia-neuron signaling mechanisms dysregulated during early diabetes that underlie harmful microglial phenotypes and are amenable to therapeutic targeting.

Here we show that during early-stage DR, activated microglia upregulate receptors (CD200R1, CD200R4) for the immunomodulatory transmembrane glycoprotein CD200, which

is decreased in the diabetic retina but primarily on amacrine cells. We provide additional evidence of dysregulated CD200-CD200R signaling correlating with retinal inflammation and pathological microglia contact with amacrine cells. In an attempt to correct this perturbed signaling axis, we show that CD200 protein can attenuate high glucose-induced microglial phagocytosis, inflammation, and transcriptional changes *in vitro*. Lastly, we demonstrate that a single intravitreal injection of CD200 protein is sufficient to suppress microglial activation, retinal inflammation, and visual dysfunction during early-stage DR. These studies present a primary signaling mechanism shared between microglia and amacrine cells that is dysregulated in early diabetes and correlates with features of microglia-mediated DR. Furthermore, this work demonstrates that CD200R signaling in microglia is a potent immunotherapeutic target *in vitro* and *in vivo,* providing a framework for future therapeutic testing in other animal models of DR and potentially patients.

# 4.2 Materials and Methods

**Ligand-Receptor Analysis.** Ligand-receptor pairings dysregulated in DR-associated microglia were identified by cross-referencing 8wk STZ DEGs identified in (Fig 2.9B) with the LRdb ligand-receptor interactions database. Identified pairings were then organized in signaling networks constructed in Cytoscape[210].

**Quantitative RT-PCR.** mRNA analysis was performed as previously described (*Chapter 2.2*). The following TaqMan Gene Expression probes were utilized: *Nos2* (Mm00440502_m1), *Cd200* (Mm00487740_m1), *Cd200r1* (Mm00491164_m1), *Cd200r4* (Mm02605260_s1), *Tnf* (Mm00443258_m1), *Il1b* (Mm00434228_m1), *Il6* (Mm00446190).

**Immunohistochemistry.** Retina flat mounts and frozen sections were prepared as previously describe (*Chapter 2.2*) were euthanized and eyeballs were enucleated and fixed in 10% formalin overnight at 4ºC. The following antibodies were used: anti-Iba1 (FUJIFILM Wako, 019-19741), anti-ChAT (Sigma-Aldrich, AB144P), anti-vGlut3 (Synaptic Systems, 135204), anti-CD200 (Abcam, ab33734), anti-AP2 (Abcam, ab52222), and anti-CD200R1 (R&D Systems, AF2554).

**Cell Culture.** BV2 microglial cells were purchased from AcceGen (ABC-TC212S) and maintained in our lab. Cells were cultured in normal glucose (1g/L) DMEM (Gibco Life Technologies) containing 10% FBS (Gibco) and 1% penicillin-streptomycin (Gibco) at 37ºC in a humidified incubator under 5% CO2. For experiments, cells were seeded in 12-well plates ($1x10^5$) and left overnight to adhere. The next day, plates were washed two to three times with DPBS to remove non-adherent cells and then treated with normal or high glucose (4.5g/L) DMEM (Gibco) with or without the addition of recombinant mouse CD200Fc (R&D Systems, 3355-CD-050). After 48 hours, cells were washed two to three times with DPBS before RNA was extracted with the total RNA extraction kit (Qiagen) for cDNA preparation and RT-PCR.

**Bulk RNA-Sequencing.** Total RNA was isolated BV2 microglia as previously described (Methods 2.2). Total RNA quantity and integrity was determined using 4200 Tapestation. All samples (n = 12) contained 0.5-4.0ug RNA and had RIN > 9.5. Library preparation was performed by the Genome Technology Access Center (GTAC) through the McDonnell Genome Institute (MGI) with 0.5-1.0ug of total RNA per sample. Ds-cDNA was prepared using the SMARTer Ultra Low RNA kit for Illumina Sequencing (Takara-Clontech). Fragments were sequenced on an Illumina NovaSeq-6000 using paired end reads extending 150 bases. Basecalls and demultiplexing were performed with Illumina's bcl2fastq software with a maximum of one

mismatch in the indexing read. RNA-Seq reads were then aligned to the Ensembl release 101 primary assembly with STAR version 2.7.9a1. Gene counts were derived from the number of uniquely aligned unambiguous reads by Subread:featureCount version 2.0.32. Raw gene counts were then filtered based on a ≥1 CPM threshold for (n-1) samples in a given condition. Next, a standard EdgeR-limma analysis of gene-level features was performed, defining significant up- or downregulated genes as a |fold-change| > 1.50 with a FDR < 0.05. All further analysis and figures were generated in R (R Core Team).

**Synaptosome isolation and pHrodo labeling.** Fresh mouse retinas were harvested in ice-cold HBSS. Once vitreous and residual choroid-RPE was removed, retinas were homogenized (dounce kit) in Syn-PER gradient buffer. The homogenate was centrifuged at 1000g for 20 minutes to discard cell nuclei and debris and collect supernatant, which was then centrifuged at 16000g for 10 minutes to obtain synaptosome pellet. The pellet was then resuspended in 300uL HBSS and incubated with pHrodo Red succinimidyl (NHS) ester (Life Technologies, P36000) for 2 hours at room temperature on a table shaker at a concentration of 1:100 (after initial 1:100 dilution). After incubation, unconjugated pHRodo was washed out with several cycles of HBSS.

**In vitro microglial engulfment assay.** Equal amounts of pHrodo-red conjugated synaptosomes (500uL) were added to BV2 microglial cells following 4-chamber slide seeding and 48-hour pre-treatment with conditioned media. After incubation for 2 hours at 37C/5% CO2, cells were washed several times with DPBS to remove residual synaptosomes and then fixed in warm 10% formalin for 10 minutes. After fixation, cells were washed in DPBS twice more and then mounted (Vectashield with DAPI). To quantify fluorescence, images of BV2 cells were captured

using confocal microscopy and individual cell fluorescence intensity was calculated using corrected total cell fluorescence (CTCF) to account for background fluorescence.

**Intravitreal injections.** Mice were anesthetized by intraperitoneal injection of a mixture of ketamine and xylazine. For both eyes, an incision in the pars plana region of the sclera was made with a 30 G needle and injections of CD200Fc (2ug/uL; 1.5uL total) or an equal volume of PBS were carried out with a Hamilton syringe. Following injections, ophthalmic ointment was applied to the corneal surface.

**Electroretinography.** Scotopic electroretinography testing was performed as previously described (Chapter 3.2*).*

# 4.3 Results

## 4.3.1 Dysregulated CD200-CD200R signaling between amacrine cells and microglia correlates with retinal inflammation and microglia-amacrine contact

Changes in neuro-glial signaling within CNS tissue can impact microglia activation and function in disease. While hyperglycemia can directly impact microglia, we wanted to uncover potential ligand-receptor signaling changes in the diabetic retina that might explain the unique susceptibility of amacrine cells to aberrant contact and phagocytosis by microglia. To do this, we assessed whether microglia transcriptome changes from (Chapter 2) included dysregulation of ligand-receptor interactions. Among dysregulated 8wk STZ DEGs we identified 50 corresponding to known ligand-receptor interactions (Fig.4.1A-B)[211]. We found that *Cd200r4*, which encodes the receptor CD200R4, was one of only two receptor DEGs upregulated in

microglia at both diabetic time points (4wk STZ, 8wk STZ). In fact, both CD200R isoforms (*Cd200r1, Cd200r4)* expressed in microglia samples showed a disease chronicity-dependent upregulation across STZ time points (Fig.4.1C). In models of CNS neurodegeneration and stroke, increased CD200R expression on myeloid cells, and decreased expression of cognate CD200 on neurons correlates with microglial activation, inflammation, and disease progression[212,213,214]. Thus, we investigated whether the CD200-CD200R axis was dysregulated in the mouse retina during early DR. Consistent with previous reports, we found that in 8wk STZ mouse retinas transcript levels of *Cd200* decreased, *Cd200r1* and *Cd200r4* increased, and inflammatory cytokines such as *Il1b* and *Tnf* increased compared to control retinas (Fig.4.1D). Also, immunostaining for CD200R1 revealed that expression was exclusive to microglia that displayed hyperactivated morphologies in the IPL of 8wk STZ retinas but was undetectable in control retinas (Fig.4.1F). We also examined endogenous sources of CD200 in the mouse retina and found that expression was detected in RGC, IPL, and INL layers (Fig.4.1E). Furthermore, we found that CD200 fluorescence intensity was decreased in the retinas of 8wk STZ mice compared to controls, and similar to decreases in *Cd200* transcript. In the CNS, CD200 expressed by neurons interacts with microglial CD200R to inhibit various immune response and control microglial activation through inhibition of Ras/MAPK pathways[215]. We then revisited microglia-neuron interactions in 8wk STZ retinas and found that AC subtypes such as $CHAT^{+}$ and $AP2^{+}$ GABAergic ACs express CD200 in the healthy mouse retina (Fig.4.1G-H). However, 8wk STZ retinas showed both reduced numbers of CD200-expressing ACs and loss of CD200 expression in remaining ACs, suggesting that chronic hyperglycemia may decrease AC-derived sources of CD200 in the mouse retina. Furthermore, ACs contacted by activated microglia in diabetic mouse retinas lacked expression of CD200, suggesting decreased CD200-CD200R

interactions may elicit aberrant interaction and engulfment by microglia (Fig.4.1I). These experiments provide preliminary evidence of dysregulated CD200-CD200R signaling between microglia and amacrine cells as a potential mechanism underlying aberrant microglia activation and contact with amacrine cells.

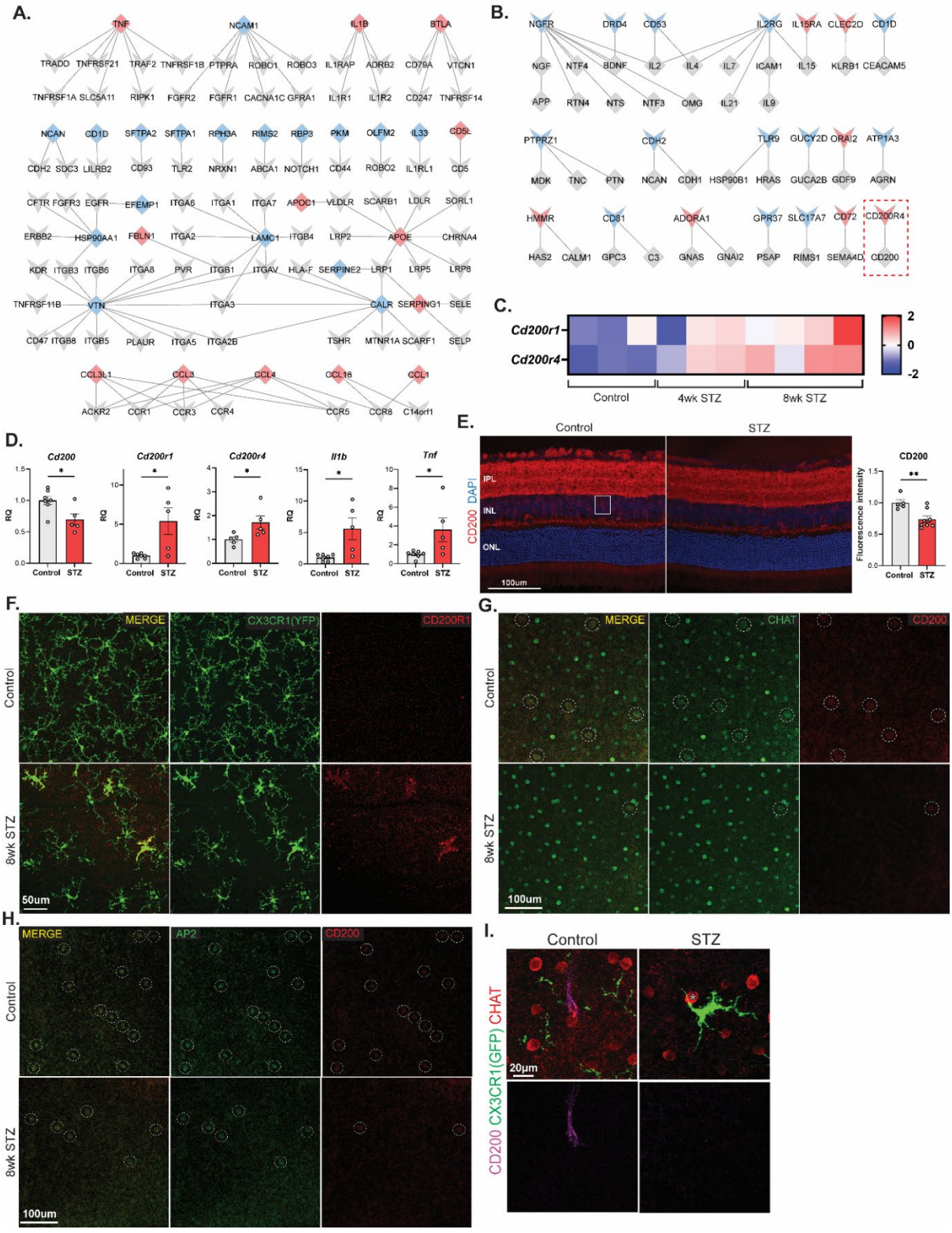


**Figure 4.1: Dysregulated CD200-CD200R signaling in early diabetes correlates with retinal inflammation and microglia-amacrine contact.** (A-B) Signaling networks for ligands (A) and receptors (B) dysregulated in 8wk STZ microglia and their cognate binding partners. Networks

were constructed in Cytoscape using DEGs identified in (*Fig.2.9B*) that correspond to known ligand-receptor pairs. Red or blue ligands and receptors correspond to increased or decreased expression compared to control microglia, respectively. CD200R4-CD200 binding partners are outlined in red. (C) Heatmap showing *Cd200r1* and *Cd200r4* expression in microglia RNA Sequencing samples from (*Fig.2.9B*). Gene expression is presented on a color gradient scale derived from normalized (Z-score) gene counts. (D) Bar graphs showing expression levels of genes analyzed by quantitative polymerase chain reaction (qPCR) using mouse retinal tissue. Each bar (n=5-7 mice per group) indicates the mean ± SEM of gene expression standardized to control values. Statistical significance among groups for each gene was determined using the Mann-Whitney U test. (E) Representative confocal images (left) and bar graph (right) showing CD200 fluorescence intensity in the retinas of control and 8wk STZ mice. These images are of immunostained cryo-sectioned retinas and are maximum projections of the section shown. Individual INL neuron expressing CD200 is outlined by a white square. Each bar (n=5-8 mice per group) indicates the mean ± SEM fluorescence intensity standardized to control values. Each mouse count is an average from four retina sections and fluorescence was calculated using corrected total cell fluorescence (CTCF). Statistical significance among groups for mean fluorescence was determined using the Mann-Whitney U test. (F) Representative confocal images showing CD200R1 expression in the retinas of control and 8wk STZ mice. These images are of immunostained flat-mounted retinas and are maximum projections of the IPL. (G-H) Representative confocal images showing CD200 expression in CHAT+ (G) and AP2+ (H) amacrine cells in the retinas of control and 8wk STZ mice. These images are of immunostained flat-mounted retinas and are maximum projections of the INL. Individual nuclei co-expressing CHAT or AP2 and CD200 are indicated by white dotted circles. (I) Representative high magnification images of CD200 expression in CHAT+ amacrine cells in the INL of control and 8wk STZ mice. These images are of immunostained flat-mounted retinas and are maximum projections of the INL. CHAT+ amacrine cells contacted by activated microglia are indicated with a white asterisk (*P<.05; **P<.01).

### 4.3.2 CD200Fc attenuates high glucose-induced microglial inflammation *in vitro*

CD200R signaling with exogenous CD200 fusion protein (CD200Fc) has been shown to ameliorate microglia activation and features of disease progression[216,217]. To examine whether CD200R binding could resolve microglia-mediated neuroinflammation in diabetes, we first created a cell culture model of hyperglycemia by treating BV2 microglia cells in normal (1g/L) or high (4.5g/L) glucose media to mimic blood-glucose concentrations of STZ diabetic (450mg/dL) and control (100mg/dL) mice used in previous experiments. We also treated cells with or without CD200Fc to examine the impact of CD200Fc on glucose-stimulated microglia

(Fig.4.2A). High glucose stimulation of microglia resulted in upregulation of nitrogen oxide species production (*Nos2)* and pro-inflammatory cytokines (*Il1b, Tnf*) similar to DR-associated microglia *in vivo* after 48hrs. Interestingly, CD200Fc suppressed high glucose-induced production of these transcripts in a concentration-dependent manner (Fig.4.2B). This *in vitro* experiment demonstrates that therapeutic targeting of the microglia-specific CD200R with CD200Fc can inhibit their inflammatory activation in BV2 microglia.

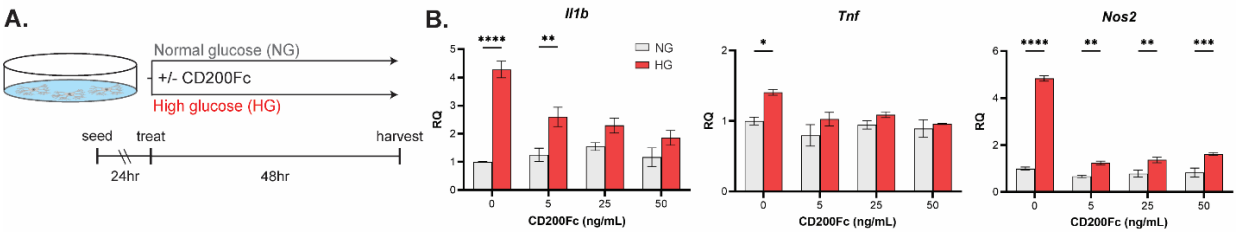


**Figure 4.2: CD200Fc attenuates high glucose-induced microglial inflammation *in vitro.*** (A) Schematic of seeding, treatment, and harvest schedule for BV2 microglia cells using normal (1.0g/L) or high (4.5g/L) glucose media with or without CD200Fc. (B) Grouped bar graphs showing expression levels of genes analyzed by quantitative polymerase chain reaction (qPCR) using BV2 microglia cell lysates following glucose-CD200Fc media treatment for 48hrs. Statistical significance among groups was determined using two-way ANOVA tests followed by Bonferonni's post hoc test for multiple comparisons (*P<.05; **P<.01; ***P<.001; ****P<.0001).

### 4.3.3 CD200Fc suppresses transcriptional programs related to inflammation, phagocytosis, and complement signaling in high glucose-treated microglia *in vitro*

In identifying an optimal concentration of CD200Fc capable of suppressing high glucose-induced production of inflammatory cytokines, we wanted to interrogate broader transcriptional programs affected by CD200Fc treatment. To do this, we generated purified mRNA samples from BV2 microglia treated with normal or high glucose cell media supplemented with or without CD200Fc (50ng/mL) as previously described (Figure 4.2). Following assessment of

RNA quantity and purity, we performed RNA sequencing and used a standard EdgeR-limma pipeline analysis on all samples (n=12) to compile differentially expressed genes (DEG; >|1.5|FC; FDR< .05) for each paired comparison of interest. Using multidimensional scaling, we found consistent clustering of samples by condition but noticed that HG and HG+CD200 clusters were separated from NG and NG+CD200 clusters, which overlapped with one another (Fig.4.3A). Consistent with this analysis, we identified 2064 total DEGs when comparing conditions but the majority of these resulted from comparing HG against NG (1329) and HG+CD200 against HG (748) (Fig.4.3B). Next, we examined genes at the intersection of these comparisons to enhance our understanding of high glucose-induced gene expression patterns suppressed by CD200Fc treatment. We found 429 DEGs within this intersection that were predominantly increased when comparing HG against NG but decreased when comparing HG+CD200 against HG. Among these were genes related to inflammation (*Mmp9, Nos2, C3, Slfn4, Adgre1, Stat2, Irf7)*, phagocytosis (*Marco, C3, Cd300lf),* and glycolysis (*Slc16a3, Slc2a6)* (Fig.4.3C). Interestingly, many of these same genes were among the most downregulated when comparing HG+CD200 against HG (Fig.4.3D). We next ran Kyoto Encyclopedia of Genes and Genomes (KEGG) pathway analysis on these downregulated genes and found that the top suppressed gene sets were related to NOD-like receptor signaling, antigen processing and presentation, complement signaling, and phagocytosis, suggesting that CD200Fc potently inhibits high glucose-induced transcription underlying inflammation and scavenger-related functions in cultured microglia. These data demonstrate that beyond suppression of primary inflammatory cytokine production, CD200Fc treatment is capable of attenuating a broad range of transcriptional changes in the context of high glucose stimulation, which may impact microglial function.

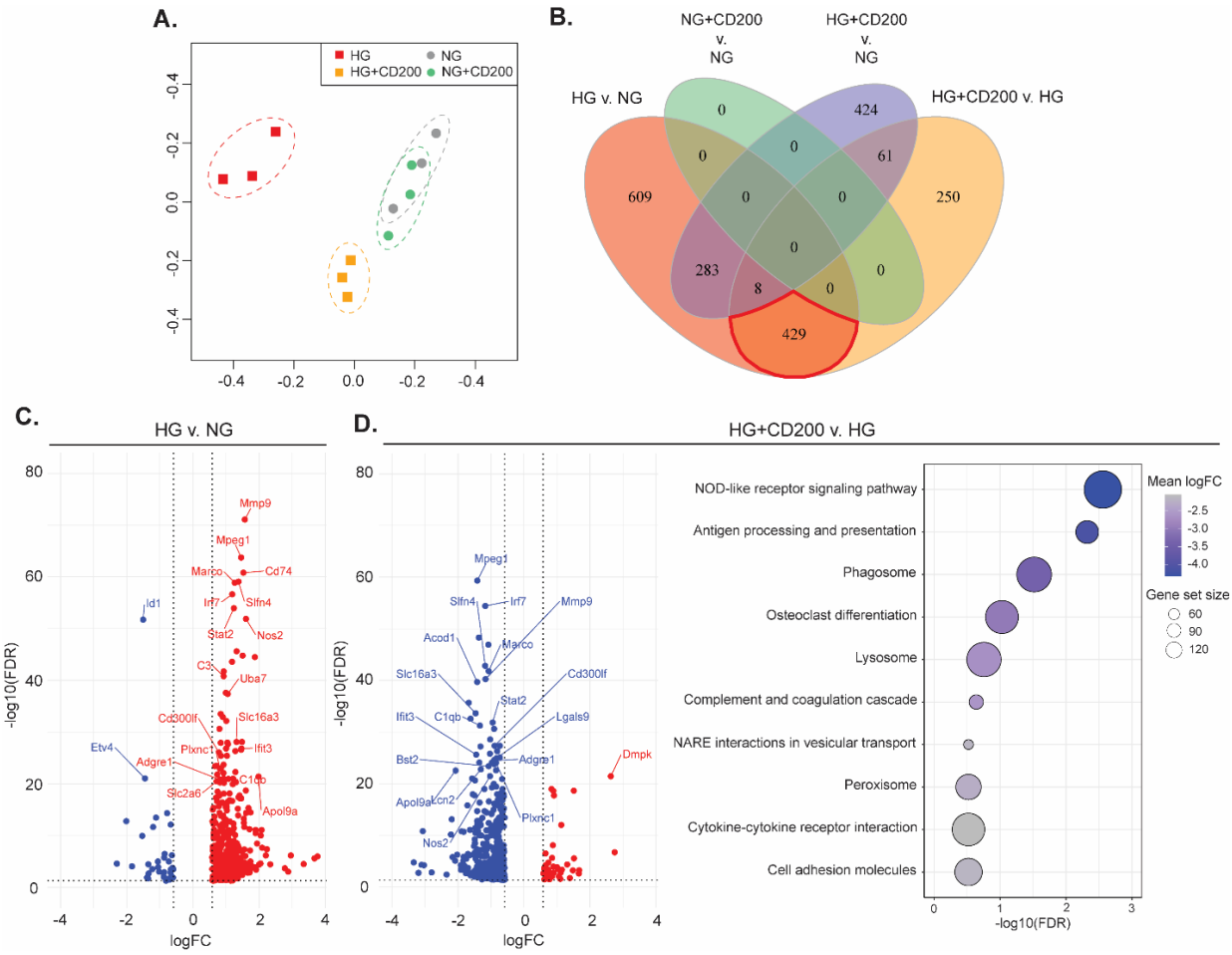


**Figure 4.3: CD200Fc suppresses high glucose-induced transcriptomic changes that drive inflammation, phagocytosis, and complement signaling.** (A) Multidimensional scaling plot (MDS) showing clustering of, and separation of, RNA-Sequencing samples (n=3 per group) for BV2 microglia. (B) Grouped Venn diagram showing the number of differentially expressed genes (DEGs) for each condition comparison of interest. DEGs at the intersection of 'HG v. NG' and 'HG+CD200 v. HG' comparisons are outlined in red. (C) Volcano plot showing DEGs that are either increased (red) or decreased (blue) in HG samples compared to NG samples. (D) Volcano plot (left) showing DEGs that are either increased (red) or decreased (blue) in HG+CD200 samples compared to HG samples and dot plot (right) showing Kyoto Encyclopedia of Genes and Genomes (KEGG) gene sets with the greatest average decreased expression in HG+CD200 samples compared to HG samples.

## 4.3.4 CD200Fc suppresses high glucose-induced microglial phagocytosis *in vitro*

Acute high glucose exposure has been shown to stimulate surveillance and scavenging functions in BV2 microglia[218]. Since CD200Fc suppressed transcriptional patterns related to

phagocytosis and lysosome function in high glucose-treated microglia, we wanted to test if microglia upregulated these functions *in vitro* similarly to aberrant phagocytosis observed in STZ mice *in vivo.* To do this, we stimulated BV2 microglia for 48 hours as previously described before exchanging for media containing isolated synaptosomes from mouse retina tagged with pHRodo conjugated dye. After 2 hours of synaptosome exposure, we found that microglia pre-treated with high glucose showed a greater accumulation of fluorescent synaptosomes compared to normal glucose-treated microglia (Fig.4.4A-B). However, microglia pre-treated with CD200Fc-supplemented high glucose media showed fluorescent profiles more similar to normal glucose-treated microglia. Furthermore, microglia pre-treated with CD200Fc-supplemented normal glucose media showed synaptosome uptake that did not significantly differ from that of normal glucose media-treated microglia, suggesting that CD200Fc suppresses high glucose-stimulated synaptosome engulfment *in vitro*. These data indicate that high glucose stimulation of microglia results in upregulated surveillance and phagocytosis *in vitro* similar to what we observe in DR-associated microglia *in vivo.* This also demonstrates that in addition to transcriptional activity, CD200Fc treatment also effects microglial function.

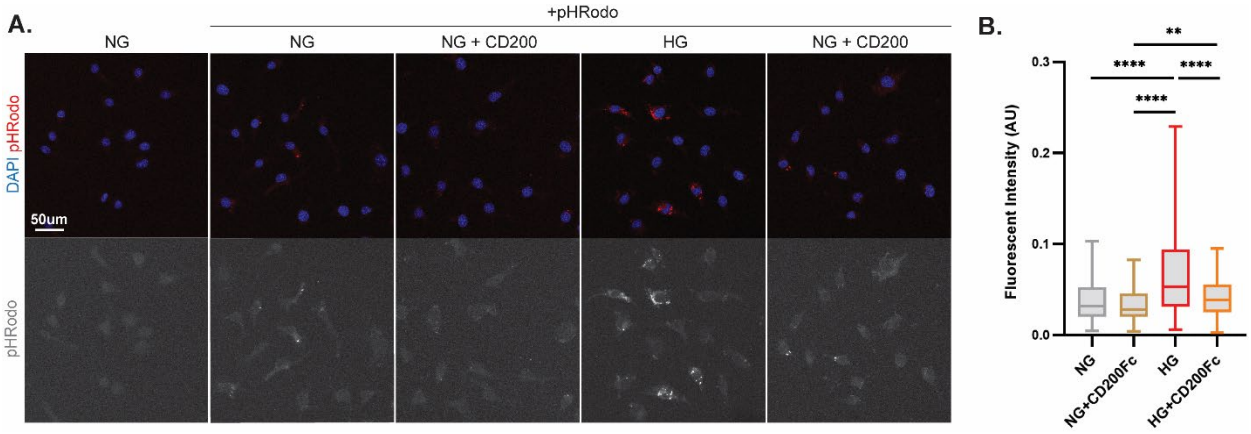


**Figure 4.4: CD200Fc suppresses high glucose-induced microglial phagocytosis *in vitro.*** (A) Representative images of BV2 microglia following pHRodo-tagged synaptosome treatment. (B) Box and whisker plot showing BV2 microglia fluorescent intensity represented in (A, pHRodo). Each plot (NG, n=245; NG+CD200, n=238; HG, n=223; HG+CD200, n=220) indicates the

median, maximum and minimum, and interquartile range. Statistical significance among groups was determined using the Kruskal-Wallis test followed by Dunn's post hoc test for multiple comparisons (**P<.01; ****P<.0001).

### 4.3.5 CD200Fc prevents DR-associated visual dysfunction, retinal inflammation, and microglia activation *in vivo*

Given the therapeutic potential of CD200Fc in models of CNS disease, and our demonstrations *in vitro*, we wanted to test whether CD200Fc could prevent features of microglia-mediated retinopathy in the STZ mouse. To do this, we administered single intravitreal injections of CD200Fc (2µg/uL; 1.5uL) or PBS into the eyes of control (CTRL+PBS) or 4wk STZ (STZ+CD200Fc; STZ+PBS) mice since we previously identified robust transcriptional changes in DR-associated microglia between 4- and 8-weeks STZ (Fig.4.5A). We then assessed visual function, microglia morphology, and retinal inflammation 4 weeks later (8wk STZ). First, CD200Fc did not alter weight change or blood glucose trends in STZ mice (Fig.4.5B). Next, we found that scotopic a- and b-wave amplitude responses were significantly increased in STZ+CD200Fc mice compared to STZ+PBS mice following mid to high intensity flash stimuli (-16 – 5db) (Fig.4.5C-D). Furthermore, combined OP amplitude responses driven by amacrine cells were significantly decreased in STZ+PBS mice compared to CTRL+PBS mice at lower flash intensities (-20db) but significantly increased in STZ+CD200Fc mice compared to STZ+PBS at mid-range flash intensities (-10 – 0db). In examining microglial morphology, we expectedly observed irregularly distributed and less ramified microglia in the OPL of STZ+PBS retinas but microglia in the OPL of STZ+CD200Fc retinas appeared highly ramified and more evenly distributed, similar to that of CTRL+PBS retinas (Fig.4.6A). Furthermore, we observed less hyperactivated microglia in the IPL of STZ+CD200Fc retinas compared to STZ+PBS retinas. Lastly, we found that transcript levels of *Cd200r1* and inflammatory cytokines (*Tnf,*

*Nos2, Il6, Il1b, Ccl2)* were expectedly increased in STZ+PBS retinas compared to CTRL+PBS retinas but expression levels were decreased in STZ+CD200Fc retinas compared to STZ+PBS, and more similar to CTRL+PBS baselines (Fig.4.6B). These data suggest that CD200Fc can prevent visual dysfunction, microglial activation, and retinal inflammation during early-stage DR in the STZ mouse. Furthermore, we show that this therapeutic effect can be achieved with a single intravitreal injection and sustains for at least 1 month after injection.

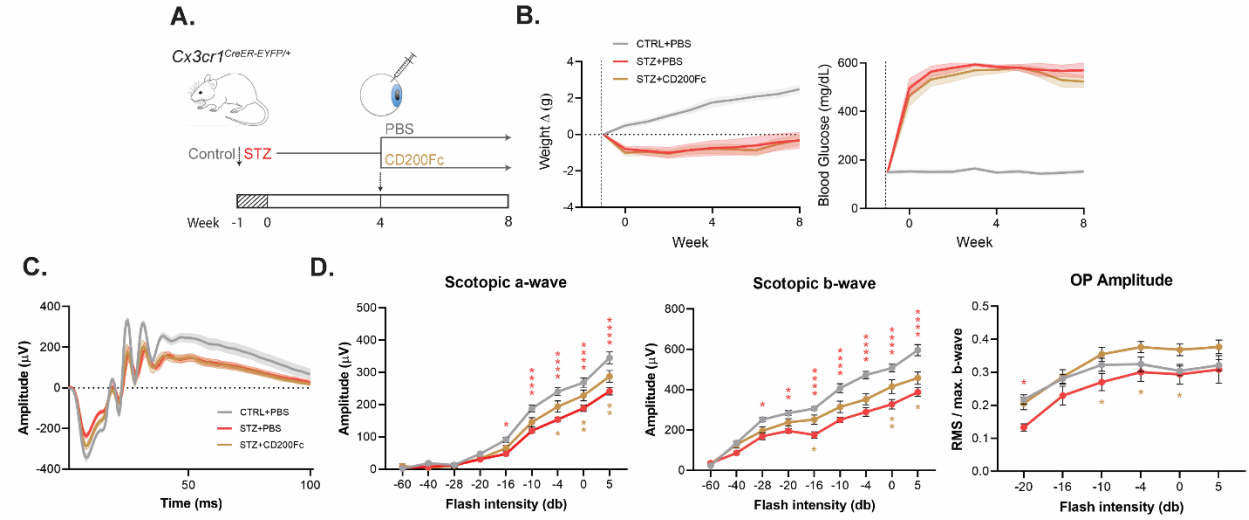


**Figure 4.5: CD200Fc prevents visual dysfunction *in vivo* during early-stage DR.** (A) Schematic of intraperitoneal (Control/STZ) and intravitreal (PBS/CD200Fc) injections for *Cx3cr1*$^{\text{CreER-YFP/+}}$ mice. (B) Line graphs showing weight change (left) and blood glucose measurements (right) in mouse groups. Each line (n=7-9 mice per group) indicates the mean ± SEM calculated for animals used in the study. Black vertical dashed line indicates time of intraperitoneal injection. (C-D) Line graphs showing scotopic electroretinogram (ERG) response waveforms (C), and a-wave, b-wave, and combined OP amplitudes (D) for each mouse group. Data (n=7-9 mice per group) indicates the mean ± SEM amplitude. Statistical significance among groups was determined using two-way ANOVA test followed by Bonferonni's post hoc test for multiple comparisons. Red asterisks in (D) indicate multiple comparisons test results between STZ+PBS and CTRL+PBS groups while beige asterisks indicate results between STZ+CD200Fc and STZ+PBS groups (*P<.05; **P<.01; ***P<.001; ****P<.0001).

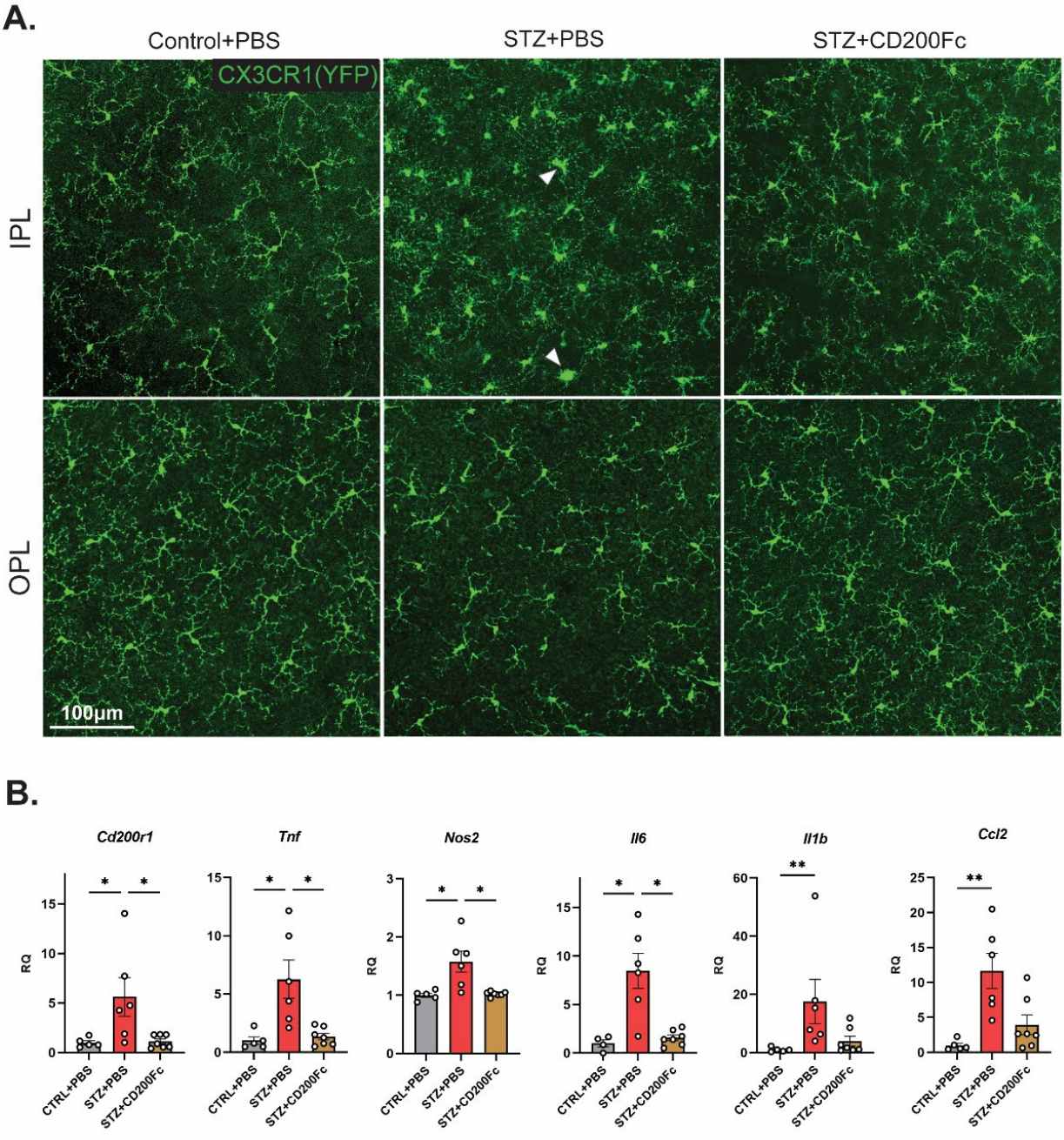


**Figure 4.6: CD200Fc prevents microglial activation and retinal inflammation *in vivo* during early-stage DR.** (A) Representative confocal images showing microglia morphology and organization in the IPL and OPL of tested mouse groups. These images are of flat-mounted retinas and are maximum projections of the retinal layers shown. Example hyperactivated microglia are indicated by white arrowheads. (B) Bar graphs showing expression levels of selected genes by qPCR. Each bar (n=5-7 mice per group) indicates the mean ± SEM of gene expression standardized to control values. Statistical significance among groups for each gene was determined using the Kruskal-Wallis test followed by Dunn's post hoc test for multiple comparisons (*P<.05; **P<.01).

## 4.4.4 Discussion

The leading observation from our ligand-receptor analysis of DR-associated microglial transcriptome dataset is that CD200R isoforms are upregulated in microglia during early-stage DR. Increased microglial expression of CD200R correlates with their activation and disease pathogenesis[219,213]. CD200 is a transmembrane glycoprotein expressed by neurons and epithelial cells that, upon interacting with its receptor, attenuates immune responses[215]. Interestingly, decreased expression of CD200 in CNS neurons, or blocking of CD200R binding, correlates with increases in myeloid cell CD200R expression, and neurodegeneration[212,220,221]. In the retina, this paradigm has also been shown to play roles in animal models of experimental autoimmune uveitis and glaucoma, suggesting that this signaling axis may play a role in other retinal diseases[98,214]. Here, we report that CD200 expression decreases broadly in the inner retinas of STZ-induced diabetic mice. Furthermore, we observe loss of CD200 expression in AC subtypes in diabetic mice, which correlates with contact by activated microglia and inflammation in the retina. In proposing that an imbalance in neuronal CD200 and microglial CD200R contributes in part to microglia-mediated retinopathy, we attempted to enhance microglial CD200R signaling via CD200Fc. Similar to benefits shown in other disease models, we show that CD200Fc attenuates high glucose-induced inflammation, transcriptomic alterations, and phagocytosis *in vitro*[216,217,222]. More importantly, we show that CD200Fc therapy at a single time point prevents visual dysfunction, microglial activation, and retinal inflammation *in vivo* one month later, providing an avenue to treat early-stage DR in the mouse (Fig.4.7). However, further testing will be necessary to determine whether CD200Fc treatment limits microglial phagocytic capacity *in vivo,* prevents neurodegeneration of amacrine cells and other key cell types, and sustains therapeutic benefits beyond the short experimental window we investigate in the present study.

To this end, future work will need to investigate whether long-term inhibition of microglia via CD200-CD200R signaling dampens potentially beneficial roles of this cell type and others within the diabetic retinal milieu.

Overall, this study represents a significant advancement in our understanding of inner retinal degeneration during early-stage DR. Microglia dominate the local immune environment of the retina and are actively involved in concurrent neurodegeneration and visual dysfunction. Within this landscape of early disease, we have identified CD200-CD200R dysregulation as a novel mechanism underlying microglia-mediated retinopathy in the diabetic mouse. Furthermore, we provide strong evidence of the therapeutic value that CD200R signaling provides in the case of hyperglycemia-induced microglia activation. Through this work, we have created a framework for future development of this novel therapy in animal models and potentially DR patients.

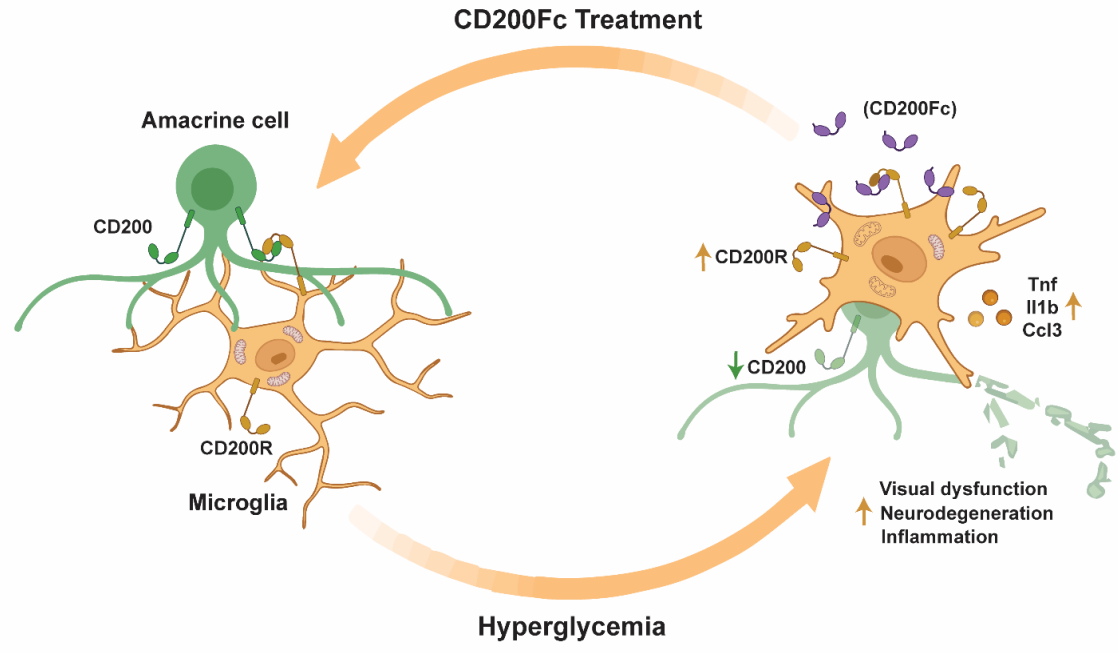


**Figure 4.7: Schematic of proposed CD200Fc treatment mechanism.** Illustration of proposed mechanism for treating CD200-CD200R dysregulation underlying microglia-mediated retinopathy during early-stage DR via CD200Fc treatment.

# Chapter 5: Future Directions

Microglia continue to prevail as a primary contributor to CNS disease pathogenesis. In this thesis, we tested this phenomenon in the context of diabetic retinopathy (DR), which poses the greatest global threat to vision. Here, we will discuss potential future directions that could be investigated to further enhance our understanding of microglial function in DR and broader CNS disease contexts.

## 5.1 Microglia-vascular interactions in DR

In chapter 2, we perform a comprehensive survey of retinal neurovascular unit components implicated in DR literature to examine the temporal emergence of phenomena such as glial reactivity, blood retina barrier (BRB) compromise, and peripheral immune cell infiltration. We convincingly show that during the first 2 months of hyperglycemia-induced DR in the STZ mouse, microglia display robust changes in morphology, ultrastructure, and transcriptome while vascular integrity, macroglial reactivity, and local immune composition remain unchanged. However, the limited methodology we implemented in these investigations prohibits us from ruling out the occurrence of more acute changes. There is a growing appreciation in the DR field for innovative imaging and analysis software that can be utilized to detect acute vascular changes in early DR prior to obvious changes in permeability. Using these methods, recent demonstrations have suggested that vessel dilation, blood flow changes, and microvascular density reductions may be early markers of retinopathy in patients[223,224,225,226]. Interestingly, a recent report has shown that microglial fractalkine signaling (CX3CL1-CX3CR1) and contact with capillary vessels underlies decreased blood flow and vasomodulation of capillary vessels during early-stage DR in the STZ rat[161]. Even in our own transcriptomic

assessment of microglia we identified a gene set related to vascular permeability during acute inflammatory response upregulated in 8wk STZ microglia (Figure 2.10B). To this end, microglia may mediate various features of diabetic vasculopathy in addition to their role in neuroinflammation. To interrogate this further, we could implement a longitudinal tail vein sodium fluorescein study in diabetic microglia-privileged and microglia-ablated mice to track primary arteriole and venule blood flow dynamics and vessel diameter to evaluate phenotypes from the previous study in higher order vessels. Acellular capillaries, pericyte dropout, and microvascular density are additional features of DR that we could evaluate as well. Seeing as ophthalmic imaging in our lab is limited by the Phoenix Micron instrument, we may also implement *in vivo* two-photon microscopy through collaboration within our department, to enhance resolution and precision of blood flow and microglia-vessel contact in real time. By combining our refined approaches to studying microglia with improved methods for ophthalmic imaging we may be able to advance the field's understanding of microglial involvement in vascular features of DR across various stages of pathogenesis.

## 5.2 Microglia-mediated recruitment of peripheral immune responses during DR

We report that local immune cell composition in the retinal parenchyma does not significantly change during early-stage DR, distinguishing microglia as the prominent resident immune cell species. However, flow cytometry analysis of dissociated retinal tissue prevents our ability to examine whether intravascular leukocyte adhesion is increasing in retinal vessels. Increased "rolling" and adhesion of leukocytes inside vessel walls has been shown to occur prior to extravasation into the retinal parenchyma in inflammatory eye diseases, including DR[227,228,229].

Although we did not observe significant peripheral immune cell infiltration during early-stage DR, we are interested in whether ablation of microglia, or inhibition of microglia via CD200Fc, may prevent intravascular adherence of leukocytes and their infiltration of the retina during established stages of DR. This is supported by our data showing increased chemokine (*Ccl2, Ccl3)* transcript production in DR-associated microglia (Fig.2.8) and suppression these transcript levels in the diabetic retina following intravitreal injection of CD200Fc (Fig.4.6). To investigate this question, we could implement tail vein injections of FITC-conjugated dye and cardiac perfusion procedures to label adherent leukocytes in the retinal vasculature followed by confocal imaging and quantification to compare adherent cells in high and low-order vessels among diabetic microglia-privileged and microglia-ablated animals. We could also take blood samples from these mice to investigate circulating levels of monocytes via flow cytometry or inflammatory mediators via qPCR to assess whether microglial inflammatory responses in the retina make meaningful contributions to peripheral immune responses during early-stage DR. Through these experiments, we could expand our understanding of microglial involvement in DR pathogenesis beyond local signaling within the retina.

## 5.3 Non-microglial immune cell contributions to DR

In chapter 3, we show that chronic ablation of retinal microglia prevents visual dysfunction and neurodegeneration associated with early-stage DR. However, we cannot exclude that depletion of resident non-microglial macrophages (<1%), intravascular adherent leukocytes, and a portion of circulating monocytes via tamoxifen treatment in $Cx3cr1^{CreER\text{-}YFP/+};Rosa26^{DTA/+}$ mice may also contribute to these observed phenotypes. Furthermore, our method is systemic, meaning all CNS *Cx3cr1*-expressing cells are ablated, so we are unable to control for the effects

of microglia ablation in the diabetic brain and spinal cord. This is important given that diabetes has been shown to induce brain atrophy and cognitive decline[230,231]. While our DTA control allowed us to rule out effects of *Cx3cr1*-expressing cell ablation in healthy animals, we are interested in further teasing apart the relative contributions of resident non-microglia macrophages, intravascular leukocytes, and monocytes in diabetes, as they have been implicated independently in DR pathogenesis[232,233,175]. To accomplish this, we could implement $Ccr2^{CreER/+}$ and $Lysm^{CreER/+}$ crosses with $Rosa26^{DTA/+}$ mice to continuously ablate monocytes and monocyte-derived macrophages, respectively, and perform similar experiments to those performed in chapter 3. To target the retina specifically, we could attempt intravitreal injections of tamoxifen, which has not been attempted previously and would require some troubleshooting, but would allow us to eliminate potentially confounded phenotypes based on non-retinal CNS ablation of microglia. We also could administer PLX5622, a CSF1R inhibitor that induces myeloid cell ablation, to healthy and diabetic mice to assess whether observed phenotypes parallel those generated with $Cx3cr1^{CreER\text{-}EYFP/+}$; $Rosa26^{DTA/+}$ mice[234]. These experiments have the ability to not only strengthen our claims of microglia-mediated features of DR but untangle the relative contributions of other immune cell types known to contribute to DR pathogenesis. In doing this, development of alternative therapies to target the peripheral immune response, in addition to the innate immune response, in DR may be possible.

## 5.4 Exploring the triggers of CD200-CD200R dysregulation

We show that dysregulation of CD200-CD200R signaling contributes to microglia-mediatedretinopathy in early diabetes but how and why these proteins decrease and increase in amacrine cells and microglia, respectively, remains unclear. By investigating dysregulated neuro-glial signaling in other disease contexts we may be able to generate potential explanations

for this phenomena in DR. Fractalkine-mediated (CX3CL1-CX3CR1) communication between neurons and microglia has been shown to mediate microglia activation and disease progression[235]. Similar to the CD200-CD200R axis, studies have demonstrated that decreased neuronal CX3CL1 as a function of CNS disease, or absence of CX3CR1 in transgenic mouse species, exacerbates disease phenotypes and microglial activation but is amenable to exogenous sources of CX3CL1[236,237,238]. To test whether CD200-CD200R dynamics are a direct result of hyperglycemia we could implement additional models of retinal neurodegeneration such as light damage-induced or NMDA excitotoxicity models and observe if CD200 expression decreases similarly in retinal neurons such as amacrine cells. We could also develop a neuron and microglia co-culture *in vitro* model and expose both cell types to high glucose media and assess whether CD200 and CD200R expression is altered in a similar manner to our *in vivo* model. There is also the possibility that increased CD200R expression in microglia is a compensatory response to decreased CD200 expression in amacrine cells and not related to high glucose exposure. To test this, we could apply a small interfering ribonucleic acid (siRNA) to silence CD200 expression in cultured neurons plated with normal glucose media and assess whether CD200R expression increases in co-cultured microglia. These experiments would clarify the respective triggers of CD200-CD200R dysregulation in diabetes and further inform therapeutic development.

CD200R expression increases over the course of early DR but there is some controversy over the function of this. We observe this increased expression in activated microglia that is associated with aberrant phagocytosis and production of pro-inflammatory mediators. However, others have reported increased CD200R expression as a marker for alternatively activated macrophages (M2a) that increase phagocytic capacity but also produce growth factors and anti-

inflammatory mediators to promote tissue repair[239]. Admittedly, our microglia RNA-Sequencing data points to a phenotype that is puzzling – pro-inflammatory but not glycolytic, yet prone to scavenging functions and enhanced lipid metabolism. Heterogeneity among activated microglia in disease is a widely accepted phenomenon, but one that requires careful investigation. To properly resolve whether the DR-associated microglia we describe are made up of one or several subpopulations of microglia we could use single cell RNA-Sequencing (scRNA-Seq). Microglia make up 0.2% of all cells in the retina, making traditional scRNA-Seq of microglia using whole-retina suspensions difficult and inefficient[109]. Alternatively, we could implement fluorescent-activated cell sorting-driven (FACS) isolation of microglia at a 1:1 capture in wells pre-filled with master mix components for scRNA-Seq to ensure proper cell yields and maximize read depth per cell. In doing so, we may find that a predominant subpopulation of pro-inflammatory microglia exists, as we and others have observed, but also smaller M2a or similar subpopulations. Resolving this question will be important in determining whether broad inhibition of retinal microglia with CD200R signaling is the best approach to treating DR, or if this may neutralize beneficial contributions of a small yet crucial minority. This may also reveal additional genes related to activation states of detrimental subpopulations which would further refine therapeutic targeting.

## 5.5 Mechanisms of microglial phagocytosis mediated by CD200R signaling

We have shown that microglia participate in excessive phagocytosis of amacrine cells and synapses, and that CD200Fc inhibits high glucose-induced phagocytosis and supporting transcriptional changes *in vitro.* To this end, we are interested in determining whether CD200R

signaling can inhibit aberrant phagocytic behavior of microglia during DR. Microglia participate in phagocytosis of dead and dying neurons to reduce inflammation but also engulf live neurons in pathological contexts[240]. While phagocytosis is mediated by various mechanisms, excessive 'tagging' and phagocytosis of neuronal synapses through complement-mediated pathways is a consistent feature of Alzheimer's disease, multiple sclerosis, and stroke in mouse models[241,242,243,244,245]. We have shown that traditional 'eat me' signals like Calreticulin, and the bridging molecules associated with recognition and phagocytosis of the dying neurons that present them, such as *Mfge8,* are not only unchanged in diabetic mouse retinas, but also unaffected by CD200Fc treatment (Fig.5.1A). However, primary complement proteins C3, C1q, C3ar, and C5ar, are robustly increased in diabetic retinas but suppressed following CD200Fc injection (Fig.5.1B). Furthermore, we observe increased numbers of hyperactivated C3-positive microglia in the IPL of diabetic mouse retinas compared to control and diabetic CD200Fc-injected retinas (Fig.5.1C). This suggests that complement-mediated phagocytosis may be the mechanism underlying the aberrant phagocytic microglial phenotype. This is further supported by our *in vitro* data which demonstrated that transcription of C3 and other complement components in BV2 microglia was stimulated by high glucose media but suppressed following addition of CD200Fc. We hypothesize that aberrant complement-mediated synapse remodeling by microglia may lead to neuronal dysfunction and eventual apoptosis. This is supported by our data that shows robust increases in microglial contact of amacrine cells but instances of soma engulfment being rarer. One way to investigate this further would be to examine C3 expression co-localized at retinal synapses in control and diabetic retinas to first confirm increased synapse "tagging". To confirm that increased synapse tagging of C3 is due to microglia, we could then examine expression levels in STZ DTA mouse retinas expecting levels to return to that of

control. We could also examine C3 expression in retinal synapses, and their general densities, following CD200Fc treatment *in vivo* to determine whether CD200R signaling can attenuate aberrant complement-mediated phagocytosis of retinal synapses by microglia in DR. Investigating the underlying mechanism of aberrant microglial phagocytosis will not only clarify their role in DR but provide critical knowledge for enhancing our general understanding of synaptic pathology across retinal diseases.

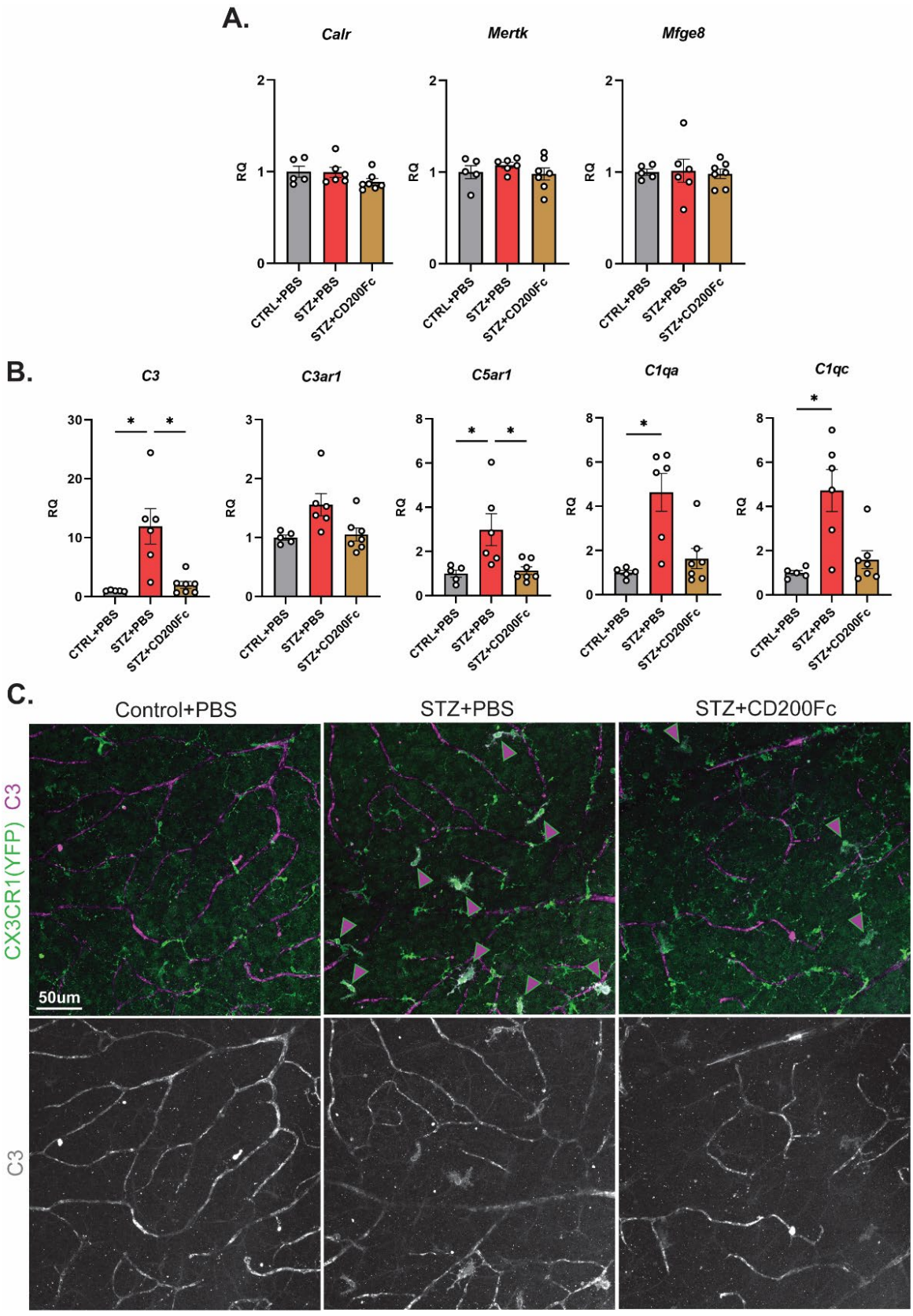
A.
Calr
Mertk
Mfge8
RQ
CTRL+PBS
STZ+PBS
STZ+CD200Fc
B.
C3
C3ar1
C5ar1
C1qa
C1qc
C.
Control+PBS
STZ+PBS
STZ+CD200Fc
CX3CR1(YFP) C3
C3
50um

**Figure 5.1: CD200Fc attenuates complement-mediated phagocytosis components in the diabetic retina while classical phagocytosis components remain unchanged.** (A-B) Bar graphs showing expression levels of selected genes related to classical (A) and complement-mediated (B) phagocytosis by qPCR. Each bar (n=5-7 mice per group) indicates the mean ± SEM of gene expression standardized to control values. Statistical significance among groups for each gene was determined using the Kruskal-Wallis test followed by Dunn's post hoc test for multiple comparisons. (C) Representative confocal images of complement-3-positive (C3) microglia in the IPL of mouse retinas. CX3CR1-positive microglia expressing C3 are indicated by purple arrowheads (*P<.05).

# 5.6 Investigating CD200-CD200R expression patterns in humans

We are interested in translating success in treating DR mice with CD200Fc to treating patients in the clinic. Currently, no treatments for early-stage DR exist, so finding a way to introduce local administration of a CD200R agonist to preserve retinal function, reduce inflammation, and improve quality of life in diabetic patients would be an immense advancement in the field. To begin this process, we have investigated CD200 expression in the human retina using a published single-nuclei RNA-seq (snRNA-seq) transcriptomic dataset of human retinal tissue and an interactive web-based resource for exploring previously published single-cell RNA sequencing data from ocular studies[246,247]. Analysis of standardized CD200 expression across major retinal cells revealed that expression was high in amacrine cells and moderate in bipolar cells (Fig.5.2A-B). Next, we looked closer at the amacrine cell cluster and found that individual cells either highly expressed CD200 or not at all (Fig.5.2C). There are currently over 40 identified amacrine cell subtypes in the human retina and over 60 subtypes in the mouse retina, with complex morphological and functional characteristics[248,249,250]. To this end, the expression pattern we observe in this human dataset may indicate that specific amacrine subtypes express CD200, but uncovering their identities will require further investigation. Through collaborative

efforts, we have also performed preliminary immunostaining of CD200 in healthy human retinas, which shows similar expression in the INL and IPL as we have found in the mouse retina (Fig.5.2D). Future efforts will be devoted to staining diabetic patient retinas to determine if diabetes causes decreases in CD200 expression. Furthermore, microglia activation has been previously described in diabetic patient retinas so examining CD200R expression, and its potential labeling of activated microglia, would further translate our findings in the mouse. Gene polymorphisms have been identified that associate with predisposition for and severity of DR[251]. This raises the question as to whether *Cd200* or *Cd200r* mutations may be associated with more severe DR or rapid progression. To evaluate this, we could look into comprehensive and interactive gene association databases such as DisGeNET to explore gene-disease associations in diabetic individuals related to the CD200-CD200R signaling axis[252]. A discovery regarding a genetic predisposition to dysregulated CD200-CD200R signaling would strengthen our claim in targeting this pathway in diabetic humans to treat DR.

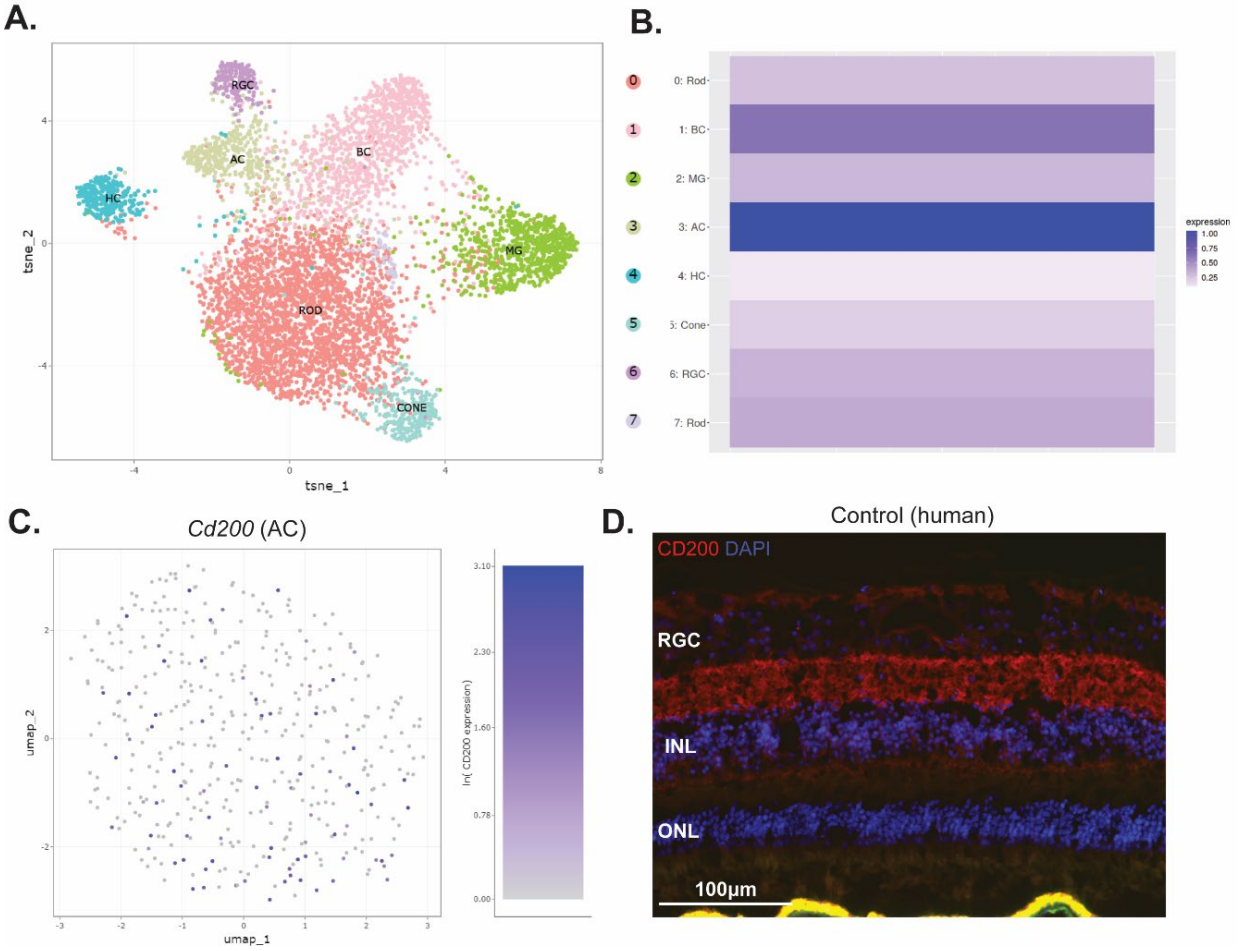


**Figure 5.2: CD200 expression in the healthy human retina.** (A) TSNE plot of single cell RNA-Sequencing data from[ref] analyzed using eye-seq.org. (B) Normalized expression of *Cd200* across all cell clusters presented on a Z-scored color gradient. (C) Log expression of *Cd200* across all cells contained within the amacrine cell (AC) cluster presented on a color gradient. (D) Representative confocal image of CD200 expression in healthy human retina. This is an image of retina crysection and is a maximum projection image of the section.

## 5.7 Conclusion

Through the combined body of work described in this thesis, we hope to have advanced our understanding of early DR pathogenesis and how microglia contribute to CNS disease pathology. Furthermore, it is our hope that the penultimate chapter of this work specifically outlines preliminary demonstrations of a potentially powerful approach to pharmacologically inhibiting microglia and the neuroinflammatory facets of DR that they contribute to. This work holds real bench-to-bedside value, particularly if similar results are reached in other animal models of diabetes. If so, this may represent a significant step forward in treating patients during early stages of disease to better preserve retinal structure and function and ultimately, quality of life.

# References


1. Virchow, R. (1858). Die Cellularpathologie in ihrer Begründung auf physiologische und pathologische Gewebelehre: zwanzig Vorlesungen, gehalten während der Monate Februar, März und April 1858 in Pathologischen Institute zu Berlin (Verlag von August Hirschwald).

2. Kettenmann, H., and Verkhratsky, A. (2008). Neuroglia: the 150 years after. Trends in Neurosciences *31*, 653–659. 10.1016/j.tins.2008.09.003.

3. Alzheimer, A. (1910). Beiträge zur Kenntnis der Pathologischen Neuroglia und ihrer Beziehungen zu den Abbauvorgängen im Nervengewebe (G. Fischer).

4. Nissl, F. (1899). Über einige Beziehungen zwischen Nervenzellerkrankungen und gliösen Erscheinungen bei verschiedenen Psychosen. Arch Psychiatr *32*, 1–21.

5. del Río Hortega, P. (1919). El tercer elemento de los centros nerviosos. I. La microglia en estado normal. II. Intervencion de la microglia en los procesos patologicos. III. Naturaleza probable de la microglia. Bol. de la Soc. esp. de biol. *9*, 69.

6. Rio-Hortega, P. (1939). THE MICROGLIA. The Lancet *233*, 1023–1026. 10.1016/S0140-6736(00)60571-8.

7. Fujita, S., and Kitamura, T. (1975). Origin of Brain Macrophages and the Nature of the So-Called Microglia. In Malignant Lymphomas of the Nervous System, K. Jellinger and F. Seitelberger, eds. (Springer Berlin Heidelberg), pp. 291–296. 10.1007/978-3-662-08456-4_51.

8. Kitamura, T., Miyake, T., and Fujita, S. (1984). Genesis of resting microglia in the gray matter of mouse hippocampus. J. Comp. Neurol. *226*, 421–433. 10.1002/cne.902260310.

9. Hao, C., Richardson, A., and Fedoroff, S. (1991). Macrophage-like cells originate from neuroepithelium in culture: Characterization and properties of the macrophage-like cells. International Journal of Developmental Neuroscience *9*, 1–14. 10.1016/0736-5748(91)90067-V.

10. Ginhoux, F., Lim, S., Hoeffel, G., Low, D., and Huber, T. (2013). Origin and differentiation of microglia. Front. Cell. Neurosci. *7*. 10.3389/fncel.2013.00045.

11. Ginhoux, F., and Guilliams, M. (2016). Tissue-Resident Macrophage Ontogeny and Homeostasis. Immunity *44*, 439–449. 10.1016/j.immuni.2016.02.024.

12. Hoeffel, G., and Ginhoux, F. (2015). Ontogeny of Tissue-Resident Macrophages. Front. Immunol. *6*. 10.3389/fimmu.2015.00486.

13. Ginhoux, F., Greter, M., Leboeuf, M., Nandi, S., See, P., Gokhan, S., Mehler, M.F., Conway, S.J., Ng, L.G., Stanley, E.R., et al. (2010). Fate Mapping Analysis Reveals That Adult Microglia Derive from Primitive Macrophages. Science *330*, 841–845. 10.1126/science.1194637.

14. Menassa, D.A., and Gomez-Nicola, D. (2018). Microglial Dynamics During Human Brain Development. Front. Immunol. *9*, 1014. 10.3389/fimmu.2018.01014.

15. Ajami, B., Bennett, J.L., Krieger, C., Tetzlaff, W., and Rossi, F.M.V. (2007). Local self-renewal can sustain CNS microglia maintenance and function throughout adult life. Nat Neurosci *10*, 1538–1543. 10.1038/nn2014.

16. Hashimoto, D., Chow, A., Noizat, C., Teo, P., Beasley, M.B., Leboeuf, M., Becker, C.D., See, P., Price, J., Lucas, D., et al. (2013). Tissue-Resident Macrophages Self-Maintain Locally throughout Adult Life with Minimal Contribution from Circulating Monocytes. Immunity *38*, 792–804. 10.1016/j.immuni.2013.04.004.

17. Sheng, J., Ruedl, C., and Karjalainen, K. (2015). Most Tissue-Resident Macrophages Except Microglia Are Derived from Fetal Hematopoietic Stem Cells. Immunity *43*, 382–393. 10.1016/j.immuni.2015.07.016.

18. Huang, Y., Xu, Z., Xiong, S., Qin, G., Sun, F., Yang, J., Yuan, T.-F., Zhao, L., Wang, K., Liang, Y.-X., et al. (2018). Dual extra-retinal origins of microglia in the model of retinal microglia repopulation. Cell Discov *4*, 9. 10.1038/s41421-018-0011-8.

19. Zhang, Y., Zhao, L., Wang, X., Ma, W., Lazere, A., Qian, H., Zhang, J., Abu-Asab, M., Fariss, R.N., Roger, J.E., et al. (2018). Repopulating retinal microglia restore endogenous organization and function under CX3CL1-CX3CR1 regulation. Sci. Adv. *4*, eaap8492. 10.1126/sciadv.aap8492.

20. O'Koren, E.G., Yu, C., Klingeborn, M., Wong, A.Y.W., Prigge, C.L., Mathew, R., Kalnitsky, J., Msallam, R.A., Silvin, A., Kay, J.N., et al. (2019). Microglial Function Is Distinct in Different Anatomical Locations during Retinal Homeostasis and Degeneration. Immunity *50*, 723-737.e7. 10.1016/j.immuni.2019.02.007.

21. Nayak, D., Roth, T.L., and McGavern, D.B. (2014). Microglia Development and Function. Annu. Rev. Immunol. *32*, 367–402. 10.1146/annurev-immunol-032713-120240.

22. Kierdorf, K., Erny, D., Goldmann, T., Sander, V., Schulz, C., Perdiguero, E.G., Wieghofer, P., Heinrich, A., Riemke, P., Hölscher, C., et al. (2013). Microglia emerge from erythromyeloid precursors via Pu.1- and Irf8-dependent pathways. Nat Neurosci *16*, 273–280. 10.1038/nn.3318.

23. Huang, G., Zhang, P., Hirai, H., Elf, S., Yan, X., Chen, Z., Koschmieder, S., Okuno, Y., Dayaram, T., Growney, J.D., et al. (2008). PU.1 is a major downstream target of AML1 (RUNX1) in adult mouse hematopoiesis. Nat Genet *40*, 51–60. 10.1038/ng.2007.7.

24. Okuda, T., Van Deursen, J., Hiebert, S.W., Grosveld, G., and Downing, J.R. (1996). AML1, the Target of Multiple Chromosomal Translocations in Human Leukemia, Is Essential for Normal Fetal Liver Hematopoiesis. Cell *84*, 321–330. 10.1016/S0092-8674(00)80986-1.

25. Smith, A.M., Gibbons, H.M., Oldfield, R.L., Bergin, P.M., Mee, E.W., Faull, R.L.M., and Dragunow, M. (2013). The transcription factor PU.1 is critical for viability and function of human brain microglia: Critical Role of PU.1 in Human Microglia. Glia *61*, 929–942. 10.1002/glia.22486.

26. Walton, M.R., Gibbons, H., MacGibbon, G.A., Sirimanne, E., Saura, J., Gluckman, P.D., and Dragunow, M. (2000). PU.1 expression in microglia. Journal of Neuroimmunology *104*, 109–115. 10.1016/S0165-5728(99)00262-3.

27. Olson, M.C., Scott, E.W., Hack, A.A., Su, G.H., Tenen, D.G., Singh, H., and Simon, M.C. (1995). PU.1 is not essential for early myeloid gene expression but is required for terminal myeloid differentiation. Immunity *3*, 703–714. 10.1016/1074-7613(95)90060-8.

28. Wiktor-Jedrzejczak, W., Bartocci, A., Ferrante, A.W., Ahmed-Ansari, A., Sell, K.W., Pollard, J.W., and Stanley, E.R. (1990). Total absence of colony-stimulating factor 1 in the macrophage-deficient osteopetrotic (op/op) mouse. Proc. Natl. Acad. Sci. U.S.A. *87*, 4828–4832. 10.1073/pnas.87.12.4828.

29. Dai, X.-M., Ryan, G.R., Hapel, A.J., Dominguez, M.G., Russell, R.G., Kapp, S., Sylvestre, V., and Stanley, E.R. (2002). Targeted disruption of the mouse colony-stimulating factor 1 receptor gene results in osteopetrosis, mononuclear phagocyte deficiency, increased primitive progenitor cell frequencies, and reproductive defects. Blood *99*, 111–120. 10.1182/blood.V99.1.111.

30. Wang, Y., Szretter, K.J., Vermi, W., Gilfillan, S., Rossini, C., Cella, M., Barrow, A.D., Diamond, M.S., and Colonna, M. (2012). IL-34 is a tissue-restricted ligand of CSF1R required for the development of Langerhans cells and microglia. Nat Immunol *13*, 753–760. 10.1038/ni.2360.

31. Minten, C., Terry, R., Deffrasnes, C., King, N.J.C., and Campbell, I.L. (2012). IFN Regulatory Factor 8 Is a Key Constitutive Determinant of the Morphological and Molecular Properties of Microglia in the CNS. PLoS ONE *7*, e49851. 10.1371/journal.pone.0049851.

32. Ponomarev, E.D., Veremeyko, T., Barteneva, N., Krichevsky, A.M., and Weiner, H.L. (2011). MicroRNA-124 promotes microglia quiescence and suppresses EAE by deactivating macrophages via the C/EBP-α–PU.1 pathway. Nat Med *17*, 64–70. 10.1038/nm.2266.

33. Simó, R., Villarroel, M., Corraliza, L., Hernández, C., and Garcia-Ramírez, M. (2010). The Retinal Pigment Epithelium: Something More than a Constituent of the Blood-Retinal Barrier—Implications for the Pathogenesis of Diabetic Retinopathy. Journal of Biomedicine and Biotechnology *2010*, 1–15. 10.1155/2010/190724.

34. Yang, S., Zhou, J., and Li, D. (2021). Functions and Diseases of the Retinal Pigment Epithelium. Front. Pharmacol. *12*, 727870. 10.3389/fphar.2021.727870.

35. Hoon, M., Okawa, H., Della Santina, L., and Wong, R.O.L. (2014). Functional architecture of the retina: Development and disease. Progress in Retinal and Eye Research *42*, 44–84. 10.1016/j.preteyeres.2014.06.003.

36. London, A., Benhar, I., and Schwartz, M. (2013). The retina as a window to the brain—from eye research to CNS disorders. Nat Rev Neurol *9*, 44–53. 10.1038/nrneurol.2012.227.

37. Reichenbach, A., and Bringmann, A. (2013). New functions of Müller cells: New Functions of Müller Cells. Glia *61*, 651–678. 10.1002/glia.22477.

38. Bringmann, A., and Wiedemann, P. (2012). Müller Glial Cells in Retinal Disease. Ophthalmologica *227*, 1–19. 10.1159/000328979.

39. Kur, J., Newman, E.A., and Chan-Ling, T. (2012). Cellular and physiological mechanisms underlying blood flow regulation in the retina and choroid in health and disease. Progress in Retinal and Eye Research *31*, 377–406. 10.1016/j.preteyeres.2012.04.004.

40. Streilein, J.W. (2003). Ocular immune privilege: therapeutic opportunities from an experiment of nature. Nat Rev Immunol *3*, 879–889. 10.1038/nri1224.

41. Medawar, P.B. (1948). Immunity to Homologous Grafted Skin. III. The Fate of Skin Homographs Transplanted to the Brain, to Subcutaneous Tissue, and to the Anterior Chamber of the Eye. Br J Exp Pathol *29*, 58–69.

42. Diaz-Araya, C.M., Provis, J.M., Penfold, P.L., and Billson, F.A. (1995). Development of microglial topography in human retina. J. Comp. Neurol. *363*, 53–68. 10.1002/cne.903630106.

43. Santos, A.M., Calvente, R., Tassi, M., Carrasco, M.-C., Martín-Oliva, D., Marín-Teva, J.L., Navascués, J., and Cuadros, M.A. (2008). Embryonic and postnatal development of microglial cells in the mouse retina. J. Comp. Neurol. *506*, 224–239. 10.1002/cne.21538.

44. Provis, J.M., Diaz, C.M., and Penfold, P.L. (1996). Microglia in human retina: a heterogeneous population with distinct ontogenies. Perspect Dev Neurobiol *3*, 213–222.

45. Marn-Teva, J.L., Calvente, R., Cuadros, M.A., Almendros, A., and Navascus, J. (1999). Circumferential migration of ameboid microglia in the margin of the developing quail retina. Glia *27*, 226–238. 10.1002/(SICI)1098-1136(199909)27:3<226::AID-GLIA4>3.0.CO;2-T.

46. Chen, L., Yang, P., and Kijlstra, A. (2002). Distribution, markers, and functions of retinal microglia. Ocular Immunology and Inflammation *10*, 27–39. 10.1076/ocii.10.1.27.10328.

47. Fruttiger, M. (2007). Development of the retinal vasculature. Angiogenesis *10*, 77–88. 10.1007/s10456-007-9065-1.

48. Bodeutsch, N., and Thanos, S. (2000). Migration of phagocytotic cells and development of the murine intraretinal microglial network: An in vivo study using fluorescent dyes. Glia *32*, 91–101. 10.1002/1098-1136(200010)32:1<91::AID-GLIA90>3.0.CO;2-X.

49. Endo, Y., Asanuma, D., Namiki, S., Sugihara, K., Hirose, K., Uemura, A., Kubota, Y., and Miura, T. (2021). Quantitative modeling of regular retinal microglia distribution. Sci Rep *11*, 22671. 10.1038/s41598-021-01820-3.

50. Silverman, S.M., and Wong, W.T. (2018). Microglia in the Retina: Roles in Development, Maturity, and Disease. Annu. Rev. Vis. Sci. *4*, 45–77. 10.1146/annurev-vision-091517-034425.

51. Checchin, D., Sennlaub, F., Levavasseur, E., Leduc, M., and Chemtob, S. (2006). Potential Role of Microglia in Retinal Blood Vessel Formation. Invest. Ophthalmol. Vis. Sci. *47*, 3595. 10.1167/iovs.05-1522.

52. Outtz, H.H., Tattersall, I.W., Kofler, N.M., Steinbach, N., and Kitajewski, J. (2011). Notch1 controls macrophage recruitment and Notch signaling is activated at sites of endothelial cell anastomosis during retinal angiogenesis in mice. Blood *118*, 3436–3439. 10.1182/blood-2010-12-327015.

53. Foulquier, S., Caolo, V., Swennen, G., Milanova, I., Reinhold, S., Recarti, C., Alenina, N., Bader, M., Steckelings, U.M., Vanmierlo, T., et al. (2019). The role of receptor MAS in microglia-driven retinal vascular development. Angiogenesis *22*, 481–489. 10.1007/s10456-019-09671-3.

54. Cunningham, C.L., Martínez-Cerdeño, V., and Noctor, S.C. (2013). Microglia Regulate the Number of Neural Precursor Cells in the Developing Cerebral Cortex. J. Neurosci. *33*, 4216–4233. 10.1523/JNEUROSCI.3441-12.2013.

55. Ueno, M., Fujita, Y., Tanaka, T., Nakamura, Y., Kikuta, J., Ishii, M., and Yamashita, T. (2013). Layer V cortical neurons require microglial support for survival during postnatal development. Nat Neurosci *16*, 543–551. 10.1038/nn.3358.

56. Wakselman, S., Béchade, C., Roumier, A., Bernard, D., Triller, A., and Bessis, A. (2008). Developmental Neuronal Death in Hippocampus Requires the Microglial CD11b Integrin and DAP12 Immunoreceptor. J. Neurosci. *28*, 8138–8143. 10.1523/JNEUROSCI.1006-08.2008.

57. Marín-Teva, J.L., Dusart, I., Colin, C., Gervais, A., Van Rooijen, N., and Mallat, M. (2004). Microglia Promote the Death of Developing Purkinje Cells. Neuron *41*, 535–547. 10.1016/S0896-6273(04)00069-8.

58. Frade, J.M., and Barde, Y.-A. (1998). Microglia-Derived Nerve Growth Factor Causes Cell Death in the Developing Retina. Neuron *20*, 35–41. 10.1016/S0896-6273(00)80432-8.

59. Schafer, D.P., Lehrman, E.K., Kautzman, A.G., Koyama, R., Mardinly, A.R., Yamasaki, R., Ransohoff, R.M., Greenberg, M.E., Barres, B.A., and Stevens, B. (2012). Microglia Sculpt Postnatal Neural Circuits in an Activity and Complement-Dependent Manner. Neuron *74*, 691–705. 10.1016/j.neuron.2012.03.026.

60. Stevens, B., Allen, N.J., Vazquez, L.E., Howell, G.R., Christopherson, K.S., Nouri, N., Micheva, K.D., Mehalow, A.K., Huberman, A.D., Stafford, B., et al. (2007). The Classical Complement Cascade Mediates CNS Synapse Elimination. Cell *131*, 1164–1178. 10.1016/j.cell.2007.10.036.

61. Noda, M., Doi, Y., Liang, J., Kawanokuchi, J., Sonobe, Y., Takeuchi, H., Mizuno, T., and Suzumura, A. (2011). Fractalkine Attenuates Excito-neurotoxicity via Microglial Clearance of Damaged Neurons and Antioxidant Enzyme Heme Oxygenase-1 Expression. Journal of Biological Chemistry *286*, 2308–2319. 10.1074/jbc.M110.169839.

62. Paolicelli, R.C., Bolasco, G., Pagani, F., Maggi, L., Scianni, M., Panzanelli, P., Giustetto, M., Ferreira, T.A., Guiducci, E., Dumas, L., et al. (2011). Synaptic Pruning by Microglia Is Necessary for Normal Brain Development. Science *333*, 1456–1458. 10.1126/science.1202529.

63. Squarzoni, P., Oller, G., Hoeffel, G., Pont-Lezica, L., Rostaing, P., Low, D., Bessis, A., Ginhoux, F., and Garel, S. (2014). Microglia Modulate Wiring of the Embryonic Forebrain. Cell Reports *8*, 1271–1279. 10.1016/j.celrep.2014.07.042.

64. Pont-Lezica, L., Beumer, W., Colasse, S., Drexhage, H., Versnel, M., and Bessis, A. (2014). Microglia shape corpus callosum axon tract fasciculation: functional impact of prenatal inflammation. Eur J Neurosci *39*, 1551–1557. 10.1111/ejn.12508.

65. Hoshiko, M., Arnoux, I., Avignone, E., Yamamoto, N., and Audinat, E. (2012). Deficiency of the Microglial Receptor CX3CR1 Impairs Postnatal Functional Development of Thalamocortical Synapses in the Barrel Cortex. J. Neurosci. *32*, 15106–15111. 10.1523/JNEUROSCI.1167-12.2012.

66. Ueno, M., and Yamashita, T. (2014). Bidirectional tuning of microglia in the developing brain: from neurogenesis to neural circuit formation. Current Opinion in Neurobiology *27*, 8–15. 10.1016/j.conb.2014.02.004.

67. Nimmerjahn, A., Kirchhoff, F., and Helmchen, F. (2005). Resting Microglial Cells Are Highly Dynamic Surveillants of Brain Parenchyma in Vivo. Science *308*, 1314–1318. 10.1126/science.1110647.

68. Wake, H., Moorhouse, A.J., Jinno, S., Kohsaka, S., and Nabekura, J. (2009). Resting Microglia Directly Monitor the Functional State of Synapses *In Vivo* and Determine the Fate of Ischemic Terminals. J. Neurosci. *29*, 3974–3980. 10.1523/JNEUROSCI.4363-08.2009.

69. Joseph, A., Power, D., and Schallek, J. (2021). Imaging the dynamics of individual processes of microglia in the living retina in vivo. Biomed. Opt. Express *12*, 6157. 10.1364/BOE.426157.

70. Schafer, D.P., and Stevens, B. (2015). Microglia Function in Central Nervous System Development and Plasticity. Cold Spring Harb Perspect Biol *7*, a020545. 10.1101/cshperspect.a020545.

71. Colonna, M., and Butovsky, O. (2017). Microglia Function in the Central Nervous System During Health and Neurodegeneration. Annu. Rev. Immunol. *35*, 441–468. 10.1146/annurev-immunol-051116-052358.

72. Ransohoff, R.M. (2016). A polarizing question: do M1 and M2 microglia exist? Nat Neurosci *19*, 987–991. 10.1038/nn.4338.

73. Paolicelli, R.C., Sierra, A., Stevens, B., Tremblay, M.-E., Aguzzi, A., Ajami, B., Amit, I., Audinat, E., Bechmann, I., Bennett, M., et al. (2022). Microglia states and nomenclature: A field at its crossroads. Neuron *110*, 3458–3483. 10.1016/j.neuron.2022.10.020.

74. Keren-Shaul, H., Spinrad, A., Weiner, A., Matcovitch-Natan, O., Dvir-Szternfeld, R., Ulland, T.K., David, E., Baruch, K., Lara-Astaiso, D., Toth, B., et al. (2017). A Unique Microglia Type Associated with Restricting Development of Alzheimer's Disease. Cell *169*, 1276-1290.e17. 10.1016/j.cell.2017.05.018.

75. Smajić, S., Prada-Medina, C.A., Landoulsi, Z., Ghelfi, J., Delcambre, S., Dietrich, C., Jarazo, J., Henck, J., Balachandran, S., Pachchek, S., et al. (2022). Single-cell sequencing of human midbrain reveals glial activation and a Parkinson-specific neuronal state. Brain *145*, 964–978. 10.1093/brain/awab446.

76. Limone, F., Mordes, D.A., Couto, A., Joseph, B.J., Mitchell, J.M., Therrien, M., Ghosh, S.D., Meyer, D., Zhang, Y., Goldman, M., et al. (2021). Single-nucleus sequencing reveals enriched expression of genetic risk factors in Extratelencephalic Neurons sensitive to degeneration in ALS (Neuroscience) 10.1101/2021.07.12.452054.

77. Marschallinger, J., Iram, T., Zardeneta, M., Lee, S.E., Lehallier, B., Haney, M.S., Pluvinage, J.V., Mathur, V., Hahn, O., Morgens, D.W., et al. (2020). Lipid-droplet-accumulating microglia represent a dysfunctional and proinflammatory state in the aging brain. Nat Neurosci *23*, 194–208. 10.1038/s41593-019-0566-1.

78. Krasemann, S., Madore, C., Cialic, R., Baufeld, C., Calcagno, N., El Fatimy, R., Beckers, L., O'Loughlin, E., Xu, Y., Fanek, Z., et al. (2017). The TREM2-APOE Pathway Drives the Transcriptional Phenotype of Dysfunctional Microglia in Neurodegenerative Diseases. Immunity *47*, 566-581.e9. 10.1016/j.immuni.2017.08.008.

79. Absinta, M., Maric, D., Gharagozloo, M., Garton, T., Smith, M.D., Jin, J., Fitzgerald, K.C., Song, A., Liu, P., Lin, J.-P., et al. (2021). A lymphocyte–microglia–astrocyte axis in chronic active multiple sclerosis. Nature *597*, 709–714. 10.1038/s41586-021-03892-7.

80. Ajami, B., Bennett, J.L., Krieger, C., McNagny, K.M., and Rossi, F.M.V. (2011). Infiltrating monocytes trigger EAE progression, but do not contribute to the resident microglia pool. Nat Neurosci *14*, 1142–1149. 10.1038/nn.2887.

81. Yamasaki, R., Lu, H., Butovsky, O., Ohno, N., Rietsch, A.M., Cialic, R., Wu, P.M., Doykan, C.E., Lin, J., Cotleur, A.C., et al. (2014). Differential roles of microglia and monocytes in the inflamed central nervous system. Journal of Experimental Medicine *211*, 1533–1549. 10.1084/jem.20132477.

82. Ritzel, R.M., Patel, A.R., Grenier, J.M., Crapser, J., Verma, R., Jellison, E.R., and McCullough, L.D. (2015). Functional differences between microglia and monocytes after ischemic stroke. J Neuroinflammation *12*, 106. 10.1186/s12974-015-0329-1.

83. Su, F., Yi, H., Xu, L., and Zhang, Z. (2015). Fluoxetine and S-citalopram inhibit M1 activation and promote M2 activation of microglia in vitro. Neuroscience *294*, 60–68. 10.1016/j.neuroscience.2015.02.028.

84. Lam, D., Lively, S., and Schlichter, L.C. (2017). Responses of rat and mouse primary microglia to pro- and anti-inflammatory stimuli: molecular profiles, K+ channels and migration. J Neuroinflammation *14*, 166. 10.1186/s12974-017-0941-3.

85. Siddiqui, T.A., Lively, S., and Schlichter, L.C. (2016). Complex molecular and functional outcomes of single versus sequential cytokine stimulation of rat microglia. J Neuroinflammation *13*, 66. 10.1186/s12974-016-0531-9.

86. Karlstetter, M., Scholz, R., Rutar, M., Wong, W.T., Provis, J.M., and Langmann, T. (2015). Retinal microglia: Just bystander or target for therapy? Progress in Retinal and Eye Research *45*, 30–57. 10.1016/j.preteyeres.2014.11.004.

87. Wang, X., Zhao, L., Zhang, J., Fariss, R.N., Ma, W., Kretschmer, F., Wang, M., Qian, H.H., Badea, T.C., Diamond, J.S., et al. (2016). Requirement for Microglia for the Maintenance of Synaptic Function and Integrity in the Mature Retina. J. Neurosci. *36*, 2827–2842. 10.1523/JNEUROSCI.3575-15.2016.

88. Karlstetter, M., Ebert, S., and Langmann, T. (2010). Microglia in the healthy and degenerating retina: Insights from novel mouse models. Immunobiology *215*, 685–691. 10.1016/j.imbio.2010.05.010.

89. Rathnasamy, G., Foulds, W.S., Ling, E.-A., and Kaur, C. (2019). Retinal microglia – A key player in healthy and diseased retina. Progress in Neurobiology *173*, 18–40. 10.1016/j.pneurobio.2018.05.006.

90. Zhao, L., Zabel, M.K., Wang, X., Ma, W., Shah, P., Fariss, R.N., Qian, H., Parkhurst, C.N., Gan, W., and Wong, W.T. (2015). Microglial phagocytosis of living photoreceptors contributes to inherited retinal degeneration. EMBO Mol Med *7*, 1179–1197. 10.15252/emmm.201505298.

91. Zeng, H., Zhu, X., Zhang, C., Yang, L.-P., Wu, L., and Tso, M.O.M. (2005). Identification of Sequential Events and Factors Associated with Microglial Activation, Migration, and Cytotoxicity in Retinal Degeneration in *rd* Mice. Invest. Ophthalmol. Vis. Sci. *46*, 2992. 10.1167/iovs.05-0118.

92. Paglinawan, R., Malipiero, U., Schlapbach, R., Frei, K., Reith, W., and Fontana, A. (2003). TGF? directs gene expression of activated microglia to an anti-inflammatory phenotype strongly focusing on chemokine genes and cell migratory genes. Glia *44*, 219–231. 10.1002/glia.10286.

93. D'Orazio, T.J., and Niederkorn, J.Y. (1998). A Novel Role for TGF-β and IL-10 in the Induction of Immune Privilege. The Journal of Immunology *160*, 2089–2098. 10.4049/jimmunol.160.5.2089.

94. Ma, W., Zhao, L., and Wong, W.T. (2012). Microglia in the Outer Retina and Their Relevance to Pathogenesis of Age-Related Macular Degeneration. In Retinal Degenerative Diseases Advances in Experimental Medicine and Biology., M. M. LaVail, J. D. Ash, R. E. Anderson, J. G. Hollyfield, and C. Grimm, eds. (Springer US), pp. 37–42. 10.1007/978-1-4614-0631-0_6.

95. Wang, M., Wang, X., Zhao, L., Ma, W., Rodriguez, I.R., Fariss, R.N., and Wong, W.T. (2014). Macroglia-Microglia Interactions via TSPO Signaling Regulates Microglial Activation in the Mouse Retina. J. Neurosci. *34*, 3793–3806. 10.1523/JNEUROSCI.3153-13.2014.

96. Karlstetter, M., Nothdurfter, C., Aslanidis, A., Moeller, K., Horn, F., Scholz, R., Neumann, H., Weber, B.H.F., Rupprecht, R., and Langmann, T. (2014). Translocator protein (18 kDa) (TSPO) is expressed in reactive retinal microglia and modulates microglial inflammation and phagocytosis. J Neuroinflammation *11*, 3. 10.1186/1742-2094-11-3.

97. Nathan, C., and Muller, W.A. (2001). Putting the brakes on innate immunity: a regulatory role for CD200? Nat Immunol *2*, 17–19. 10.1038/83124.

98. Broderick, C., Hoek, R.M., Forrester, J.V., Liversidge, J., Sedgwick, J.D., and Dick, A.D. (2002). Constitutive Retinal CD200 Expression Regulates Resident Microglia and Activation State of Inflammatory Cells during Experimental Autoimmune Uveoretinitis. The American Journal of Pathology *161*, 1669–1677. 10.1016/S0002-9440(10)64444-6.

99. Carter, D., and Dick, A. (2004). CD200 maintains microglial potential to migrate in adult human retinal explant model. Current Eye Research *28*, 427–436. 10.1080/02713680490503778.

100. Denieffe, S., Kelly, R.J., McDonald, C., Lyons, A., and Lynch, M.A. (2013). Classical activation of microglia in CD200-deficient mice is a consequence of blood brain barrier permeability and infiltration of peripheral cells. Brain, Behavior, and Immunity *34*, 86–97. 10.1016/j.bbi.2013.07.174.

101. Copland, D.A., Calder, C.J., Raveney, B.J.E., Nicholson, L.B., Phillips, J., Cherwinski, H., Jenmalm, M., Sedgwick, J.D., and Dick, A.D. (2007). Monoclonal Antibody-Mediated CD200 Receptor Signaling Suppresses Macrophage Activation and Tissue Damage in Experimental Autoimmune Uveoretinitis. The American Journal of Pathology *171*, 580–588. 10.2353/ajpath.2007.070272.

102. Bazan, J.F., Bacon, K.B., Hardiman, G., Wang, W., Soo, K., Rossi, D., Greaves, D.R., Zlotnik, A., and Schall, T.J. (1997). A new class of membrane-bound chemokine with a CX3C motif. Nature *385*, 640–644. 10.1038/385640a0.

103. Cardona, A.E., Pioro, E.P., Sasse, M.E., Kostenko, V., Cardona, S.M., Dijkstra, I.M., Huang, D., Kidd, G., Dombrowski, S., Dutta, R., et al. (2006). Control of microglial neurotoxicity by the fractalkine receptor. Nat Neurosci *9*, 917–924. 10.1038/nn1715.

104. Liang, K.J., Lee, J.E., Wang, Y.D., Ma, W., Fontainhas, A.M., Fariss, R.N., and Wong, W.T. (2009). Regulation of Dynamic Behavior of Retinal Microglia by CX3CR1 Signaling. Invest. Ophthalmol. Vis. Sci. *50*, 4444. 10.1167/iovs.08-3357.

105. Zabel, M.K., Zhao, L., Zhang, Y., Gonzalez, S.R., Ma, W., Wang, X., Fariss, R.N., and Wong, W.T. (2016). Microglial phagocytosis and activation underlying photoreceptor degeneration is regulated by CX3CL1-CX3CR1 signaling in a mouse model of retinitis pigmentosa. Glia *64*, 1479–1491. 10.1002/glia.23016.

106. Combadière, C., Feumi, C., Raoul, W., Keller, N., Rodéro, M., Pézard, A., Lavalette, S., Houssier, M., Jonet, L., Picard, E., et al. (2007). CX3CR1-dependent subretinal microglia cell accumulation is associated with cardinal features of age-related macular degeneration. J. Clin. Invest. *117*, 2920–2928. 10.1172/JCI31692.

107. Eyo, U.B., Peng, J., Swiatkowski, P., Mukherjee, A., Bispo, A., and Wu, L.-J. (2014). Neuronal Hyperactivity Recruits Microglial Processes via Neuronal NMDA Receptors and Microglial P2Y12 Receptors after Status Epilepticus. Journal of Neuroscience *34*, 10528–10540. 10.1523/JNEUROSCI.0416-14.2014.

108. Fontainhas, A.M., Wang, M., Liang, K.J., Chen, S., Mettu, P., Damani, M., Fariss, R.N., Li, W., and Wong, W.T. (2011). Microglial Morphology and Dynamic Behavior Is Regulated by Ionotropic Glutamatergic and GABAergic Neurotransmission. PLoS ONE *6*, e15973. 10.1371/journal.pone.0015973.

109. Macosko, E.Z., Basu, A., Satija, R., Nemesh, J., Shekhar, K., Goldman, M., Tirosh, I., Bialas, A.R., Kamitaki, N., Martersteck, E.M., et al. (2015). Highly Parallel Genome-wide Expression Profiling of Individual Cells Using Nanoliter Droplets. Cell *161*, 1202–1214. 10.1016/j.cell.2015.05.002.

110. Gupta, N., Brown, K.E., and Milam, A.H. (2003). Activated microglia in human retinitis pigmentosa, late-onset retinal degeneration, and age-related macular degeneration. Experimental Eye Research *76*, 463–471. 10.1016/S0014-4835(02)00332-9.

111. Yuan, L., and Neufeld, A.H. (2001). Activated microglia in the human glaucomatous optic nerve head. J. Neurosci. Res. *64*, 523–532. 10.1002/jnr.1104.

112. Yoshida, N., Ikeda, Y., Notomi, S., Ishikawa, K., Murakami, Y., Hisatomi, T., Enaida, H., and Ishibashi, T. (2013). Laboratory Evidence of Sustained Chronic Inflammatory Reaction in Retinitis Pigmentosa. Ophthalmology *120*, e5–e12. 10.1016/j.ophtha.2012.07.008.

113. Zeng, H. (2008). Microglial Activation in Human Diabetic Retinopathy. Arch Ophthalmol *126*, 227. 10.1001/archophthalmol.2007.65.

114. Okunuki, Y., Mukai, R., Pearsall, E.A., Klokman, G., Husain, D., Park, D.-H., Korobkina, E., Weiner, H.L., Butovsky, O., Ksander, B.R., et al. (2018). Microglia inhibit photoreceptor cell death and regulate immune cell infiltration in response to retinal detachment. Proc. Natl. Acad. Sci. U.S.A. *115*. 10.1073/pnas.1719601115.

115. Tan, Z., Guo, Y., Shrestha, M., Gregory-Ksander, M.S., and Jakobs, T.C. (2021). Depletion of optic nerve microglia does not improve visual function in experimental glaucoma. Investigative Ophthalmology & Visual Science *62*, 2383.

116. Hilla, A.M., Diekmann, H., and Fischer, D. (2017). Microglia Are Irrelevant for Neuronal Degeneration and Axon Regeneration after Acute Injury. J. Neurosci. *37*, 6113–6124. 10.1523/JNEUROSCI.0584-17.2017.

117. Rashid, K., Akhtar-Schaefer, I., and Langmann, T. (2019). Microglia in Retinal Degeneration. Front. Immunol. *10*, 1975. 10.3389/fimmu.2019.01975.

118. American Diabetes Association (2010). Diagnosis and Classification of Diabetes Mellitus. Diabetes Care *33*, S62–S69. 10.2337/dc10-S062.

119. Saeedi, P., Petersohn, I., Salpea, P., Malanda, B., Karuranga, S., Unwin, N., Colagiuri, S., Guariguata, L., Motala, A.A., Ogurtsova, K., et al. (2019). Global and regional diabetes prevalence estimates for 2019 and projections for 2030 and 2045: Results from the International Diabetes Federation Diabetes Atlas, 9th edition. Diabetes Research and Clinical Practice *157*, 107843. 10.1016/j.diabres.2019.107843.

120. Harding, J.L., Pavkov, M.E., Magliano, D.J., Shaw, J.E., and Gregg, E.W. (2019). Global trends in diabetes complications: a review of current evidence. Diabetologia *62*, 3–16. 10.1007/s00125-018-4711-2.

121. Flaxman, S.R., Bourne, R.R.A., Resnikoff, S., Ackland, P., Braithwaite, T., Cicinelli, M.V., Das, A., Jonas, J.B., Keeffe, J., Kempen, J.H., et al. (2017). Global causes of blindness and distance vision impairment 1990–2020: a systematic review and meta-analysis. The Lancet Global Health *5*, e1221–e1234. 10.1016/S2214-109X(17)30393-5.

122. Wang, W., and Lo, A. (2018). Diabetic Retinopathy: Pathophysiology and Treatments. IJMS *19*, 1816. 10.3390/ijms19061816.

123. Brownlee, M. (2005). The Pathobiology of Diabetic Complications. Diabetes *54*, 1615–1625. 10.2337/diabetes.54.6.1615.

124. Rübsam, A., Parikh, S., and Fort, P. (2018). Role of Inflammation in Diabetic Retinopathy. IJMS *19*, 942. 10.3390/ijms19040942.

125. Sohn, E.H., Van Dijk, H.W., Jiao, C., Kok, P.H.B., Jeong, W., Demirkaya, N., Garmager, A., Wit, F., Kucukevcilioglu, M., Van Velthoven, M.E.J., et al. (2016). Retinal neurodegeneration may precede microvascular changes characteristic of diabetic retinopathy in diabetes mellitus. Proc. Natl. Acad. Sci. U.S.A. *113*. 10.1073/pnas.1522014113.

126. Abcouwer, S.F., and Gardner, T.W. (2014). Diabetic retinopathy: loss of neuroretinal adaptation to the diabetic metabolic environment. Ann. N.Y. Acad. Sci. *1311*, 174–190. 10.1111/nyas.12412.

127. Kern, T.S., and Berkowitz, B.A. (2015). Photoreceptors in diabetic retinopathy. J Diabetes Invest *6*, 371–380. 10.1111/jdi.12312.

128. Sinclair, S.H., and Schwartz, S.S. (2019). Diabetic Retinopathy–An Underdiagnosed and Undertreated Inflammatory, Neuro-Vascular Complication of Diabetes. Front. Endocrinol. *10*, 843. 10.3389/fendo.2019.00843.

129. Honasoge, A., Nudleman, E., Smith, M., and Rajagopal, R. (2019). Emerging Insights and Interventions for Diabetic Retinopathy. Curr Diab Rep *19*, 100. 10.1007/s11892-019-1218-2.

130. Duh, E.J., Sun, J.K., and Stitt, A.W. (2017). Diabetic retinopathy: current understanding, mechanisms, and treatment strategies. JCI Insight *2*, e93751. 10.1172/jci.insight.93751.

131. Silva, P.S., Sun, J.K., and Aiello, L.P. (2009). Role of Steroids in the Management of Diabetic Macular Edema and Proliferative Diabetic Retinopathy. Seminars in Ophthalmology *24*, 93–99. 10.1080/08820530902800355.

132. Bolinger, M., and Antonetti, D. (2016). Moving Past Anti-VEGF: Novel Therapies for Treating Diabetic Retinopathy. IJMS *17*, 1498. 10.3390/ijms17091498.

133. Chen, X., Zhou, H., Gong, Y., Wei, S., and Zhang, M. (2015). Early spatiotemporal characterization of microglial activation in the retinas of rats with streptozotocin-induced diabetes. Graefes Arch Clin Exp Ophthalmol *253*, 519–525. 10.1007/s00417-014-2727-y.

134. Zeng, X.-X., Ng, Y.-K., and Ling, E.-A. (2000). Neuronal and microglial response in the retina of streptozotocin-induced diabetic rats. Vis Neurosci *17*, 463–471. 10.1017/S0952523800173122.

135. Xia, Y., Luo, Q., Chen, J., Huang, C., Jahangir, A., Pan, T., Wei, X., Liu, W., and Chen, Z. (2022). Retinal Astrocytes and Microglia Activation in Diabetic Retinopathy Rhesus Monkey Models. Current Eye Research *47*, 297–303. 10.1080/02713683.2021.1984535.

136. Kaštelan, S., Orešković, I., Bišćan, F., Kaštelan, H., and Gverović Antunica, A. (2020). Inflammatory and angiogenic biomarkers in diabetic retinopathy. Biochem. med. (Online) *30*, 385–399. 10.11613/BM.2020.030502.

137. Sorrentino, F.S., Allkabes, M., Salsini, G., Bonifazzi, C., and Perri, P. (2016). The importance of glial cells in the homeostasis of the retinal microenvironment and their pivotal role in the course of diabetic retinopathy. Life Sciences *162*, 54–59. 10.1016/j.lfs.2016.08.001.

138. Xu, H., and Chen, M. (2017). Diabetic retinopathy and dysregulated innate immunity. Vision Research *139*, 39–46. 10.1016/j.visres.2017.04.013.

139. Lechner, J., O'Leary, O.E., and Stitt, A.W. (2017). The pathology associated with diabetic retinopathy. Vision Research *139*, 7–14. 10.1016/j.visres.2017.04.003.

140. Garcia-Martin, E., Cipres, M., Melchor, I., Gil-Arribas, L., Vilades, E., Polo, V., Rodrigo, M.J., and Satue, M. (2019). Neurodegeneration in Patients with Type 2 Diabetes Mellitus without Diabetic Retinopathy. Journal of Ophthalmology *2019*, 1–8. 10.1155/2019/1825819.

141. Jackson, G.R., Scott, I.U., Quillen, D.A., Walter, L.E., and Gardner, T.W. (2012). Inner retinal visual dysfunction is a sensitive marker of non-proliferative diabetic retinopathy. Br J Ophthalmol *96*, 699–703. 10.1136/bjophthalmol-2011-300467.

142. Vujosevic, S., and Simó, R. (2017). Local and Systemic Inflammatory Biomarkers of Diabetic Retinopathy: An Integrative Approach. Invest. Ophthalmol. Vis. Sci. *58*, BIO68. 10.1167/iovs.17-21769.

143. Safi, S.Z., Qvist, R., Kumar, S., Batumalaie, K., and Ismail, I.S.B. (2014). Molecular Mechanisms of Diabetic Retinopathy, General Preventive Strategies, and Novel Therapeutic Targets. BioMed Research International *2014*, 1–18. 10.1155/2014/801269.

144. Brownlee, M. (2001). Biochemistry and molecular cell biology of diabetic complications. Nature *414*, 813–820. 10.1038/414813a.

145. Rungger-Brändle, E., Dosso, A.A., and Leuenberger, P.M. (2000). Glial reactivity, an early feature of diabetic retinopathy. Invest Ophthalmol Vis Sci *41*, 1971–1980.

146. Vujosevic, S., Micera, A., Bini, S., Berton, M., Esposito, G., and Midena, E. (2016). Proteome analysis of retinal glia cells-related inflammatory cytokines in the aqueous humour of diabetic patients. Acta Ophthalmol *94*, 56–64. 10.1111/aos.12812.

147. Boss, J.D., Singh, P.K., Pandya, H.K., Tosi, J., Kim, C., Tewari, A., Juzych, M.S., Abrams, G.W., and Kumar, A. (2017). Assessment of Neurotrophins and Inflammatory Mediators in Vitreous of Patients With Diabetic Retinopathy. Invest. Ophthalmol. Vis. Sci. *58*, 5594. 10.1167/iovs.17-21973.

148. Beli, E., Dominguez, J.M., Hu, P., Thinschmidt, J.S., Caballero, S., Li Calzi, S., Luo, D., Shanmugam, S., Salazar, T.E., Duan, Y., et al. (2016). CX3CR1 deficiency accelerates the development of retinopathy in a rodent model of type 1 diabetes. J Mol Med *94*, 1255–1265. 10.1007/s00109-016-1433-0.

149. Cerani, A., Tetreault, N., Menard, C., Lapalme, E., Patel, C., Sitaras, N., Beaudoin, F., Leboeuf, D., De Guire, V., Binet, F., et al. (2013). Neuron-Derived Semaphorin 3A Is an Early Inducer of Vascular Permeability in Diabetic Retinopathy via Neuropilin-1. Cell Metabolism *18*, 505–518. 10.1016/j.cmet.2013.09.003.

150. Yokomizo, H., Maeda, Y., Park, K., Clermont, A.C., Hernandez, S.L., Fickweiler, W., Li, Q., Wang, C.-H., Paniagua, S.M., Simao, F., et al. (2019). Retinol binding protein 3 is increased in the retina of patients with diabetes resistant to diabetic retinopathy. Sci. Transl. Med. *11*, eaau6627. 10.1126/scitranslmed.aau6627.

151. Miyamoto, K., Khosrof, S., Bursell, S.-E., Rohan, R., Murata, T., Clermont, A.C., Aiello, L.P., Ogura, Y., and Adamis, A.P. (1999). Prevention of leukostasis and vascular leakage in streptozotocin-induced diabetic retinopathy via intercellular adhesion molecule-1 inhibition. Proc. Natl. Acad. Sci. U.S.A. *96*, 10836–10841. 10.1073/pnas.96.19.10836.

152. Jung, S., Aliberti, J., Graemmel, P., Sunshine, M.J., Kreutzberg, G.W., Sher, A., and Littman, D.R. (2000). Analysis of Fractalkine Receptor CX $_3$ CR1 Function by Targeted Deletion and Green Fluorescent Protein Reporter Gene Insertion. Molecular and Cellular Biology *20*, 4106–4114. 10.1128/MCB.20.11.4106-4114.2000.

153. Mattapallil, M.J., Wawrousek, E.F., Chan, C.-C., Zhao, H., Roychoudhury, J., Ferguson, T.A., and Caspi, R.R. (2012). The *Rd8* Mutation of the *Crb1* Gene Is Present in Vendor Lines of C57BL/6N Mice and Embryonic Stem Cells, and Confounds Ocular Induced Mutant Phenotypes. Invest. Ophthalmol. Vis. Sci. *53*, 2921. 10.1167/iovs.12-9662.

154. Maclaren, N.K., Neufeld, M., McLaughlin, J.V., and Taylor, G. (1980). Androgen Sensitization of Streptozotocin-induced Diabetes in Mice. Diabetes *29*, 710–716. 10.2337/diab.29.9.710.

155. Brucklacher, R.M., Patel, K.M., VanGuilder, H.D., Bixler, G.V., Barber, A.J., Antonetti, D.A., Lin, C.-M., LaNoue, K.F., Gardner, T.W., Bronson, S.K., et al. (2008). Whole genome assessment of the retinal response to diabetes reveals a progressive neurovascular inflammatory response. BMC Med Genomics *1*, 26. 10.1186/1755-8794-1-26.

156. Furman, B.L. (2021). Streptozotocin-Induced Diabetic Models in Mice and Rats. Current Protocols *1*. 10.1002/cpz1.78.

157. Bisht, K., Sharma, K.P., Lecours, C., Gabriela Sánchez, M., El Hajj, H., Milior, G., Olmos-Alonso, A., Gómez-Nicola, D., Luheshi, G., Vallières, L., et al. (2016). Dark microglia: A new phenotype predominantly associated with pathological states. Glia *64*, 826–839. 10.1002/glia.22966.

158. Hammond, T.R., Dufort, C., Dissing-Olesen, L., Giera, S., Young, A., Wysoker, A., Walker, A.J., Gergits, F., Segel, M., Nemesh, J., et al. (2019). Single-Cell RNA Sequencing of Microglia throughout the Mouse Lifespan and in the Injured Brain Reveals Complex Cell-State Changes. Immunity *50*, 253-271.e6. 10.1016/j.immuni.2018.11.004.

159. Sousa, C., Golebiewska, A., Poovathingal, S.K., Kaoma, T., Pires-Afonso, Y., Martina, S., Coowar, D., Azuaje, F., Skupin, A., Balling, R., et al. (2018). Single-cell transcriptomics reveals distinct inflammation-induced microglia signatures. EMBO Reports *19*, e46171. 10.15252/embr.201846171.

160. Chiu, I.M., Morimoto, E.T.A., Goodarzi, H., Liao, J.T., O'Keeffe, S., Phatnani, H.P., Muratet, M., Carroll, M.C., Levy, S., Tavazoie, S., et al. (2013). A Neurodegeneration-Specific Gene-Expression Signature of Acutely Isolated Microglia from an Amyotrophic Lateral Sclerosis Mouse Model. Cell Reports *4*, 385–401. 10.1016/j.celrep.2013.06.018.

161. Mills, S.A., Jobling, A.I., Dixon, M.A., Bui, B.V., Vessey, K.A., Phipps, J.A., Greferath, U., Venables, G., Wong, V.H.Y., Wong, C.H.Y., et al. (2021). Fractalkine-induced microglial vasoregulation occurs within the retina and is altered early in diabetic retinopathy. Proc. Natl. Acad. Sci. U.S.A. *118*, e2112561118. 10.1073/pnas.2112561118.

162. Guillaumond, F., Gréchez-Cassiau, A., Subramaniam, M., Brangolo, S., Peteri-Brünback, B., Staels, B., Fiévet, C., Spelsberg, T.C., Delaunay, F., and Teboul, M. (2010). Krüppel-Like Factor KLF10 Is a Link between the Circadian Clock and Metabolism in Liver. Molecular and Cellular Biology *30*, 3059–3070. 10.1128/MCB.01141-09.

163. Ly, A., Yee, P., Vessey, K.A., Phipps, J.A., Jobling, A.I., and Fletcher, E.L. (2011). Early Inner Retinal Astrocyte Dysfunction during Diabetes and Development of Hypoxia, Retinal Stress, and Neuronal Functional Loss. Invest. Ophthalmol. Vis. Sci. *52*, 9316. 10.1167/iovs.11-7879.

164. Olivares, A.M., Althoff, K., Chen, G.F., Wu, S., Morrisson, M.A., DeAngelis, M.M., and Haider, N. (2017). Animal Models of Diabetic Retinopathy. Curr Diab Rep *17*, 93. 10.1007/s11892-017-0913-0.

165. Like, A.A., and Rossini, A.A. (1976). Streptozotocin-Induced Pancreatic Insulitis: New Model of Diabetes Mellitus. Science *193*, 415–417. 10.1126/science.180605.

166. Pardue, M.T., Barnes, C.S., Kim, M.K., Aung, M.H., Amarnath, R., Olson, D.E., and Thulé, P.M. (2014). Rodent Hyperglycemia-Induced Inner Retinal Deficits are Mirrored in Human Diabetes. Trans. Vis. Sci. Tech. *3*, 6. 10.1167/tvst.3.3.6.

167. El Hajj, H., Savage, J.C., Bisht, K., Parent, M., Vallières, L., Rivest, S., and Tremblay, M.-È. (2019). Ultrastructural evidence of microglial heterogeneity in Alzheimer's disease amyloid pathology. J Neuroinflammation *16*, 87. 10.1186/s12974-019-1473-9.

168. Hayden, M., Grant, D., Aroor, A., and DeMarco, V. (2018). Ultrastructural Remodeling of the Neurovascular Unit in the Female Diabetic db/db Model–Part II: Microglia and Mitochondria. Neuroglia *1*, 311–326. 10.3390/neuroglia1020021.

169. Hsieh, C.-F., Liu, C.-K., Lee, C.-T., Yu, L.-E., and Wang, J.-Y. (2019). Acute glucose fluctuation impacts microglial activity, leading to inflammatory activation or self-degradation. Sci Rep *9*, 840. 10.1038/s41598-018-37215-0.

170. Quan, Y., Jiang, C., Xue, B., Zhu, S., and Wang, X. (2011). High glucose stimulates TNFα and MCP-1 expression in rat microglia via ROS and NF-κB pathways. Acta Pharmacol Sin *32*, 188–193. 10.1038/aps.2010.174.

171. Lv, K., Ying, H., Hu, G., Hu, J., Jian, Q., and Zhang, F. (2022). Integrated multi-omics reveals the activated retinal microglia with intracellular metabolic reprogramming contributes to inflammation in STZ-induced early diabetic retinopathy. Front. Immunol. *13*, 942768. 10.3389/fimmu.2022.942768.

172. Kolliniati, O., Ieronymaki, E., Vergadi, E., and Tsatsanis, C. (2022). Metabolic Regulation of Macrophage Activation. J Innate Immun *14*, 51–68. 10.1159/000516780.

173. Mehla, K., and Singh, P.K. (2019). Metabolic Regulation of Macrophage Polarization in Cancer. Trends in Cancer *5*, 822–834. 10.1016/j.trecan.2019.10.007.

174. Gaucher, D., Chiappore, J.-A., Pâques, M., Simonutti, M., Boitard, C., Sahel, J.A., Massin, P., and Picaud, S. (2007). Microglial changes occur without neural cell death in diabetic retinopathy. Vision Research *47*, 612–623. 10.1016/j.visres.2006.11.017.

175. Omri, S., Behar-Cohen, F., De Kozak, Y., Sennlaub, F., Mafra Verissimo, L., Jonet, L., Savoldelli, M., Omri, B., and Crisanti, P. (2011). Microglia/Macrophages Migrate through Retinal Epithelium Barrier by a Transcellular Route in Diabetic Retinopathy. The American Journal of Pathology *179*, 942–953. 10.1016/j.ajpath.2011.04.018.

176. Vujosevic, S., Bini, S., Midena, G., Berton, M., Pilotto, E., and Midena, E. (2013). Hyperreflective Intraretinal Spots in Diabetics without and with Nonproliferative Diabetic Retinopathy: An *In Vivo* Study Using Spectral Domain OCT. Journal of Diabetes Research *2013*, 1–5. 10.1155/2013/491835.

177. Arroba, A.I., Alcalde-Estevez, E., García-Ramírez, M., Cazzoni, D., De La Villa, P., Sánchez-Fernández, E.M., Mellet, C.O., García Fernández, J.M., Hernández, C., Simó, R., et al. (2016). Modulation of microglia polarization dynamics during diabetic retinopathy in db / db mice. Biochimica et Biophysica Acta (BBA) - Molecular Basis of Disease *1862*, 1663–1674. 10.1016/j.bbadis.2016.05.024.

178. Schwarzer, P., Kokona, D., Ebneter, A., and Zinkernagel, M.S. (2020). Effect of Inhibition of Colony-Stimulating Factor 1 Receptor on Choroidal Neovascularization in Mice. The American Journal of Pathology *190*, 412–425. 10.1016/j.ajpath.2019.10.011.

179. Okunuki, Y., Mukai, R., Nakao, T., Tabor, S.J., Butovsky, O., Dana, R., Ksander, B.R., and Connor, K.M. (2019). Retinal microglia initiate neuroinflammation in ocular autoimmunity. Proc. Natl. Acad. Sci. U.S.A. *116*, 9989–9998. 10.1073/pnas.1820387116.

180. Littman, D.R. An inducible cre recombinase driven by Cx3cr1.

181. Voehringer, D., Liang, H.-E., and Locksley, R.M. (2008). Homeostasis and Effector Function of Lymphopenia-Induced "Memory-Like" T Cells in Constitutively T Cell-Depleted Mice. The Journal of Immunology *180*, 4742–4753. 10.4049/jimmunol.180.7.4742.

182. Barber, A.J., Lieth, E., Khin, S.A., Antonetti, D.A., Buchanan, A.G., and Gardner, T.W. (1998). Neural apoptosis in the retina during experimental and human diabetes. Early onset and effect of insulin. J. Clin. Invest. *102*, 783–791. 10.1172/JCI2425.

183. Jackson, G.R., and Barber, A.J. (2010). Visual Dysfunction Associated with Diabetic Retinopathy. Curr Diab Rep *10*, 380–384. 10.1007/s11892-010-0132-4.

184. Peng, J., Zou, Q., Chen, M.-J., Ma, C.-L., and Li, B.-M. (2022). Motor deficits seen in microglial ablation mice could be due to non-specific damage from high dose diphtheria toxin treatment. Nat Commun *13*, 3874. 10.1038/s41467-022-31562-3.

185. Lei, F., Cui, N., Zhou, C., Chodosh, J., Vavvas, D.G., and Paschalis, E.I. (2020). CSF1R inhibition by a small-molecule inhibitor is not microglia specific; affecting hematopoiesis and the function of macrophages. Proc. Natl. Acad. Sci. U.S.A. *117*, 23336–23338. 10.1073/pnas.1922788117.

186. Bruttger, J., Karram, K., Wörtge, S., Regen, T., Marini, F., Hoppmann, N., Klein, M., Blank, T., Yona, S., Wolf, Y., et al. (2015). Genetic Cell Ablation Reveals Clusters of Local Self-Renewing Microglia in the Mammalian Central Nervous System. Immunity *43*, 92–106. 10.1016/j.immuni.2015.06.012.

187. Van Dijk, H.W., Kok, P.H.B., Garvin, M., Sonka, M., DeVries, J.H., Michels, R.P.J., Van Velthoven, M.E.J., Schlingemann, R.O., Verbraak, F.D., and Abra`moff, M.D. (2009). Selective Loss of Inner Retinal Layer Thickness in Type 1 Diabetic Patients with Minimal Diabetic Retinopathy. Invest. Ophthalmol. Vis. Sci. *50*, 3404. 10.1167/iovs.08-3143.

188. Sergeys, J., Etienne, I., Van Hove, I., Lefevere, E., Stalmans, I., Feyen, J.H.M., Moons, L., and Van Bergen, T. (2019). Longitudinal In Vivo Characterization of the Streptozotocin-Induced Diabetic Mouse Model: Focus on Early Inner Retinal Responses. Invest. Ophthalmol. Vis. Sci. *60*, 807. 10.1167/iovs.18-25372.

189. Nian, S., Lo, A.C.Y., Mi, Y., Ren, K., and Yang, D. (2021). Neurovascular unit in diabetic retinopathy: pathophysiological roles and potential therapeutical targets. Eye and Vis *8*, 15. 10.1186/s40662-021-00239-1.

190. Wachtmeister, L. (1998). Oscillatory potentials in the retina: what do they reveal. Progress in Retinal and Eye Research *17*, 485–521. 10.1016/S1350-9462(98)00006-8.

191. Dai, J., He, J., Wang, G., Wang, M., Li, S., and Yin, Z.Q. (2017). Contribution of GABAa, GABAc and glycine receptors to rat dark-adapted oscillatory potentials in the time and frequency domain. Oncotarget *8*, 77696–77709. 10.18632/oncotarget.20770.

192. Gastinger, M.J., Singh, R.S.J., and Barber, A.J. (2006). Loss of Cholinergic and Dopaminergic Amacrine Cells in Streptozotocin-Diabetic Rat and Ins2 $^{Akita}$ -Diabetic Mouse Retinas. Invest. Ophthalmol. Vis. Sci. *47*, 3143. 10.1167/iovs.05-1376.

193. Park, S.-H., Park, J.-W., Park, S.-J., Kim, K.-Y., Chung, J.-W., Chun, M.-H., and Oh, S.-J. (2003). Apoptotic death of photoreceptors in the streptozotocin-induced diabetic rat retina. Diabetologia *46*, 1260–1268. 10.1007/s00125-003-1177-6.

194. Park, H.-Y.L., Kim, J.H., and Park, C.K. (2014). Neuronal Cell Death in the Inner Retina and the Influence of Vascular Endothelial Growth Factor Inhibition in a Diabetic Rat Model. The American Journal of Pathology *184*, 1752–1762. 10.1016/j.ajpath.2014.02.016.

195. Anderson, J.R., Jones, B.W., Watt, C.B., Shaw, M.V., Yang, J.-H., DeMill, D., Lauritzen, J.S., Lin, Y., Rapp, K.D., Mastronarde, D., et al. (2011). Exploring the retinal connectome. Mol Vis *17*, 355–379.

196. Martin, P.M., Roon, P., Van Ells, T.K., Ganapathy, V., and Smith, S.B. (2004). Death of Retinal Neurons in Streptozotocin-Induced Diabetic Mice. Invest. Ophthalmol. Vis. Sci. *45*, 3330. 10.1167/iovs.04-0247.

197. Shi, J., Hua, L., Harmer, D., Li, P., and Ren, G. (2018). Cre Driver Mice Targeting Macrophages. In Macrophages Methods in Molecular Biology., G. Rousselet, ed. (Springer New York), pp. 263–275. 10.1007/978-1-4939-7837-3_24.

198. Ferro, A., Auguste, Y.S.S., and Cheadle, L. (2021). Microglia, Cytokines, and Neural Activity: Unexpected Interactions in Brain Development and Function. Front. Immunol. *12*, 703527. 10.3389/fimmu.2021.703527.

199. Portillo, J.-A.C., Lopez Corcino, Y., Miao, Y., Tang, J., Sheibani, N., Kern, T.S., Dubyak, G.R., and Subauste, C.S. (2017). CD40 in Retinal Müller Cells Induces P2X7-Dependent Cytokine Expression in Macrophages/Microglia in Diabetic Mice and Development of Early Experimental Diabetic Retinopathy. Diabetes *66*, 483–493. 10.2337/db16-0051.

200. Tonade, D., and Kern, T.S. (2021). Photoreceptor cells and RPE contribute to the development of diabetic retinopathy. Progress in Retinal and Eye Research *83*, 100919. 10.1016/j.preteyeres.2020.100919.

201. Church, K.A., Rodriguez, D., Lopez-Gutierrez, I., Vanegas, D.V., Cardona, S.M., and Cardonaa, A.E. (2022). Microglia depletion elicits neuroprotective effects to alleviate

vascular damage and neuronal cell loss in the diabetic retina. The Journal of Immunology *208*, 54.14-54.14. 10.4049/jimmunol.208.Supp.54.14.

202. Church, K.A., Rodriguez, D., Vanegas, D., Gutierrez, I.L., Cardona, S.M., Madrigal, J.L.M., Kaur, T., and Cardona, A.E. (2022). Models of microglia depletion and replenishment elicit protective effects to alleviate vascular and neuronal damage in the diabetic murine retina. J Neuroinflammation *19*, 300. 10.1186/s12974-022-02659-9.

203. Yuan, T., Dong, L., Pearsall, E.A., Zhou, K., Cheng, R., and Ma, J.-X. (2022). The Protective Role of Microglial PPARα in Diabetic Retinal Neurodegeneration and Neurovascular Dysfunction. Cells *11*, 3869. 10.3390/cells11233869.

204. Krady, J.K., Basu, A., Allen, C.M., Xu, Y., LaNoue, K.F., Gardner, T.W., and Levison, S.W. (2005). Minocycline Reduces Proinflammatory Cytokine Expression, Microglial Activation, and Caspase-3 Activation in a Rodent Model of Diabetic Retinopathy. Diabetes *54*, 1559–1565. 10.2337/diabetes.54.5.1559.

205. Cukras, C.A., Petrou, P., Chew, E.Y., Meyerle, C.B., and Wong, W.T. (2012). Oral Minocycline for the Treatment of Diabetic Macular Edema (DME): Results of a Phase I/II Clinical Study. Invest. Ophthalmol. Vis. Sci. *53*, 3865. 10.1167/iovs.11-9413.

206. Sfikakis, P.P., Grigoropoulos, V., Emfietzoglou, I., Theodossiadis, G., Tentolouris, N., Delicha, E., Katsiari, C., Alexiadou, K., Hatziagelaki, E., and Theodossiadis, P.G. (2010). Infliximab for Diabetic Macular Edema Refractory to Laser Photocoagulation. Diabetes Care *33*, 1523–1528. 10.2337/dc09-2372.

207. Nakazawa, T., Kayama, M., Ryu, M., Kunikata, H., Watanabe, R., Yasuda, M., Kinugawa, J., Vavvas, D., and Miller, J.W. (2011). Tumor Necrosis Factor-α Mediates Photoreceptor Death in a Rodent Model of Retinal Detachment. Invest. Ophthalmol. Vis. Sci. *52*, 1384. 10.1167/iovs.10-6509.

208. Huang, H., Gandhi, J.K., Zhong, X., Wei, Y., Gong, J., Duh, E.J., and Vinores, S.A. (2011). TNFα Is Required for Late BRB Breakdown in Diabetic Retinopathy, and Its Inhibition Prevents Leukostasis and Protects Vessels and Neurons from Apoptosis. Invest. Ophthalmol. Vis. Sci. *52*, 1336. 10.1167/iovs.10-5768.

209. Stahel, M., Becker, M., Graf, N., and Michels, S. (2016). SYSTEMIC INTERLEUKIN 1β INHIBITION IN PROLIFERATIVE DIABETIC RETINOPATHY: A Prospective Open-Label Study Using Canakinumab. Retina *36*, 385–391. 10.1097/IAE.0000000000000701.

210. Otasek, D., Morris, J.H., Bouças, J., Pico, A.R., and Demchak, B. (2019). Cytoscape Automation: empowering workflow-based network analysis. Genome Biol *20*, 185. 10.1186/s13059-019-1758-4.

211. Cabello-Aguilar, S., Alame, M., Kon-Sun-Tack, F., Fau, C., Lacroix, M., and Colinge, J. (2020). SingleCellSignalR: inference of intercellular networks from single-cell transcriptomics. Nucleic Acids Research *48*, e55–e55. 10.1093/nar/gkaa183.

212. Oria, M., Figueira, R.L., Scorletti, F., Sbragia, L., Owens, K., Li, Z., Pathak, B., Corona, M.U., Marotta, M., Encinas, J.L., et al. (2018). CD200-CD200R imbalance correlates with microglia and pro-inflammatory activation in rat spinal cords exposed to amniotic fluid in retinoic acid-induced spina bifida. Sci Rep *8*, 10638. 10.1038/s41598-018-28829-5.

213. Zhao, S., Heng, X., Ya-ping, W., Di, L., Wen-qian, W., Ling-song, M., Chu, Z., and Xu, Y. (2020). CD200-CD200R1 signaling pathway regulates neuroinflammation after stroke. Brain Behav *10*. 10.1002/brb3.1882.

214. Taylor, S., Calder, C.J., Albon, J., Erichsen, J.T., Boulton, M.E., and Morgan, J.E. (2011). Involvement of the CD200 receptor complex in microglia activation in experimental glaucoma. Experimental Eye Research *92*, 338–343. 10.1016/j.exer.2011.01.012.

215. Kotwica-Mojzych, K., Jodłowska-Jędrych, B., and Mojzych, M. (2021). CD200:CD200R Interactions and Their Importance in Immunoregulation. IJMS *22*, 1602. 10.3390/ijms22041602.

216. Jiang, L., Xu, F., He, W., Chen, L., Zhong, H., Wu, Y., Zeng, S., Li, L., and Li, M. (2016). CD200Fc reduces TLR4-mediated inflammatory responses in LPS-induced rat primary microglial cells via inhibition of the NF-κB pathway. Inflamm. Res. *65*, 521–532. 10.1007/s00011-016-0932-3.

217. Hernangómez, M., Klusáková, I., Joukal, M., Hradilová-Svíženská, I., Guaza, C., and Dubový, P. (2016). CD200R1 agonist attenuates glial activation, inflammatory reactions, and hypersensitivity immediately after its intrathecal application in a rat neuropathic pain model. J Neuroinflammation *13*, 43. 10.1186/s12974-016-0508-8.

218. Iannucci, J., Rao, H.V., and Grammas, P. (2022). High Glucose and Hypoxia-Mediated Damage to Human Brain Microvessel Endothelial Cells Induces an Altered, Pro-Inflammatory Phenotype in BV-2 Microglia In Vitro. Cell Mol Neurobiol *42*, 985–996. 10.1007/s10571-020-00987-z.

219. Lunnon, K., Teeling, J.L., Tutt, A.L., Cragg, M.S., Glennie, M.J., and Perry, V.H. (2011). Systemic Inflammation Modulates Fc Receptor Expression on Microglia during Chronic Neurodegeneration. The Journal of Immunology *186*, 7215–7224. 10.4049/jimmunol.0903833.

220. Zhang, S., Wang, X.-J., Tian, L.-P., Pan, J., Lu, G.-Q., Zhang, Y.-J., Ding, J.-Q., and Chen, S.-D. (2011). CD200-CD200R dysfunction exacerbates microglial activation and dopaminergic neurodegeneration in a rat model of Parkinson's disease. J Neuroinflammation *8*, 154. 10.1186/1742-2094-8-154.

221. Lyons, A., Downer, E.J., Crotty, S., Nolan, Y.M., Mills, K.H.G., and Lynch, M.A. (2007). CD200 Ligand–Receptor Interaction Modulates Microglial Activation *In Vivo* and *In Vitro* : A Role for IL-4. J. Neurosci. *27*, 8309–8313. 10.1523/JNEUROSCI.1781-07.2007.

222. Liu, Y., Bando, Y., Vargas-Lowy, D., Elyaman, W., Khoury, S.J., Huang, T., Reif, K., and Chitnis, T. (2010). CD200R1 Agonist Attenuates Mechanisms of Chronic Disease in a Murine Model of Multiple Sclerosis. J. Neurosci. *30*, 2025–2038. 10.1523/JNEUROSCI.4272-09.2010.

223. Ghassemi, F., Fadakar, K., Berijani, S., Babeli, A., Gholizadeh, A., and Sabour, S. (2021). Quantitative assessment of vascular density in diabetic retinopathy subtypes with optical coherence tomography angiography. BMC Ophthalmol *21*, 82. 10.1186/s12886-021-01831-8.

224. Klein, R., Myers, C.E., Lee, K.E., Gangnon, R., and Klein, B.E.K. (2012). Changes in Retinal Vessel Diameter and Incidence and Progression of Diabetic Retinopathy. Arch Ophthalmol *130*. 10.1001/archophthalmol.2011.2560.

225. Ueno, Y., Iwase, T., Goto, K., Tomita, R., Ra, E., Yamamoto, K., and Terasaki, H. (2021). Association of changes of retinal vessels diameter with ocular blood flow in eyes with diabetic retinopathy. Sci Rep *11*, 4653. 10.1038/s41598-021-84067-2.

226. De Carlo, T.E., Chin, A.T., Bonini Filho, M.A., Adhi, M., Branchini, L., Salz, D.A., Baumal, C.R., Crawford, C., Reichel, E., Witkin, A.J., et al. (2015). DETECTION OF MICROVASCULAR CHANGES IN EYES OF PATIENTS WITH DIABETES BUT NOT CLINICAL DIABETIC RETINOPATHY USING OPTICAL COHERENCE TOMOGRAPHY ANGIOGRAPHY. Retina *35*, 2364–2370. 10.1097/IAE.0000000000000882.

227. McLeod, D.S., Lefer, D.J., Merges, C., and Lutty, G.A. (1995). Enhanced expression of intracellular adhesion molecule-1 and P-selectin in the diabetic human retina and choroid. Am J Pathol *147*, 642–653.

228. Lutty, G.A., Cao, J., and McLeod, D.S. (1997). Relationship of polymorphonuclear leukocytes to capillary dropout in the human diabetic choroid. Am J Pathol *151*, 707–714.

229. Noda, K., Nakao, S., Ishida, S., and Ishibashi, T. (2012). Leukocyte Adhesion Molecules in Diabetic Retinopathy. Journal of Ophthalmology *2012*, 1–6. 10.1155/2012/279037.

230. Moran, C., Beare, R., Wang, W., Callisaya, M., Srikanth, V., and for the Alzheimer's Disease Neuroimaging Initiative (ADNI) (2019). Type 2 diabetes mellitus, brain atrophy, and cognitive decline. Neurology *92*, e823–e830. 10.1212/WNL.0000000000006955.

231. Moheet, A., Mangia, S., and Seaquist, E.R. (2015). Impact of diabetes on cognitive function and brain structure: Impact of diabetes on brain. Ann. N.Y. Acad. Sci. *1353*, 60–71. 10.1111/nyas.12807.

232. Saadane, A., Veenstra, A.A., Minns, M.S., Tang, J., Du, Y., Abubakr Elghazali, F., Lessieur, E.M., Pearlman, E., and Kern, T.S. (2023). CCR2-positive monocytes contribute to the pathogenesis of early diabetic retinopathy in mice. Diabetologia *66*, 590–602. 10.1007/s00125-022-05860-w.

233. Talahalli, R., Zarini, S., Tang, J., Li, G., Murphy, R., Kern, T.S., and Gubitosi-Klug, R.A. (2013). Leukocytes regulate retinal capillary degeneration in the diabetic mouse via generation of leukotrienes. Journal of Leukocyte Biology *93*, 135–143. 10.1189/jlb.0112025.

234. Spangenberg, E., Severson, P.L., Hohsfield, L.A., Crapser, J., Zhang, J., Burton, E.A., Zhang, Y., Spevak, W., Lin, J., Phan, N.Y., et al. (2019). Sustained microglial depletion with CSF1R inhibitor impairs parenchymal plaque development in an Alzheimer's disease model. Nat Commun *10*, 3758. 10.1038/s41467-019-11674-z.

235. Pawelec, P., Ziemka-Nalecz, M., Sypecka, J., and Zalewska, T. (2020). The Impact of the CX3CL1/CX3CR1 Axis in Neurological Disorders. Cells *9*, 2277. 10.3390/cells9102277.

236. Zujovic, V., Schussler, N., Jourdain, D., Duverger, D., and Taupin, V. (2001). In vivo neutralization of endogenous brain fractalkine increases hippocampal TNFα and 8-isoprostane production induced by intracerebroventricular injection of LPS. Journal of Neuroimmunology *115*, 135–143. 10.1016/S0165-5728(01)00259-4.

237. Joaquín Merino, J., Muñetón-Gómez, V., Alvárez, M.-I., and Toledano-Díaz, A. (2016). Effects of CX3CR1 and Fractalkine Chemokines in Amyloid Beta Clearance and p-Tau Accumulation in Alzheimer,s Disease (AD) Rodent Models: Is Fractalkine a Systemic Biomarker for AD? CAR *13*, 403–412. 10.2174/1567205013666151116125714.

238. Nash, K.R., Moran, P., Finneran, D.J., Hudson, C., Robinson, J., Morgan, D., and Bickford, P.C. (2015). Fractalkine Over Expression Suppresses α-Synuclein-mediated Neurodegeneration. Molecular Therapy *23*, 17–23. 10.1038/mt.2014.175.

239. Walker, D.G., and Lue, L.-F. (2015). Immune phenotypes of microglia in human neurodegenerative disease: challenges to detecting microglial polarization in human brains. Alz Res Therapy *7*, 56. 10.1186/s13195-015-0139-9.

240. Brown, G.C., and Neher, J.J. (2014). Microglial phagocytosis of live neurons. Nat Rev Neurosci *15*, 209–216. 10.1038/nrn3710.

241. Alawieh, A.M., Langley, E.F., Feng, W., Spiotta, A.M., and Tomlinson, S. (2020). Complement-Dependent Synaptic Uptake and Cognitive Decline after Stroke and Reperfusion Therapy. J. Neurosci. *40*, 4042–4058. 10.1523/JNEUROSCI.2462-19.2020.

242. Alawieh, A., Langley, E.F., and Tomlinson, S. (2018). Targeted complement inhibition salvages stressed neurons and inhibits neuroinflammation after stroke in mice. Sci. Transl. Med. *10*, eaao6459. 10.1126/scitranslmed.aao6459.

243. Michailidou, I., Willems, J.G.P., Kooi, E.-J., Van Eden, C., Gold, S.M., Geurts, J.J.G., Baas, F., Huitinga, I., and Ramaglia, V. (2015). Complement C1q-C3-associated synaptic changes in multiple sclerosis hippocampus: Complement and Synapses in MS. Ann Neurol. *77*, 1007–1026. 10.1002/ana.24398.

244. Hong, S., Beja-Glasser, V.F., Nfonoyim, B.M., Frouin, A., Li, S., Ramakrishnan, S., Merry, K.M., Shi, Q., Rosenthal, A., Barres, B.A., et al. (2016). Complement and microglia mediate early synapse loss in Alzheimer mouse models. Science *352*, 712–716. 10.1126/science.aad8373.

245. Zhong, L., Sheng, X., Wang, W., Li, Y., Zhuo, R., Wang, K., Zhang, L., Hu, D.-D., Hong, Y., Chen, L., et al. (2023). TREM2 receptor protects against complement-mediated synaptic loss by binding to complement C1q during neurodegeneration. Immunity *56*, 1794-1808.e8. 10.1016/j.immuni.2023.06.016.

246. Voigt, A.P., Whitmore, S.S., Lessing, N.D., DeLuca, A.P., Tucker, B.A., Stone, E.M., Mullins, R.F., and Scheetz, T.E. (2020). Spectacle: An interactive resource for ocular single-cell RNA sequencing data analysis. Experimental Eye Research *200*, 108204. 10.1016/j.exer.2020.108204.

247. Liang, Q., Dharmat, R., Owen, L., Shakoor, A., Li, Y., Kim, S., Vitale, A., Kim, I., Morgan, D., Liang, S., et al. (2019). Single-nuclei RNA-seq on human retinal tissue provides improved transcriptome profiling. Nat Commun *10*, 5743. 10.1038/s41467-019-12917-9.

248. Grünert, U., and Martin, P.R. (2020). Cell types and cell circuits in human and non-human primate retina. Progress in Retinal and Eye Research *78*, 100844. 10.1016/j.preteyeres.2020.100844.

249. Kolb, H., Linberg, K.A., and Fisher, S.K. (1992). Neurons of the human retina: A Golgi study. J. Comp. Neurol. *318*, 147–187. 10.1002/cne.903180204.

250. Yan, W., Laboulaye, M.A., Tran, N.M., Whitney, I.E., Benhar, I., and Sanes, J.R. (2020). Mouse Retinal Cell Atlas: Molecular Identification of over Sixty Amacrine Cell Types. J. Neurosci. *40*, 5177–5195. 10.1523/JNEUROSCI.0471-20.2020.

251. Fan, W.-Y. (2020). Association of candidate gene polymorphisms with diabetic retinopathy in Chinese patients with type 2 diabetes. Int J Ophthalmol *13*, 301–308. 10.18240/ijo.2020.02.15.

252. Pinero, J., Queralt-Rosinach, N., Bravo, A., Deu-Pons, J., Bauer-Mehren, A., Baron, M., Sanz, F., and Furlong, L.I. (2015). DisGeNET: a discovery platform for the dynamical exploration of human diseases and their genes. Database *2015*, bav028–bav028. 10.1093/database/bav028.